SAND 90-7038

Design and Cost of the First Commercial Stretched-Membrane Heliostat

Solar Kinetics, Inc.

Sandia National Laboratories

Cover design by Gene Clardy, Sandia National Laboratories.

Design and Cost of the First
Commercial Stretched-Membrane Heliostat

Dan Brown, Andrew Konnerth III,
Paul Schertz, P.E. and David White, P.E.

Solar Kinetics, Inc.
10635 King Willia Dr.
Dallas, Texas

Sandia Contract #42-9691

ABSTRACT

A complete design of a 50 m^2 stretched-membrane heliostat was developed specifically for the early stages of manufacturing. The design included mirror-module refinements, drive selection, pylon and foundation design, and detailing and tracking control design. The mirror module and rear structure are highly similar to the Mark II prototype erected at Sandia National Laboratories, Albuquerque, in 1989. The pylon and foundation consist of a single pipe set in a cast-in-place pier as successfully developed at Sandia. The unique tracking control uses only commercially available industrial control components. Also, all real-time communication requirements have been eliminated to assure against the most common source of malfunctions in previous central receiver fields. Control commands are calculated internally to the local controller using a polynomial approximation curve fitted to actual sun position and adjusted for individual heliostat requirements. Direct material costs, in 1990 dollars, were obtained for several different production volumes from material and component manufacturers and subassembly subcontractors. Manufacturing costs for a low-volume production company are projected to be competitive with glass/metal heliostats.

ACKNOWLEDGEMENT

Table of Contents

List of Figures

List of Tables

1.0 INTRODUCTION

1.1 Purpose and Goals

The purpose of this effort was to complete a comprehensive design of a stretched-membrane heliostat suitable for near-term markets. The design was to include the drive, controls, support and foundation for the heliostat, as well as the mirror module. Also required was the development of realistic manufacturing costs for this design. Solar Kinetics Inc. (SKI) performed this work under contract to Sandia National Laboratories in Albuquerque (SNLA).

Efforts in earlier contracts were aimed at determining the viability of stretched-membrane heliostats for commercial utility-scale power generation. Those efforts concentrated on demonstrating the technical feasibility of the stretched-membrane mirror module and projecting high-volume manufacturing costs. The current work is intended as a bridge to supply design and costing information to hasten the transformation of heliostat technology from the current prototype stage to low-volume commercial production.

The design and costs developed here are based upon fabrication techniques already developed for existing stretched-membrane heliostat prototypes or already in common use in industry. This means almost no development effort is required to produce this design for the costs described. The design developed here also uses off-the-shelf components whenever practical. This eliminates the need for further development before near-term markets can be satisfied. This approach is intended to minimize the typical "teething" problems associated with new technologies during the critical early, evaluation period.

1.2 Prior Work on Stretched-Membrane Heliostats

This work builds upon substantial design and development work done in earlier contracts. Heliostats with reflective surfaces of 150 m^2 and a 50 m^2 were designed by Solar Kinetics under previous contracts to Sandia (1, 2). Two generations of prototype 50-m^2 mirror modules proved to be successful. Costs to manufacture the 150-m^2 heliostats in the high volumes required for full commercialization have been estimated. Similar work was done by another contractor to SNLA, Science Applications International Corp. (SAIC) (3, 4).

Testing by SNLA of the first SKI prototype 50-m^2 stretched-membrane heliostat "demonstrated that membrane heliostats could perform at least as well as heliostats using glass mirrors" (5). The second-generation prototype testing had results that "show significant improvement in optical performance over the first-generation designs, especially in windy conditions" (5). One measure of a heliostat's performance is to quantify the mirror-normal error of the reflective surface. This compares the theoretical parabolic contour the mirror should have to the actual shape of the focused heliostat

1

membrane. Second-generation glass heliostats and the heliostats at Solar One typically had errors of 1.1 to 1.9 mrad one sigma. The SKI Mark II prototype had an error of about 1.2 mrad (5).

Cost studies in earlier works were for 150-m^2 heliostats. Significant economies of scale are available in manufacturing large units. The prototypes were built to a smaller scale to reduce development costs and because of space limitations at the Central Receiver Test Facility (CRTF) assembly building. Also, there were not many drives available for the large-area heliostats at that time.

Cost studies are often reported in terms of cost per unit heliostat area, $/m^2$. This allows quick comparison between varied approaches. The production volume selected for the first estimates was 50,000 heliostats per year. The estimators assumed that a central manufacturing facility would pre-fabricate as many readily shippable components as possible. An on-site assembly operation would be built at each central receiver power plant to assemble the heliostats, since they are too large to ship. Projected cost (in 1985 dollars) for the 50,000th heliostat was $14.69/$m^2$ for the mirror module only. The balance of the heliostat would add another $26.96/$m^2$ for a total of $41.65/$m^2$ installed cost (1). A summary of heliostat costs is in Table 1.1

SAIC projected the price for a reduced volume of 5000 units per year, with the 5,000th unit costing $107.00/$m^2$ (4). This was for a 100-m^2 unit using a unique dual-module design. The current work projects a cost for a 50-m^2 heliostat manufactured with low-volume tooling and installed in small fields at about $268/$m^2$.

Table 1.1
Projected Costs of Installed Heliostats

Source	SKI(B)	SKI*	SAIC(D)
Qnty/Yr.	50,000	2,000	5,000
Size m^2	150	50	100
Dollar year	1985	1990	1989
Annual production m^2/year	7.5×10^6	0.1×10^6	0.5×10^6
Direct Cost	$7,493.49	$11,930.50	$13,059.01
Direct Cost/m^2	$49.96	$238.61	$130.59
Selling Price	$9,573.80	$13,401.00	$16,426.28
$/m^2$	$63.83	$268.02	$164.26

* First Commercial Heliostat

1.3 The First Anticipated Markets

It is anticipated that stretched-membrane heliostats will initially be sold in smaller quantities than required for a multi-megawatt commercial utility plant. Current studies suggest that for a central receiver plant to be commercially viable in today's market it would require at least 100 to 200 megawatts generating capacity. Such a plant would require about 5,000 to 10,000 150-m^2 heliostats. It is unlikely that investors in such a project would commit to using such a new technology as stretched-membrane heliostats because of the limited manufacturing and operating experience. Traditionally, utility companies and their investors tend to be conservative.

Utility companies are accustomed, however, to very long- range planning and supporting some research for future generating requirements. The stretched-membrane technique has considerable promise for lowering heliostat manufacturing costs because of its efficient use of material and low total part count compared to a glass-metal heliostat. Therefore, it is likely that if a central receiver plant were built in the near future a nominal quantity of stretched-membrane heliostats would be installed beside the glass-metal units for long-term evaluation.

Other initial applications may include small independent fields built for heliostat, receiver, and control testing purposes. Small fields may also be built for waste detoxification applications.

The quantities of heliostats required for the applications mentioned would not justify the heavy investment in manufacturing facilities assumed in the earlier commercialization cost studies. Considerable engineering and process development work is required before the manufacturing scenarios assumed by those studies could be implemented. Consideration of those studies shows the extremely low labor content of the total manufactured cost that can only be achieved with intense automation. Automation on that scale requires heavy engineering and development effort not immediately cost justifiable.

1.4 Limitations and Assumptions

Specific limitations on the scope of the current work were defined at its outset. These were, in part, determined by available funding, and in part, by the anticipated market requirements.

It was judged that near-term demand would be sufficient to support only a low volume of production. This led to three working assumptions to guide this effort.

1. It was assumed that funding was not going to be available for a major tooling development effort. More specifically, this means no development of the proposed tension tooling concept proposed in earlier high-volume production studies. This tooling concept will require a major engineering effort with some technological risk associated with it.

2. It was assumed that, in spite of the high cost of available drives purchased in low volumes, no effort would be expended to design an alternative.

3. It was decided that wherever practical, control components would be off-the-shelf units. Reliability and minimization of field debugging would be emphasized. Also emphasized would be the flexibility of the control system to allow the inevitable modifications that come with first-of-a kind installations.

1.5 Current Design Description

The current design is for a heliostat that is nominally $50 \, m^2$. The systems that make up a heliostat are the mirror module, rear structure, drive, support pylon, foundation, and tracking controls. The mirror module and rear structure are based very closely on the commercial design developed by SKI (1 & 2) and on the reduced-scale prototype of it. Table 1.2 summarizes the specifications of the first commercial heliostat.

The mirror module is the actual reflective element. It consists of two 0.010 inch aluminum membranes stretched across an aluminum ring. The ring is standard 6-inch high aluminum channel, rolled to a 160-inch inside radius. The two membranes are tensioned and welded to the rolled ring so that they retain a pre-tension at all times. The front membrane is laminated with a silvered-acrylic reflective film. The front membrane has a hole in its center where a fan draws air from the plenum formed between the two membranes. The fan causes the front membrane to be drawn inward to form a parabolic contour, which provides a concentrating effect on the reflected beam of incident sunlight. The rear membrane is linked to the rear supporting structure near its center.

The rear support structure attaches to the mirror module at six equally spaced points about its periphery. The attachment links are pinned to control the manner in which loads are imposed on the mirror-module ring. The rear structure restrains the module to maintain its planarity. The rear structure also serves as the path for wind loads to be conducted to ground. The structure consists of six trusses fabricated from steel bar angles. The trusses are two feet high at their root, tapered toward the tips. They are arranged radially about a central hub weldment. The hub is a 2-foot section of 10-inch diameter steel tubing with a flange at either end.

The drive specified for the first commercial heliostats is a Winsmith torque tube azimuth/elevation gear drive currently only available as pre-owned units. These drives were used for Lugo and Carizzo Plains photovoltaic systems. A custom drive adapter is required to interface this drive to the three mounting pads located on three of the rear structure trusses near the structure center. A different drive adapter would need to be designed if a different drive were used.

The support pylon design is based upon a successful approach used at SNLA for several experimental heliostats. A single 24-inch diameter; 375 in. thick steel tube is set in a

4

bored hole. The concrete pier is poured around it. A single heavy flange is welded to the top of the pylon for the drive to bolt to. In this project, the pier size was determined for soil conditions representative of those at the CRTF in Albuquerque.

The tracking controls are based upon available industrial control components. The controls require no real time communication for tracking. Each controller can track independently for a minimum period of one day. A simple on/off signal selects the operating mode. Periodically, during nonoperating hours, a set of identical coefficients is broadcast on a simple low-speed buss. Each local controller uses the coefficients for the next operating period, (day or week depending upon resident memory capacity).

Table 1.2
HELIOSTAT SPECIFICATIONS

Heliostat diameter	324 in.	8.2 m
Total area	573 sq.ft.	53.2 m^2
Effective area	530 sq.ft.	49.2 m^2
Membrane		
Material	5052-H34 Aluminum	
Thickness	.010 in.	.25 mm
Panel width	36 in.	91.4 cm
Reflective material	ECP-305 by 3M Co.	
Reflective film width	24 in.	61 cm
Front membrane hole	17 in.	43.2 cm
Rear membrane hole	44 in.	111.8 cm
Weight	87 lbs ea.	39.5 kg ea.
Ring		
Material	6061-T6 Aluminum	
Shape	6 in. x 1.92 in. Am. Std. Channel	
	3.63 #/ft.	5.40 kg/m
Cross sectional area	2.403 sq. in.	15.5 cm^2
In-plane area moment	0.72 in.^{4}	30 cm^4
Out-of-plane area moment	13.0 in.^{4}	541.1 cm^4
Weight	251 lbs.	113.9 kg
Trusses		
Quantity	6	
Primary material	ASTM A36 Steel	
Secondary material	ASTM A36 Steel	
Height	24 in. at root	61 cm
	13 in. at tip	33 cm
Weight	205 lbs ea.	93 kg ea.
Hub		
Body material	AISI type 1026 steel	
	10 in. dia. x .25 in. thick	25.4 cm x 6.4 cm
Flanges	3/8 in. ASTM A36 steel	1 cm
Length	24 in.	61 cm
Weight of hub assembly	126 lbs.	57.2 kg
Controls		
Fan motor	1/4hp 90VDCPM	.2 kw
Fan diameter	14 in.	35.6 cm
Position sensor	2 in. stroke LVDT	5.1 cm
Logic controller	Siemans S5-102 U	

2.0 DESIGN LOADS

Wind and gravity loads were defined so that the drive, pedestal, and foundation could be sized. This effort considered only existing wind tunnel data on models with similar configurations. The analysis was based on estimates for component weights. Many significant assumptions were made during this work. These assumptions are discussed first, followed by a discussion of the results.

The source of the wind tunnel data was a report by Colorado State University for the Solar Energy Research Institute (6). The heliostat models were tested in a turbulent boundary layer that produced fluxuating local wind speeds and loads on the heliostats. The data are reported in terms of the mean, maximum and minimum aerodynamic coefficients. For purposes of this design effort, the mean coefficients were used. These coefficients were used with the defined peak wind speeds. The load reducing effects of wind fences and other heliostats were neglected; an isolated heliostat was assumed.

Three modes of operations, each with different loads and requirements, were considered. First, the stow mode was considered. It was assumed that the heliostat would face the zenith when subjected to peak wind speeds up to 90 mph. The 90-mph wind was assumed to vary slightly from true horizontal, but to stay within 6 degrees of horizontal. Second, the go-to-stow mode was considered. It was assumed that the heliostat might experience peak wind speeds up to 50 mph at any orientation before it reached stow. This could occur in any heliostat orientation. Operation was the third mode considered. No excessive deflection was allowed at peak wind speeds of 27 mph with any heliostat orientation.

Several assumptions were made with respect to the geometry and weight of the drive and optical element. Assumptions were required because in many cases the geometry and components had not yet been selected (pending definition of the loads), and modifications were planned for other components. The distance from the elevation axis to the heliostat face (Dimension a in Figure 2.1) strongly influences the moment load about the elevation axis. A distance of 51.5 inches was assumed for calculation of loads and was later used in the final design. It was assumed that the elevation axis crossed the axis of the optical element (Dimension b = 0 in Figure 2.1). The final design has an 11-inch off-set (Dimension b = 11"). This difference would cause the actual elevation moment loads to be higher than design by approximately 15%, and the base moment loads to be higher by approximately 5%. The distance between the elevation axis and the foundation was assumed to be 186 inches. The dimension selected for the final design was 184 inches, an insignificant difference. The weight of the optical element was assumed to be 1,980 lbs with its center of gravity located 13.5 inches behind the ring plane (front surface of the ring). The final design was very close with 1,880 lbs and 13.5 inches. The weight of the drive adaptor (500 lbs in the final design) was neglected because of its small significance. The combined weight of the drive and the pedestal was assumed to be 4,000 lbs. The final design weight was determined to be 3,500 lbs, an insignificant difference.

The combined loads from the wind and gravity were resolved into loads about the drive and about the foundation, as shown in Figure 2.1. All elevation angles with the heliostat facing toward the wind were considered. Also considered were all azimuth angles (with respect to the wind) with the heliostat facing the horizon. All load coefficients as a function of azimuth angle were not provided, so the coefficients as a function of elevation angle were used (Peterka, 6). Orientations that produced a maximum wind load vector (force or moment) were used for loading calculations.

The results of this work showed that the loads on the drive, pedestal, and foundation are higher in the go-to-stow mode than in the stow mode. Therefore, the go-to-stow loads were used for calculations of the support's strength. Table 2.1 shows the orientations that produced the maximum loads and the values for the maximum loads. Note that the peak loads do not all occur at the same orientation, and therefore would not be imposed simultaneously. The actual loads for the other vectors were used in conjunction with the peak loads for determination of combined effects. Operational loads were similar and are summarized in Table 2.2.

Table 2.1
50 MPH Wind and Gravity Loads on Heliostat and Foundation.

		Elevation Angle (gamma, degrees)	Azimuth Angle (beta, degrees)
Drive Loads			
Max Fx' =	+/- 7000 lbs	90 degrees	0,180 degrees
Max Fy' =	+/- 7000 lbs	90 degrees	+/- 90 degrees
Max Fz' =	+ 2900 lbs	40 degrees	0,180 degrees
	- 6900 lbs	40 degrees	0,180 degrees
Max Mx' =	+/- 497000 in-lbs	30 degrees	+/- 90 degrees
Max My' =	+/- 497000 in-lbs	30 degrees	0,180 degrees
Max Mz' =	+/- 460000 in-lbs	90 degrees	+/- 30 degrees
Foundation Loads			
Max Fx" =	+/- 7000 lbs	90 degrees	0,180 degrees
Max Fy" =	+/- 7000 lbs	90 degrees	+/- 90 degrees
Max Fz" =	-11000 lbs	40 degrees	0,180 degrees
Max Mx" =	+/-1400000 in-lbs	90 degrees	0,180 degrees
Max My" =	+/-1400000 in-lbs	90 degrees	+/- 90 degrees
Max Mz" =	+/- 460000 in-lbs	90 degrees	+/- 30 degrees

Table 2.2
27 MPH Wind and Gravity Loads on Heliostat and Foundation.

		Elevation Angle (gamma, degrees)	Azimuth Angle (beta, degrees)
Drive Loads			
Max Fx' =	+/- 2000 lbs	90 degrees	0,180 degrees
Max Fy' =	+/- 2000 lbs	90 degrees	+/- 90 degrees
Max Fz' =	+ 3400 lbs	40 degrees	0,180 degrees
Max Mx' =	+/- 172000 in-lbs	30 degrees	+/- 90 degrees
Max My' =	+/- 172000 in-lbs	30 degrees	0,180 degrees
Max Mz' =	+/- 134000 in-lbs	90 degrees	+/- 30 degrees
Foundation Loads			
Max Fx" =	+/- 2000 lbs	90 degrees	0,180 degrees
Max Fy" =	+/- 2000 lbs	90 degrees	+/- 90 degrees
Max Fz" =	- 6700 lbs	40 degrees	0,180 degrees
Max Mx" =	+/-482000 in-lbs	90 degrees	0,180 degrees
Max My" =	+/-482000 in-lbs	90 degrees	+/- 90 degrees
Max Mz" =	+/-133400 in-lbs	90 degrees	+/- 30 degrees
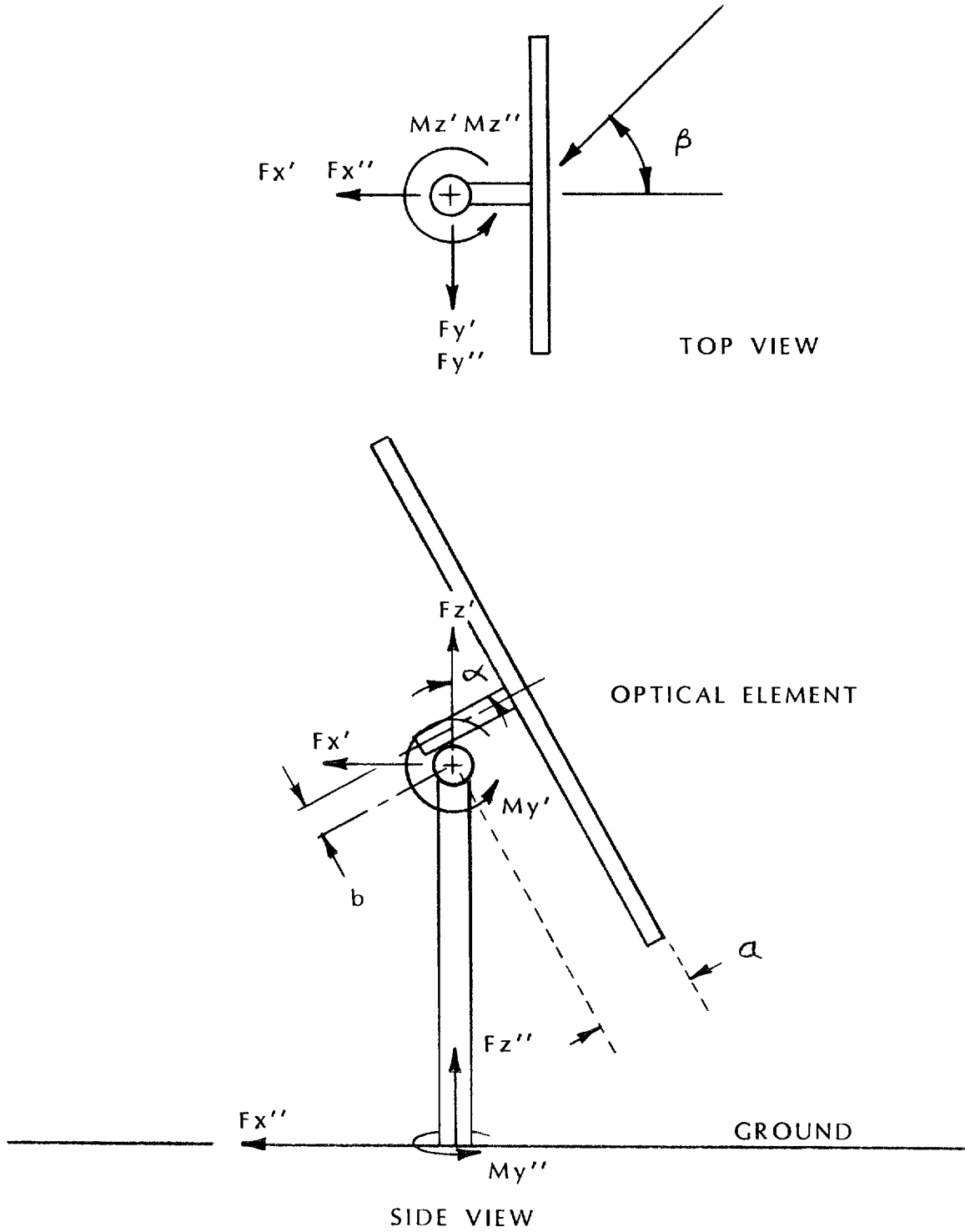
Figure 2.1 Heliostat Load Vector Definition.

10

3.0 DESIGN MODIFICATIONS TO MIRROR MODULE

3.1 Mirror Module

The mirror module design used for the 50-m^2 prototype was used as the baseline design for this work. The original prototype design included some compromises that would be inappropriate for a production design. These items were changed in the current work. Several of these improvements suggested themselves during the prototype fabrication process. Additional changes which would simplify manufacturing became apparent during the work being reported on here. The changes and improvements were included where they could be made without adversely affecting related components or adding technical risk.

3.1.1 Laminating

A dry laminating process is used to apply the reflective film to the aluminum coil stock from which the membrane will be fabricated. Dry lamination is a standard industrial process commonly used to apply decorative and protective films to metal coil stock. The film is normally manufactured with a pressure-sensitive adhesive on one side protected by a removable thinner plastic film or release liner. The process is conducted in a laminator line as shown in Figure 3.1. The laminator removes the release liner and applies the film to the coil stock and then uses a pair of pinch rollers to set the adhesive.

The laminating procedure used for the Mark II prototype included the use of paper templates that attached to the membrane coil stock as a mask before laminating. This mask was applied where the presence of laminate would interfere with subsequent welding of the coil stock to the heliostat ring (see Figure 3.2). Use of masking avoided the necessity of stripping the laminate and its adhesive in areas where welding was to occur. The film was manually sliced with a razor knife along the clearly visible edge of the mask. The masking paper with the unneeded film could then be lifted off the area where welding was to be done.

The masking technique was developed because early experience with laminate stripping revealed it to be very time consuming. The stripping technique combined solvents, heat and mechanical scraping. This subjected the membrane coil stock to risk of damage. The long-term effects of the solvent on the edge of the laminated area were unknown and a cause for concern.

Stripping techniques were recently reinvestigated with positive results. A heated blade was used to scrape the laminate, while the coil stock was securely backed up against a smooth hard surface. This was demonstrated to be practical. An important step was to first use a heated blade to score the edges of the area to be stripped. The low-volume

Dust Free Temp. &
Humidity Controlled
Room

Al. Coil Stock

Coil Washer / Wiper

Solar
Clean

Leveler

Uncoiler

Release Liner Take-Up

Reflective Film Stock

Protective Pre-Mask Stock

Dust "Tack" Cloth

Tape Applicator

Main Laminator

Pre-Mask Laminator

Recoiler
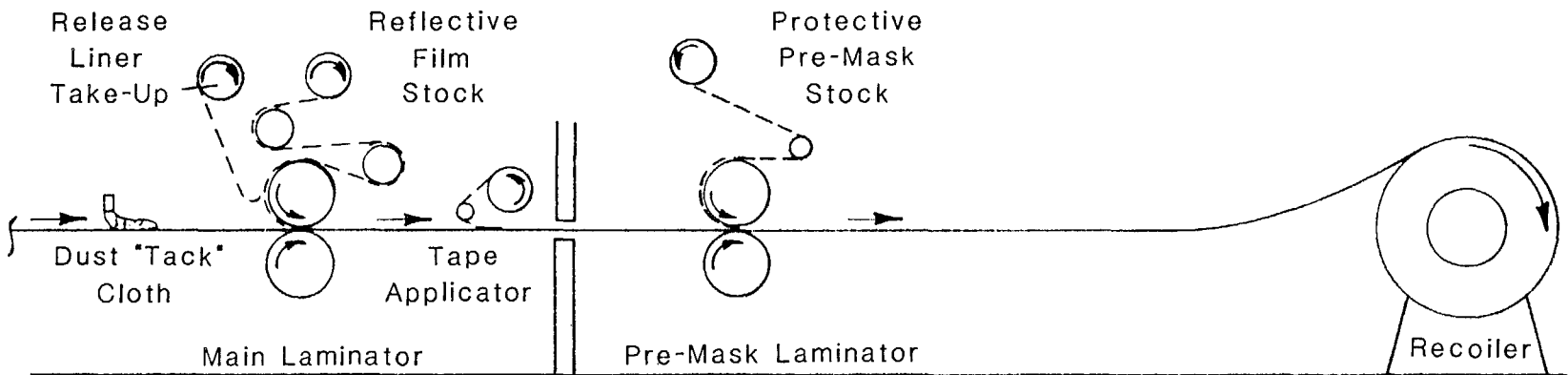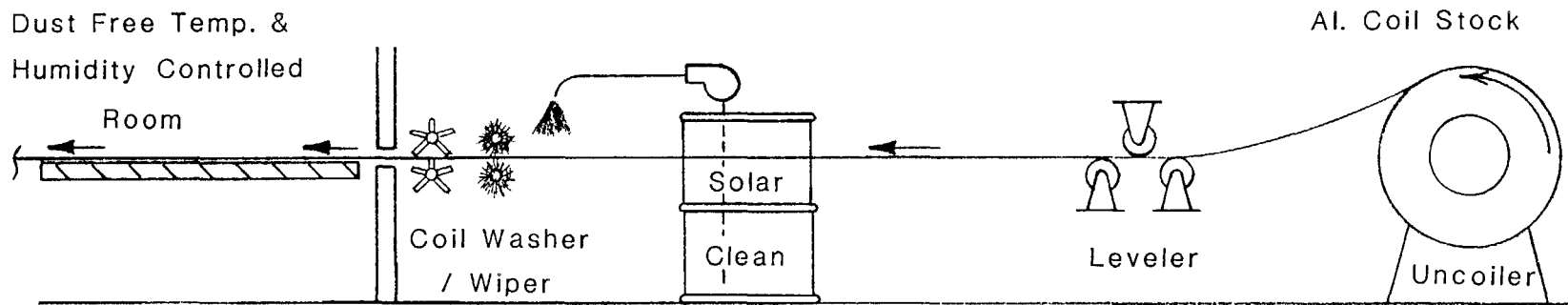
Figure 3.1 Reflective Film Laminating Coil Line.
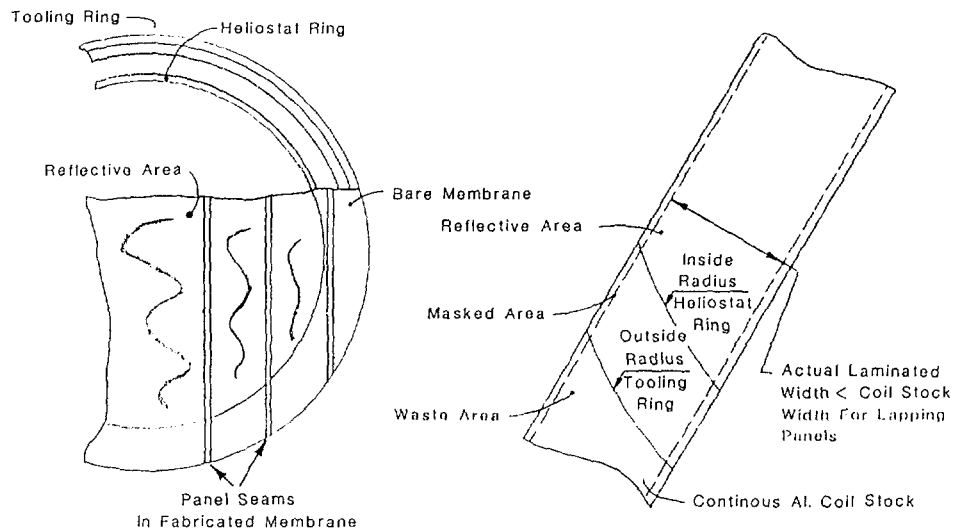
Figure 3.2   Masks used in Coil Line to Selectively Laminate to Prototype Coil Stock.

production plans include use of this technique instead of masking to prepare the weld area before final assembly.

The elimination of the use of paper masks during laminating provides a minimum 50% increase in laminating productivity. It also means that the inventory of laminated stock can be used for any panel of the front membrane. When the coil stock is masked, each panel is unique, requiring inventory of five different parts plus spares in case of damage.

In the prototype fabrication procedure, the membranes had to be laid out and attached to the tooling sequentially. This could not be done until after the ring had been assembled and a temporary membrane support layout table was erected in the center of the tooling. This approach is not viable even for a low-volume production scenario because it prevents quick cycling of the expensive tooling. The production plan will allow two membranes to be fitted to their respective tensioning rings simultaneously. This can be done while the ring is being assembled in a seperate operation.

The tensioning rings will be very similar to the prototype tooling rings. A circumferential bladder will provide the tensioning force. A peripheral membrane mechanical clamp system will fixture the membrane. A permanent vacuum layout table in the center of each ring will ensure accurate and even fit-up of the membrane to the tooling. The tensioning rings may then be lifted, complete with an attached membrane, and moved to the membrane welding station. When production requirements justify it, two

pairs of tensioning rings may be used to permit fixturing of additional membranes during the welding of the previous pair.

There have been difficulties with past laminating activities when using the 0.010-inch thick coil stock with maintaining material alignment. The thin material is more difficult to keep aligned as it passes through the lamination than the thicker stock used in most commercial applications. Future production of membrane stock will involve the use of additional active tracking controls. An edge-locating sensor will detect any off-track condition and control two actuators to steer the pinch rollers to bring the coil stock back on center. This addition will improve laminating production rate about another 25%.

A final rate of 2,200 feet per day is used for these estimating purposes.

The specified coil stock will be supplied in a width of 48 inches. This will allow best use of the 3M ECP-305 reflective film used for heliostats in the past. ECP-305 is available in 24 inches maximum width. If another film is selected, it will be specified to be 48 inches wide nominally for simplified laminating.

Also visible in Figure 3.1 is a tape applicator. This device applies strips of Tedlar weather-resistant tape to the edges of the laminated areas to improve the film resistance to tunneling and delaminating (see Figure 3.3). The tape applicator for production use will also be automatically controlled to follow the edge of the film.

SILVER

ACRYLIC

PRESSURE SENSITIVE ADHESIVE

PROTECTIVE TAPE ALONG EDGES

.010" ALUMINUM MEMBRANE

LAMINATED ECP-300
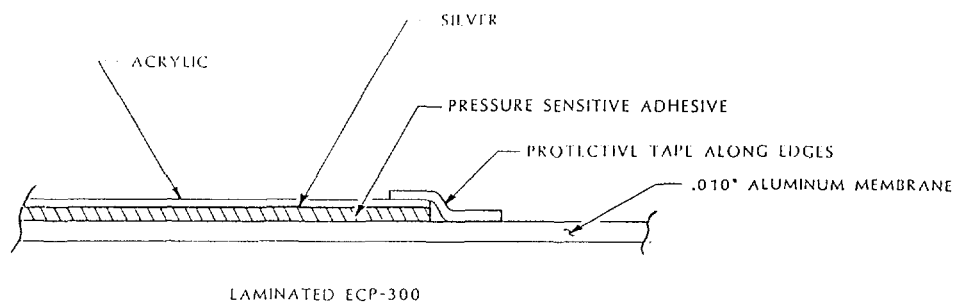
DOMINANT FAILURE MODE:

TUNNELING - SEPARATION OF ACRYLIC FROM SILVER AND SUBSEQUENT CORROSION OF SILVER

SEPARATION OF ADHESIVE/ALUMINUM BOND IS RARE

Figure 3.3 Reflective Film Attachment Detail.

14

Previous prototype lamination procedures required periodic stopping for manual adjustment of the tape applicator tracking.

The use of Tedlar tape for protecting the edge of the laminate has been developed as a method of preventing delamination and tunnelling. Past experience with acrylic reflective films has revealed a problem with failures of the bond between the silver back coat and the acrylic film itself. This separation often begins at the edge of the laminate and progresses across the reflective area as a small tunnel about 3/16 to 1/4 inch wide. In some instances, entire sections of laminate comes detached affecting from several square inches to several square feet. Several variables seem to affect the likelihood and extent of tunnelling problems. Preventing the first initiation of the effect at the laminate edge can prevent onset of this problem. Early heliostats and parabolic troughs used a reflective acrylic tape to seal the edges. This tape was not sufficiently pliable to ensure continuous complete sealing of the laminate edge. Sealing the circular outer perimeter of the heliostat reflective area was particularly difficult. The Tedlar tape was developed for other industries specifically as a weather resistant sealant tape. The Tedlar is resistant to damage by U.V. radiation. The adhesive is very aggressive and formulated for continuous exposure to weather. The Tedlar itself is ductile and easily conforms to surface irregularities and in plane curvatures. Experience to date suggests the small loss of reflective area covered by the non-reflecting tape is more than offset by the increased longevity of the reflective laminate.

3.1.2 Membrane Fabrication

The membrane coil stock must be cut into strips, which are in turn welded together to form a 30-foot wide membrane. The ends of each strip are cut to conform to a 30-foot diameter circle (see Figure 3.2). The welding seam between each panel of the membrane is formed by overlapping the materials and then resistance welding them to one another.

Membrane fabrication is identical for front and rear membranes. Strips of coil stock are unrolled and cut to length for the specific panel being welded. Extra length is allowed at each end for samples of the weld seam to be cut out for quality-control testing.

The panels are laid out on a level table surface with vacuum hold-down capabilities. The panels are aligned and overlapped along one edge. The vacuum hold down is turned on first at the center of the new strip, and then activated progressively from the center toward the ends to work out any waves in the material. As each panel is added to the membrane, it is rolled onto a single straight mandrel for handling and storage (see Figure 3.4).

The welding is performed by a rolling spot resistance welder. One electrode arm reaches under the table and contacts a copper buss bar under the seam area. The other contact wheel and arm reaches over the top. The membrane panels were originally laid out so that the overlap was positioned directly over the copper buss bar.

15

Completed Membrane
Rolled On Mandrel

Reflective Area

Waste Area
Also Used For Weld Tests

Rolling Spot Welder

Vacuum Channels In
Layout/Welding Table
Top

Copper BusBar
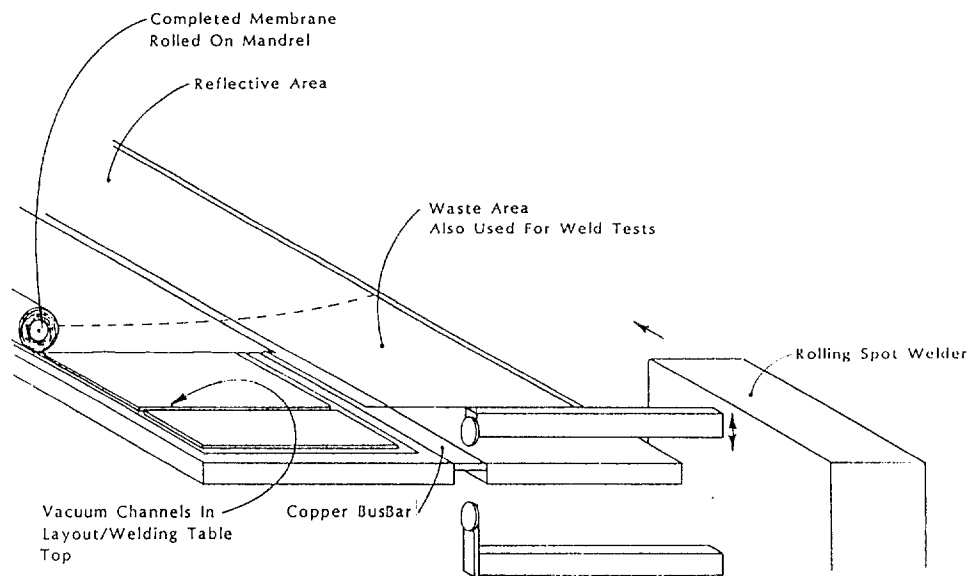
Figure 3.4 Membrane Fabrication; Welding Panels.

3.1.3 Tension Tooling

This procedure assumes several changes from the procedures used for the Mark II prototype. The changes are for the purposes of increased efficiency of manufacturing. Several changes revolve around increased use of dedicated tooling and fixtures.

It is recognized that the actual tension tooling used for the Mark II prototype differed significantly from that originally proposed for production use. The prototype tension tooling was designed to keep tooling costs moderate. The proposed high-volume production tooling will require considerable further development to implement, besides the considerable detail design and fabrication effort. Production volumes at this point are unlikely to justify the expense of this development. There is also significant technical risk associated with the proposed tooling. Therefore, early production plans use a variation of the tension tooling already demonstrated during the Mark II heliostat fabrication.

In the prototype fabrication procedure, there was a single stationary tooling set-up. The membranes had to be laid out and attached to the tooling sequentially. This could not be done until after the ring had been assembled and a temporary membrane support layout table was erected in the center of the tooling. All major assembly operations for a mirror module were performed sequentially in the same fixture (see Figure 3.5). These were ring assembly, front membrane layout and tensioning, rear membrane layout and tensioning, membrane welding to ring, membrane center hole cutting and

16
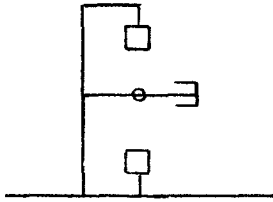
Assemble & Weld Heliostat Ring
-Tooling Rings Retracted
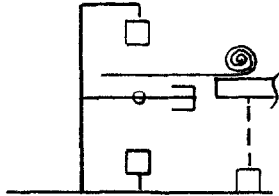
Lay Out Upper (Rear) Membrane
-Tooling Rings Retracted
-Layout Table Assembled & Extended
Level w/ Heliostat Ring
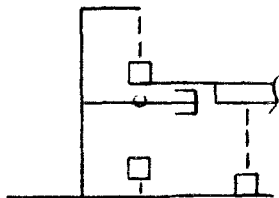
Clamp Membrane To Tooling Ring
-Upper Tooling Ring Lowered
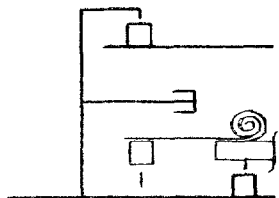
Lay Out Lower (Front) Membrane & Clamp
-Tooling Rings Retracted
-Layout Table Lowered Level w/
Tooling Ring
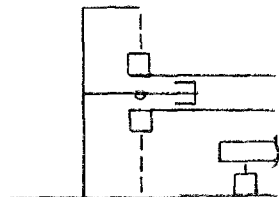
Tension & Welding
-Tooling Rings Extended To Weld Position
-Layout Table Remains Lowered

Figure 3.5 Tooling Procedure for Prototype.

17

reinforcing, and rear structure attachment. This approach is not viable even for a low-volume production scenario because it prevents quick cycling of the expensive tooling.

The production plan allows two membranes to be fitted to their respective tensioning rings simultaneously. This in turn can be done while the ring is being assembled and while the previous mirror module is being welded.

The tensioning rings are very similar to the prototype tooling rings (see Figure 3.6). A circumferential bladder provides the tensioning force. A peripheral membrane mechanical clamp system fixtures the membrane. A permanent vacuum layout table in the center of each ring ensures accurate and even fit-up of the membrane to the tooling. The rings may then be lifted, complete with an attached membrane, and moved to the module assembly station. When production requirements justify it, two pairs of tensioning rings may be used to permit fixturing of additional membranes during the assembly of the previous pair.
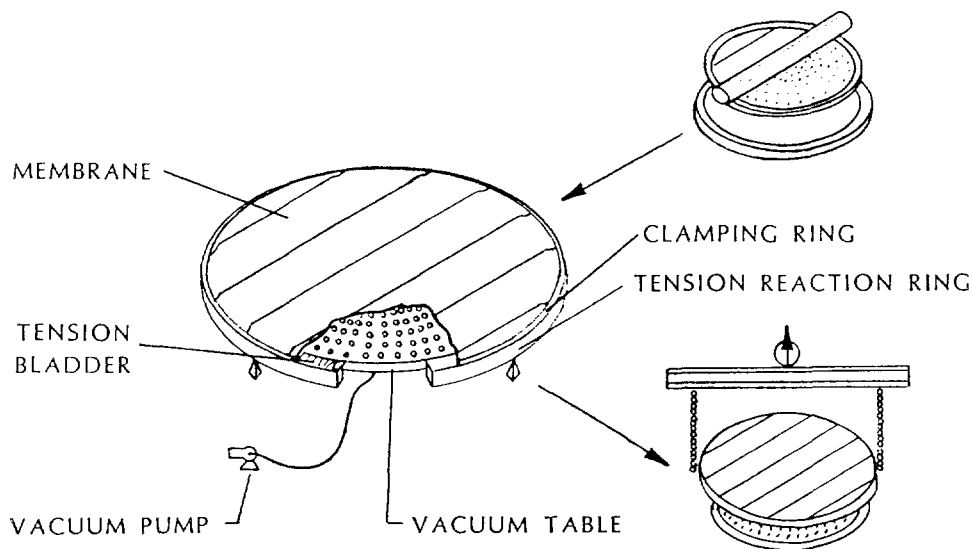
Figure 3.6 Production Tension Tooling Setup.

3.1.4 Heliostat Ring Fabrication

Two major changes to the heliostat ring design will reduce assembly cost and decrease assembly time. The ring will be made from three segments of channel instead of four. The butt joints between the segments will not be welded, but rather they will use a bolt splice plate.

By special-ordering longer lengths of aluminum channel, the heliostat ring can be made from three segments instead of four, as in the Mark II prototype. This will reduce scrap because each rolled ring section has extra material cut off each end where the rolling machine cannot form it. Fewer segments means less material wasted. Reduction in assembly time is achieved by reducing the total number of butt joints in each ring.

The ring was also redesigned to eliminate the use of welding in joining the segments. Instead, a high-strength nonremovable fastener is now used to bolt a splice plate across each butt joint (see Figure 3.7). The standard commercial fasteners are not true bolts. Each fastener has a grooved shank below the head. When the fastener is installed, a collar is swaged onto the grooved pin by a special forming tool that yields the collar metal into the grooves on the pin. The collar is swaged while the pin is held under tension to ensure correct joint compression.
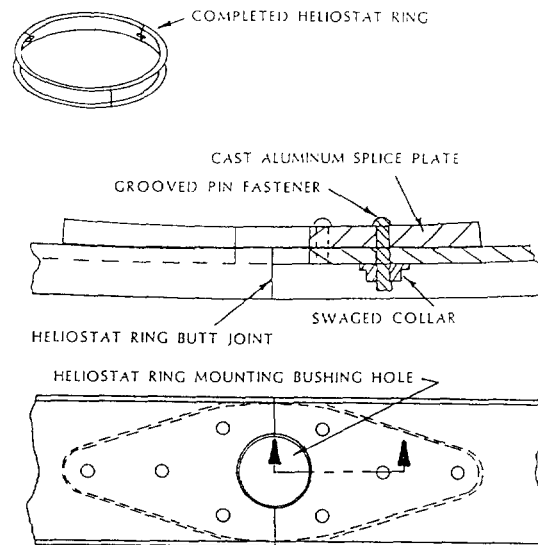
Figure 3.7 Detail of Bolted Heliostat Ring Butt Joint.

This system has advantages over high-strength threaded bolts for this application. Threaded fasteners rely on the indirect method of bolt tightening torque to determine joint compression. Many factors can contribute to causing false indications for conventional bolts. For swaged collar fasteners, the hydraulic tooling ensures that the pin and collar are set under the designed fastener tension.

This system is also faster than welding. It can be performed by less costly laborers with equal or better reliability as welding. Quality control is less expensive and easier to maintain.

The fasteners are available as aluminum parts to ensure prevention of galvanic corrosion and to maintain matched thermal expansion coefficients. The entire mirror module is aluminum. The steel rear structure is completely isolated by the use of urethane mounting bushings from the mirror module.

The splice plate is a cast aluminum part. It is cost-effective in a wide range of production volumes. The same part will serve both as a joint splice plate and as a hinge attachment point doubler at the six points where the ring is linked to the rear structure.

Ring assembly for the Mark II prototype was performed in the same fixture used for final assembly of the ring and membranes and rear structure attachment. This approach is not efficient for production operations because it forces too many assembly operations to be done sequentially. Assembly tolerances, however, must be maintained to the same degree exercised on the prototype. Thus, in the new approach, a separate fixture is used to prepare the rolled channel segments for final assembly. Drill bushings built into the fixture accurately locate all holes for segment joining, tooling attachment, and rear structure attachment. Also, the fixture ensures accurate trimming to length of the ring segment to maintain the correct assembled diameter.

After each segment is prepared, it is fitted into an assembly fixture. This fixture holds the segments to maintain planarity and concentricity while the splice plates are "bolted" in place to join them. After bolting, six temporary spokes are fitted and tensioned to maintain concentricity while the ring is removed from the assembly fixture to await final assembly.

3.1.5 Mirror Module Assembly

Mirror module assembly consists of three major steps. They are

- fixture tensioned membranes and heliostat ring for welding,
- weld membranes to ring, and
- cut and reinforce center holes in membranes.

As mentioned earlier, for the Mark II prototype this sequence was completed on a single fixture. For the low-volume production, several stations are used to allow several steps to be completed in parallel for increased production rates. In the prototype assembly operation, the welding of the membranes to the ring required too much time. This was primarily a result of the limited welding equipment available.

The heliostat ring may be completed in its assembly fixture and then moved for interim storage before final assembly. This removes ring assembly from the critical path in determining module production rate.

The membranes will be fixtured to their tensioning rings in stations dedicated to this task, as described in Section 3.1.3. The rings will then be transferred to the final assembly station.

At the final assembly station (see Figure 3.8), the tensioning rings with attached membranes will be first placed in approximate welding position. They will then be tensioned by inflating the tensioning bladders. The front membrane (assembled on bottom of stack up) will be lowered onto a fixturing ring to ensure its planarity. Next, the heliostat ring with its temporary spokes will be set on the back of the front membrane and centered. Then, the rear membrane will be lowered into place where it presses down on the ring and the front membrane below it.

There are two resistance welders, one above and one below the fixtured mirror-module components. The welders are set up for indirect rolling spot welds, as shown in Figure 3.9. In the production plan, the pair of indirect resistance welders will then be synchronized to always work opposite each other to minimize loads on the ring during welding. They also will be synchronized to avoid firing their welding circuits simultaneously. The use of indirect resistance welding allows two rows of welds to be made at a time.

Indirect welding requires accurate control of all welding parameters to ensure consistent weld quality. Surface preparation will be assured by use of a mechanized abrasion wheel for the channel and the membrane edge. The welder will be monitored by a data acquisition system that captures the electronic signature (similar to an oscilloscope) of each weld pulse and compares it to pre-established limits.

After both membranes are welded to the heliostat ring, the tension tooling bladders are de-pressurized. The membrane tension developed by the tensioning rings is transferred to the heliostat ring. The temporary spokes can now be removed because the membranes keep the heliostat ring concentric.

Another change in the assembly operation results from a minor design improvement. The membranes both have holes cut in their centers for the fan opening and the rear access opening. The holes have reinforcing rings attached around their peripheries to reduce stress concentrations (see Figure 3.10). The reinforcing rings are attached with a combination of silicone adhesive and self-clinching rivets. The rings are made from aluminum sheet stock. They are predrilled for rivet locations. The existing holes serve as guides for drilling holes in the membranes.

The hole in the front membrane has an increased clearance from that of the Mark II prototype because a separate bellows seal now attaches between the central fan shroud and the membrane. The prototype had a slip fit hole in the membrane about the fan shroud. This required a close tolerance for cutting the membrane hole, locating the membrane hole, and fabricating and locating the fan assembly. Too large a hole would have increased air leakage, and thus, focus control system parasitic power usage. The bellows completely seals this leak path and greatly reduces the required accuracy of fabrication in this area.

For a complete process plan for the assembly operation see Appendix 3.A.

UPPER MEMBRANE LAYOUT
& FIXTURE STATION

FINAL ASSEMBLY STATION

PRE-FABRICATED
HELIOSTAT RING
STORAGE

UPPER MEMBRANE WELDER
PIVOT SUPPORT

REAR STRUCTURE
ASSEMBLY FIXTURE

LOWER MEMBRANE LAYOUT
& FIXTURE STATION

MATERIAL HANDLING GANTRY
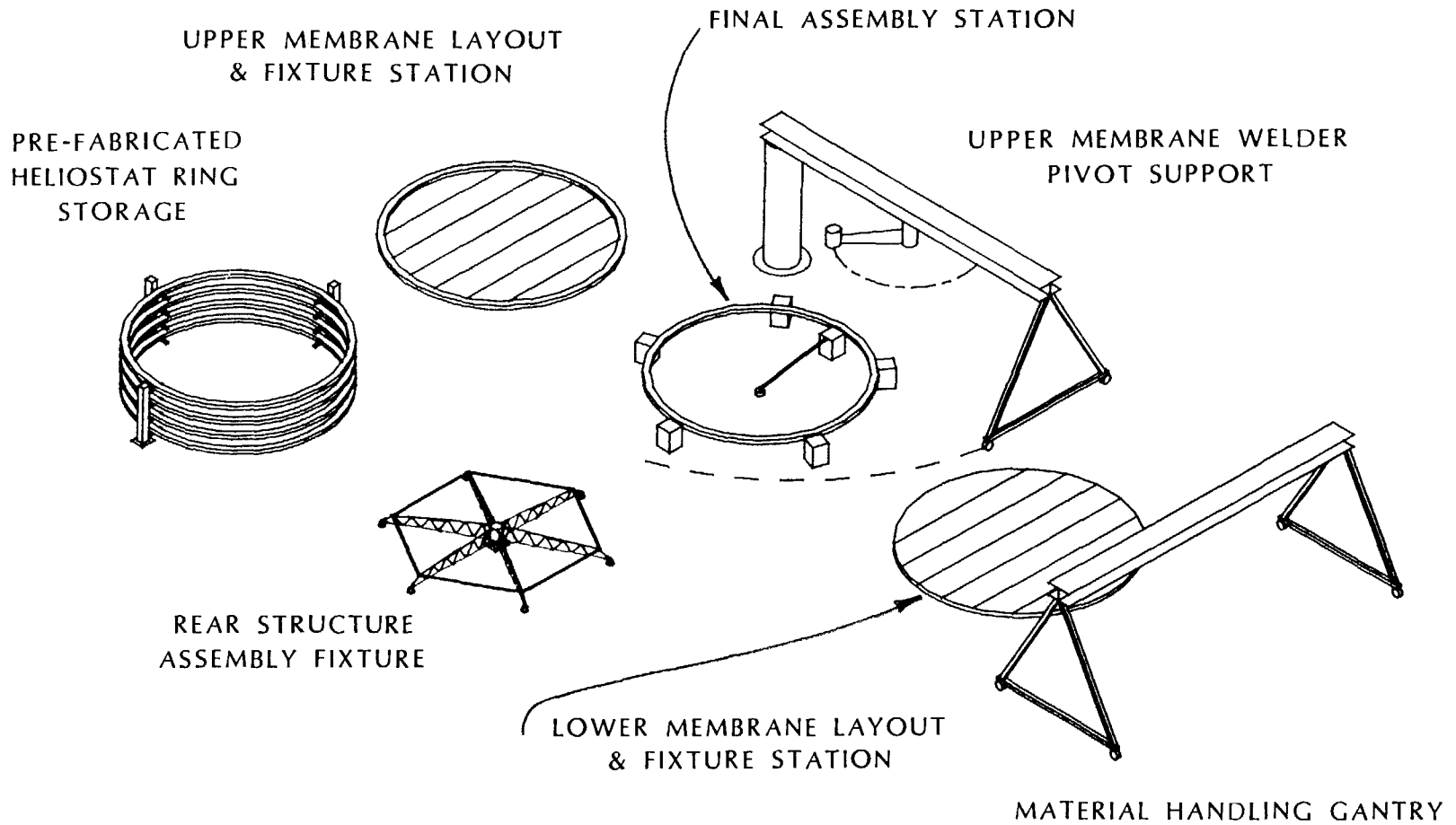
Figure 3.8 Final Assembly Station.
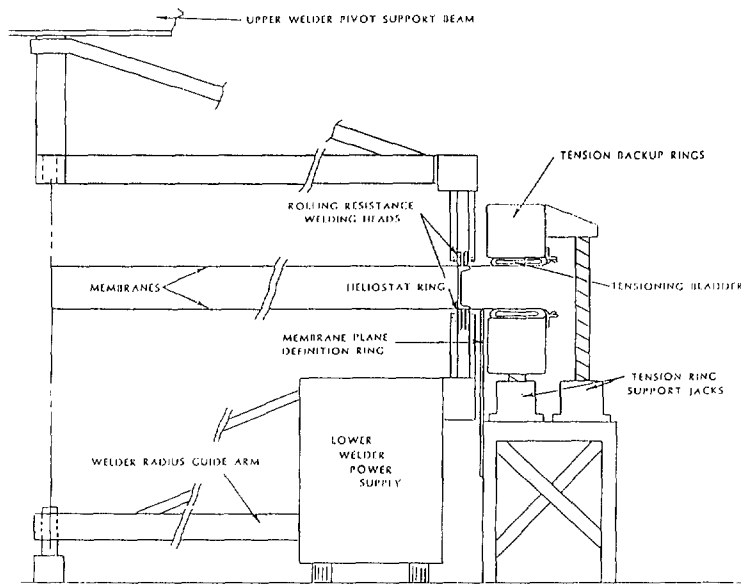
Figure 3.9 Membrane to Ring Welder Arrangement.

FRONT MEMBRANE
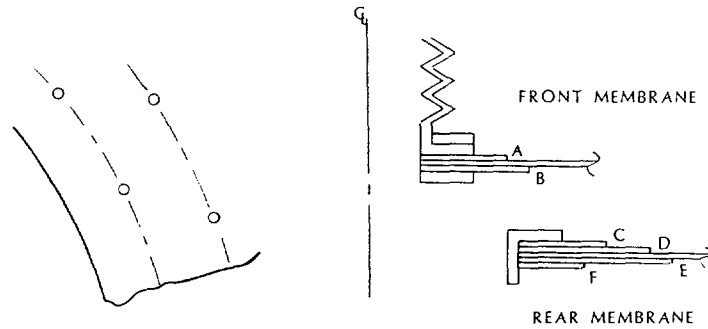
REAR MEMBRANE

	THICKNESS	ID	OD
A	.060	14 1/2"	23"
B	.020	14 1/2"	29"
C	.040	44"	68"
D	.030	44"	80"
E	.020	44"	92"
F	.060	44"	56"

Figure 3.10 Membrane Center Hole Reinforcement.

3.2 Rear Structure

The rear structure supports the mirror module and transfers wind loads imposed on the mirror module back to the drive and support pylon. The mirror module is a steel structure consisting of six bar trusses fabricated from angle iron. The trusses are arranged in a star pattern with their root ends attached to a single central hub assembly. The trusses are linked together by tie rods to distribute loads among the trusses and to limit deflection caused by truss twist.

At the tip of each truss is a hinge element that attaches to the mirror module. The hinge elements are so named because they are linked to the truss by a pin. They are linked to the mirror module by a resilient bushing. This permits differential thermal growth between the aluminum ring and the steel rear structure without imposing any loads on the ring. This arrangement also limits the bending loads that may be imposed on the heliostat ring because the resilient bushing serves almost as a ball joint, transmitting only lateral forces. The tension of the membranes imposes compressive forces on the heliostat ring. The ring, therefore, must be designed not to buckle. Eliminating bending loads in the ring reduces the tendency to buckle.

3.2.1 Hinge Element

The hinge element was redesigned from the Mark II prototype to reduce its manufacturing cost and to simplify assembly. The redesign also improved long-term maintainability by eliminating a seal. Use of steel fasteners in aluminum was also eliminated with its attendant potential for thread galling or seizure.

The new design (shown in Figure 3.11) uses a single plate for the main body, reducing total part count and fabrication complexity. Coating for protection from weather is also simplified by elimination of inaccessible interior surfaces. Attachment to the truss tip is identical to the prototype. Attachment to the mirror module is improved to allow for some misalignment during assembly.

The attachment to the mirror module uses a urethane bushing where it attaches to the aluminum ring. A bolt through the bushing compresses the bushing between two circular plates. The bushing material, when compressed axially, expands radially to grip the inside of a cylindrical hole in the heliostat ring. The compressive force is set by a spacer inside the urethane bushing that limits total compressive deflection. The compression is limited to ensure long bushing life and still provide 16,000 pounds of pull-out resistance. The hinge-element pin and the geometry of the six truss attachment points limit the forces on the bushing to all act perpendicularly to its axis. There is, therefore, almost no force acting to drive the bushing out of its hole. The resilience of the urethane material allows some relative movement of the ring to the pin, limiting bending loads introduced into the ring.
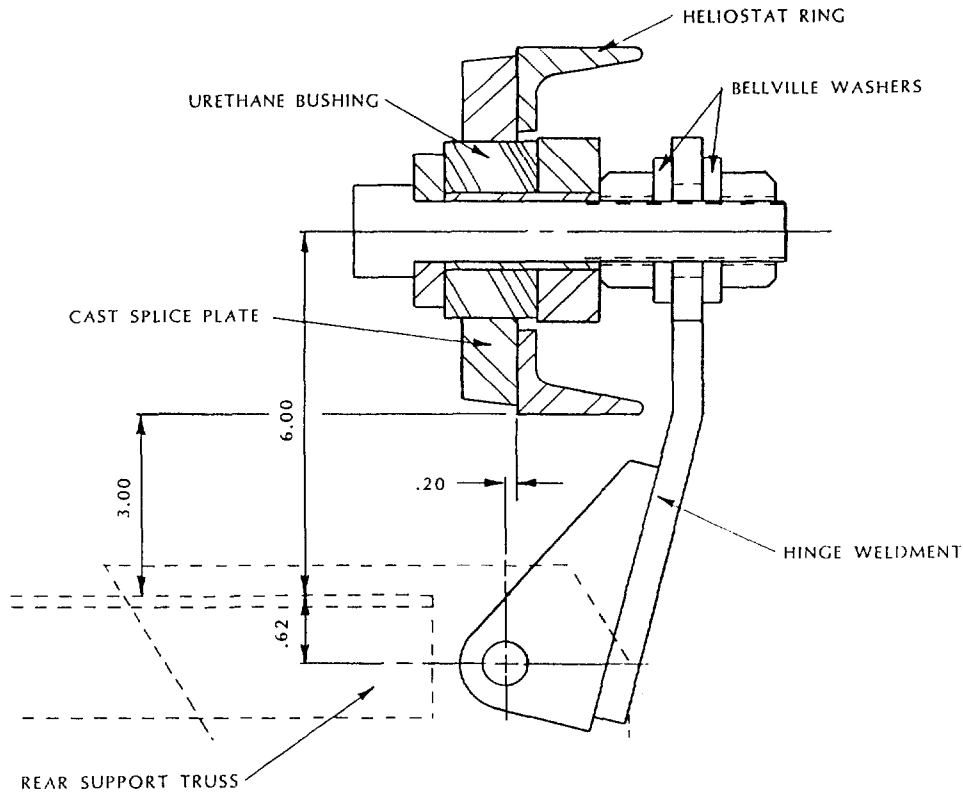
Figure 3.11 Hinge Element Detail.

The bushing, when it is expanded, completely seals the hole in the ring at its mounting point. This eliminates the need for additional silicone sealant, as used in the prototype at each hinge connection. The urethane bushing can also be readily replaced by releasing the compressive load on it until it shrinks within its mounting hole. It is then slipped off its bolt and a new one reinstalled. The urethane specified has excellent weathering properties and is well shaded from the sun. It may not need replacement for the life of the unit.

The bolt through the bushing is also used for attachment to the hinge element. The bolt passes through an oversized hole in the tip of the hinge plate. The oversized hole is used to accommodate any misalignment between the truss tip location and the attachment point hole in the heliostat ring. This reduces the assembly tolerance for the rear structure. The most difficult task in assembling the rear structure assembly is truing the truss tips during final adjustment. By having tolerant hinge attachment connections, the assembly is simplified.

To permit the use of an oversized hole in the hinge plate, the hinge assembly must depend on bolt pre-tension during assembly for its integrity. Therefore, a 1-inch, grade-8 bolt is used. Under the two nuts, which capture the hinge plate, are two Belleville washers rated at 10 times the clamping force required for the joint. The nuts will be tightened at assembly to fully compress the washers. This is a more reliable indication of bolt tension than tightening torque measurements. The washers also serve to main-

tain bolt tension if there is any creep in the joint and when the joint bulk temperature varies.

3.2.2 Tie Rods

The tie rods were redesigned to reduce the total number of parts required. The tie rod ends, where they attach to the trusses, are threaded and bent to pass through the holes in the truss primary's flanges (see Figure 3.12). An acorn nut is used at each truss connection. The thread length is arranged so that the threaded tie rod bottoms in the nut to jam it. High-strength anaerobic thread-locking solution is used. The previous design used a male threaded clevis and a long coupling nut at one end of each tie rod. The other end used a turnbuckle body and another clevis. The new design retains the turnbuckle body, but reduces the part count per tie rod from 14 to 8.
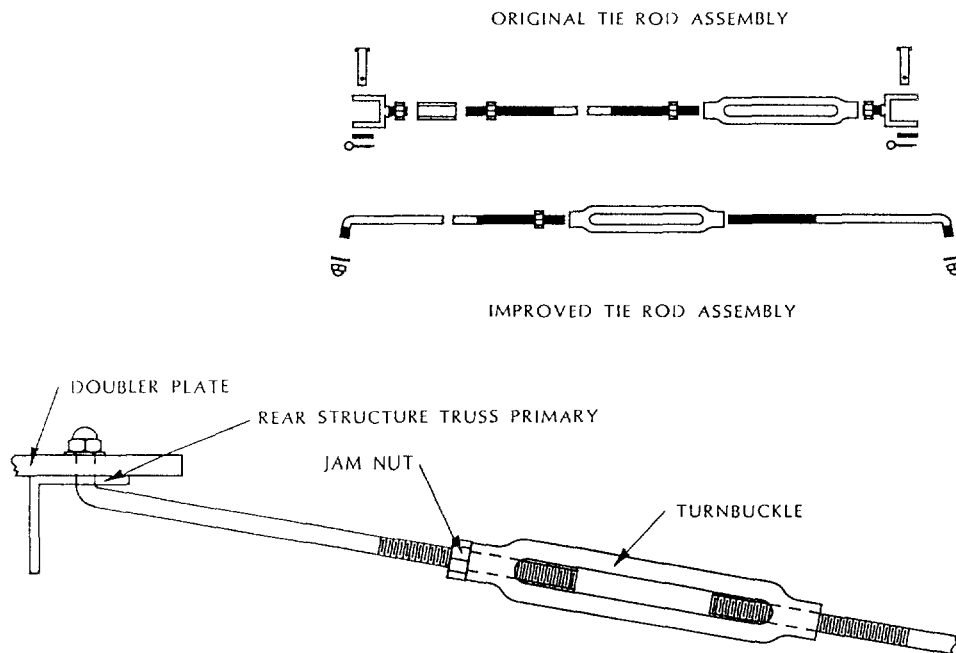
Figure 3.12 Tie Rod End Detail.

26

3.2.3 Truss-to-Hub Attachment

The truss design uses well-proven details very common in the steel joist industry. The root of each truss bolts to fins on the hub weldment and to flanges on the hub weldment (see Figure 3.13). The Mark II prototype used match drilled and reamed holes with shoulder bolts to ensure joint integrity. The revised production design uses slightly oversized holes with nonreplaceable tensioned grooved and swaged fasteners, as described in Section 3.1.4. The fasteners for the trusses will be grade-8 material, 3/4-inch diameter.
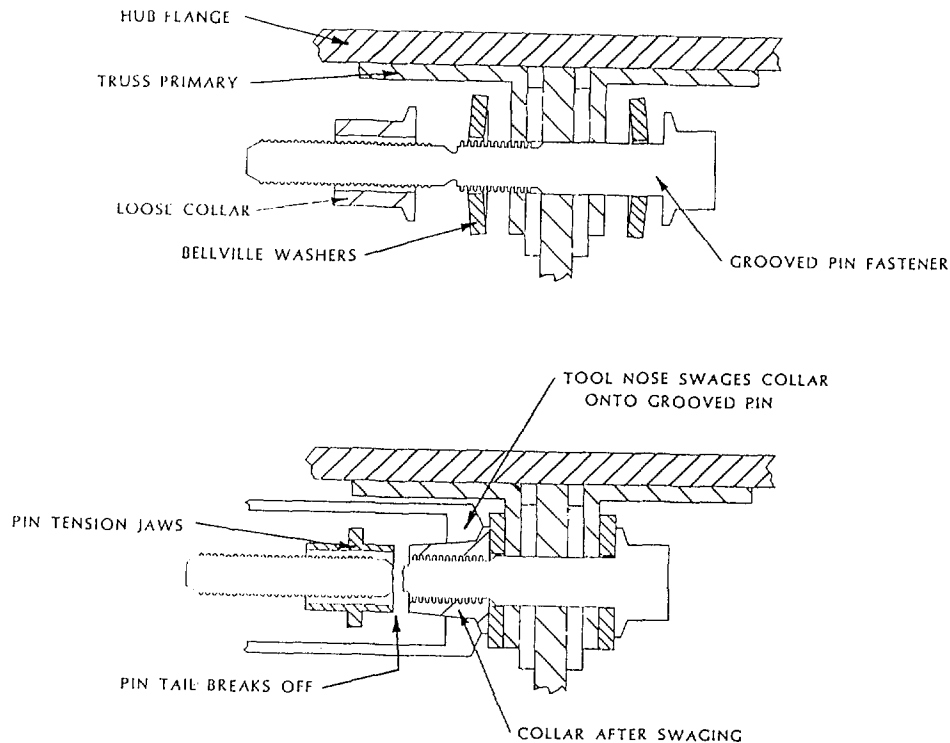
Figure 3.13 Truss-to-Hub Bolting Detail.

Elimination of the requirement for reaming the holes means that the trusses and the hub can be predrilled on separate fixtures prior to the assembly operation. The swaged-on fasteners use a power tool for assembly that is faster, as well as more reliable, than the alternative of threaded fasteners and torque wrench. These combined effects speed the assembly operation considerably. The use of the tensioned pins with swaged-on collars combined with Belleville washers ensure correct joint compression for full design strength with resistance to any loosening in service. The fasteners specified are routinely used for assembly of railway cars and heavy truck chassis, where high joint loads, reversing loads, and heavy vibration are encountered, and absolute joint reliability is essential.

27

3.2.4 Assembly Fixturing

During assembly of the rear structure, the truss tips must be kept planar. A simple fixture will securely support the hub with its axis vertical. All six trusses will be slipped onto the attachment fins, and their tips supported so that the centerline of the hinge pin bushings are planar, and the tips are equidistant apart. The swage bolts will then be inserted and set. Finally, the tie rods will be installed and tensioned. The truss tip supports will then be removed, and the trusses checked to ensure they are not pulled out of place by the tie rods. Pointers on the fixture will be used as a reference point for this. Adjustments will be made by loosening and tightening the tie rods.

When the fixture is first set up, it must be checked with a transit. It should be periodically rechecked after several rear structures have been assembled. The fixture may be designed not to require a finished floor to anchor it to. This would reduce the set-up time required and would allow more flexibility in the on-site assembly operations.

3.2.5 Corrosion Protection

Corrosion protection for the steel parts of the rear structure and for the support pylon must be supplied. With the long life these assemblies must provide, this is an important consideration even in the dry environments many will be built in. Hot dip galvanizing was selected as a proven long-term protection method suitable for many climates. Galvanizing requires little labor because little surface preparation is needed. It is also capable of protecting inside surfaces, not readily coated, using paints. This is important for the trusses with their small crevices and corners. Galvanizing also resists mechanical damage better than paints. For components that will be shipped, this is important because less expensive handling and packaging methods are needed.

3.2.6 Drive Adapter

A drive adapter is required to interface the rear structure to the azimuth/elevation drive mechanism. The drive specified is only a short-term solution because there are not many available and they are not cost-effective to reproduce. Once production volumes are high enough, a different drive will have to be specified. A drive adapter was designed for the purposes of the very near-term market. It transfers wind and gravity loads from the entire optical element to the drive. Three mounting pads on three "drive" trusses are provided on the rear structure for interface.

The selected drive was originally designed for glass-metal heliostats with a central torque tube. The elevation stage, therefore, has two opposed rotating flanges for mounting. The drive adapter has two mirror image halves that bolt to these flanges (see Figure 3.14). The adapter is very similar to that used for the Mark II prototype. It was redesigned to eliminate time-consuming fabrication of parts with compound angles. Also, the fixturing is simpler, and the fabrication tolerances are wider.

Rear
Support
Trusses

Drive Adapter

Hub

Mirror
Module

Elevation Over Azimuth Drive
(Peerless-Winsmith 1151 Shown)
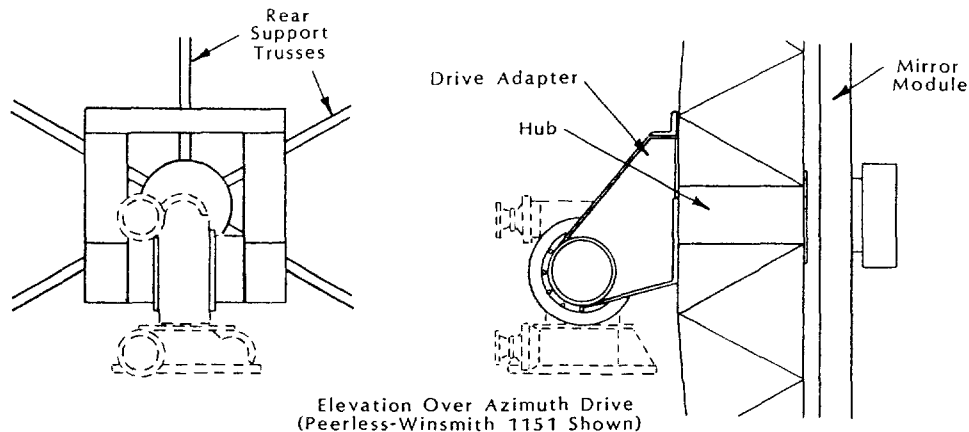
Figure 3.14 Drive Adapter Detail.

3.3 Focus Control System

The focus control system consists of two main subsystems:

- focus fan and support and
- mirror-module seals.

The focus fan is supported in the center of the front membrane so that it may exhaust air from the space between the two membranes out through a hole in the center of the reflective membrane. The first subsystem consists of the motor, fan blade, fan blade shroud, support, and weather cover. The module seals prevent air leakage in and out of the interior of the mirror module past the fan shroud and through the large access hole in the rear membrane.

3.3.1 Focus Fan and Mount

The focus fan is driven by a permanent magnet 1/4 horsepower DC motor with a type-74 frame size. A high- quality motor was specified because of the continuous duty it will see. Alternatives such as brushless DC motors and variable frequency drives with an AC motor were investigated. These alternatives were not found to be cost effective. The primary disadvantage of the selected motor is that it uses a pair of brushes to commutate the armature current. These brushes have a limited life, although some manufacturers claim up to 40,000 hours. The cost of periodic replacement was balanced against the cost of eliminating the brushes. The cost of elimination was too

high. Instead, the design of the motor mounting emphasized easy access for motor removal and brush replacement.

The fan motor is attached by a strap as found in many HVAC blower installations. No special face mounting and motor modifications are required, as in the prototype.

The design of the fan mount is greatly simplified when compared to the Mark II prototype. This is possible because a larger hole (14.5 inches instead of 14 inches) is made in the front membrane, and a bellows is used to seal the annulus created between the membrane inside edge and the fan shroud. This larger hole means the fan mount and shroud assembly can be made to much less restrictive tolerances. The fan shroud position no longer needs to be adjustable to accommodate misalignment of the membrane center hole with the true center line of the rear structure. The fan shroud is now a structural component of the support. All materials are steel, spot welded, and then hot dip galvanized.

The fan mount bolts to the front flange on the rear structure hub. It also serves as a mounting support for the LVDT that senses the front membrane position.

A simpler weather cover is used over the fan outlet. A simple flat disk of aluminum with reflective film laminated to it replaces the previous stamped dish cover. The new design is less expensive and adds 2.7 ft^2 of reflective area.

3.3.2 Mirror-Module Seals

Mirror-module seals include a front membrane bellows seal, rear membrane flexible strip seal, and six sheet metal segment on the rear structure.

The bellows on the front membrane (see Figure 3.15) prevent air flow past the front membrane inner edge around the fan shroud. The bellows allow the front membrane to move from the forward defocused position to the rear most focused position with minimal force required. The front sleeve of the bellows simply clamps to the fan shroud. The rearwards flange on the bellows is clamped to the front surface of the reflective membrane by a metal ring. The bellows is molded from Hypalon, an excellent engineering polymer for outdoor applications. It is easily replaced by removing the weather cover and its weather ring. All work can be done from the front of the mirror module.

On the rear of the mirror module is a large opening (44 inches in diameter) for access to the focus control components. This opening must be closed when the heliostat is operating. A series of separate sealing segments (see Figure 3.15) fastens to the front primaries of the six trusses. This creates a solid disk 3 inches behind the rear membrane. A flexible strip of PVC-impregnated cloth wraps about the outside diameter of this disk and closes the opening between the rear membrane and the sealing segments. The strip is attached with "hook and loop" fastener strips for easy installation and a tight recloseable fit.

30
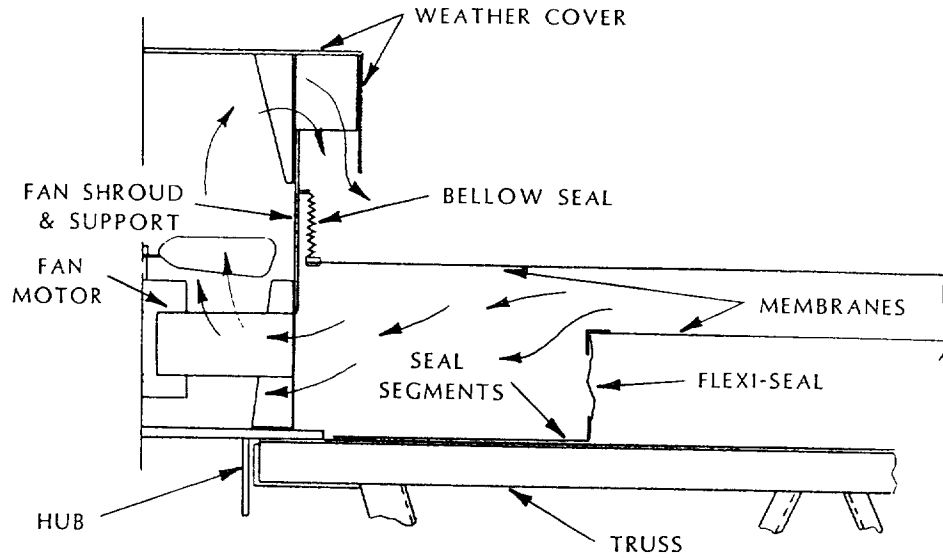
Figure 3.15 **Front Membrane Bellows Seal and Rear Membrane Sealing Detail.**

31

4.0 DRIVES

4.1 Drive Requirements

The selection of a drive for a commercial heliostat is a very important and sensitive decision. The cost of drives from any source tends to be high for low volumes of units. This is because a heliostat drive has a very unique combination of technical specifications not found in many common industrial devices. These requirements include:

> high overall gear reduction ratios (up to 30,000:1),
> high output torque (460,000 in.-lbs),
> 0 backlash gear train,
> high lateral loading on output stage (7,000 lbf), and
> high axial loading on output stage (7,000 lbf).

Several heliostat drives have been designed specifically for that purpose by various manufacturers. They have been designed for various sizes and types of heliostats, so their ratings and geometry vary. Basically, they are all elevation over azimuth drives. The azimuth stages are all gear or cycloidal gear reducers. For elevation stages, both gear drives and jack screw designs have been used.

None of the units are in production. There is no existing inventory of new units. Some of them could be built as specials, but the entire set-up and retooling costs would be charged to the actual order quantity; rather than being amortized over some projected long-term production volume. Until a ready market exists for heliostats, this is unlikely to change. When heliostats, glass or stretched-membrane, are being installed in significant quantities, it will likely be as part of a large megawatt size installation. The large quantity of heliostats and drives required for a given power plant would probably still constitute a special order from a drive manufacturer, rather than a production item for inventory. The drives would, therefore, be customized for use with the type of heliostats that field will use.

If such a full-scale plant is built using glass/metal heliostats, the owners may also want to test a limited number of stretched-membrane units, as discussed in Section 1.3. The stretched-membrane heliostats would have to be adapted to the glass/metal drives in order to take advantage of any volume cost reductions. At best, the azimuth stage could be utilized from the high-volume glass/metal drives, and a custom elevation stage adapted to it with some increased cost penalty for the small quantity.

If an order for drives for commercial stretched-membrane heliostat drives cannot be "piggy backed" on some other larger order, there is almost no possibility of volume discounts.

This scenario was essentially understood at the beginning of the current effort. It was also recognized that through a DOE-funded development effort Peerless-Winsmith

had designed and prototyped a promising drive that had reasonable cost projections for volume production (7). The design was also amenable to scaling to other sizes through a limited additional engineering effort. The level of funding available for the current effort was insufficient to design a drive specifically for low volume 50 m^2 heliostat applications. It was decided instead to review the drives that were already available. It was assumed that an available design would be used, even if it was oversized for this 50 m^2 heliostat. A quick investigation of nonsolar-specific industrial components was made to look for something currently available that could be adapted for use as a drive.

4.2 Existing Heliostat Drives

Three manufacturers of heliostat drives were identified. They are Peerless-Winsmith, Inc., Hub City Inc., and Flenders Corp. Each manufacturer was solicited to recommend one existing drive and supply costs at several different production quantities. They were given the specifications for drive loads and tracking accuracy as described in Table 4.1.

Table 4.1
Partial Heliostat Drive Specifications for First Commercial Heliostat.

Worst Case Loads

Elevation torque	497,000	in-lbs
Azimuth torque	460,000	in-lbs (+ /-)
Horizontal load	7,000	lbs
Vertical load	6,900	lbs.....downward
	2,900	lbs.....upwards
Gear backlash	0.50 mrad maximum	

Flenders Corp. expressed little interest in continuing involvement in heliostat drive manufacture. Hub City supplied costs to reproduce one of its existing torque tube designs in a wide range of volumes. The specifications of its recommended drive, design model #99-22-00351, are summarized in Table 4.2. Peerless-Winsmith provided similar information for the low-cost drive mentioned previously. Its specifications are also shown in Table 4.2. The Peerless-Winsmith unit was selected as the lowest cost option of these three.

Table 4.2
Specifications for Several Heliostat Drives.

		Peerless-Winsmith		Hub-City
		Low-cost	#1151	#99-22-00351
Max. rate of rotation, degrees/min.				
	Azimuth	12	11.7	7.4
	Elevation	12	11.7	7.4
Torque capability, ft-lb				
Elevation,	operate	32053		
	drive to stow	65547		29000
	maximum	87403	* 18500	60000
Azimuth,	operate	30118		
	drive to stow		29000	
	maximum	61364	18500	60000
Output shaft tolerance, (backlash)				
	mrad	1.5	.38 max.	.5
Output shaft deflection				
	mrad	2.0	2.8 El.	< +3
	@	32000 ft-lb	6000 ft-lb	20000 ft-lb
Effective drive ratio.				
	Azimuth	33120:1	18400:1	29200:1
	Elevation	31640:1	18400:1	29200:1

* Tested to excess of 80,000 ft-lbs operating torque. Ratings are calculated values for cast iron. Nodular iron increases safety factor by factor of 2. Another factor of 2 is included for fatigue.

A limited source of pre-owned Peerless-Winsmith torque tube type drives was also found. They were originally sold to support a 93 m^2 heliostat. The specifications are shown in Table 4.2. The Carrizo Solar Corp. is selling some units that were originally installed at the Taft Solar Thermal site and from the Carrizo Plains Field. The cost of these units is reasonable, but there are only a few available. This was the option selected for very low, 1 to 50, production volumes of heliostats.

5.0 SUPPORT AND FOUNDATION

The heliostat drive must be mounted at an elevation high enough to allow the mirror module to rotate to face the horizon. An additional foot of height is added to ensure clearance from low vegetation and snow fall. For the drive designs considered here, the support is a single vertically positioned piece of structural steel tubing with a flange on the upper end to adapt to the drive mechanism (see Figure 5.1). The base of this pylon must be anchored to a foundation that resists all forces and moments from gravity and wind. The support and foundation design must prevent excessive mirror module movement at operating wind speeds. At higher wind speeds, it must not deflect permanently.

The final design (see Figure 5.2) uses a section of tubing that is continuous from the top flange to ground level and into the cast-in-place concrete pier. The embedded section of tubing extends to the bottom of the pier and serves as the steel reinforcing, thus eliminating the steel rebar cage. Experience at the CRTF with installing heliostat pylons led to the development and demonstration of this efficient method of pylon installation. This approach eliminates having to fabricate and place a reinforcing cage of rebar in the bored hole. It also eliminates the J-bolts at the top surface of the pier and their positioning fixture. A pylon bottom end flange to interface with the pier J-bolts is also eliminated. This results in a significant labor and cost savings.

Pylon design initially followed the conventional approach of a reinforced pier with J-bolts for interface to the pylon (see Figure 5.2). This was simplified to using a tube as reinforcement and with a flange on the top to provide an interface to the pylon. The ground-level flange set was retained in this design to allow final adjustment of the pylon to ensure it is kept vertical. The cost of this approach led to a decision to eliminate the expensive ground level flanges and put more care at installation into assuring that the continuous pylon is kept vertical. The control algorithm can also effectively correct for axis tilt, making this issue less critical.

5.1 Pylon Design

The pylon design considered: pylon tube,
                                base flange,
                                top flange,
                                tube to flange welds, and
                                flange bolts.

When the design was simplified to eliminate the ground-level flange set, the ground-level flange and bolt issues were also eliminated. Each step considers both material stresses at survival conditions and displacement errors at operational conditions.
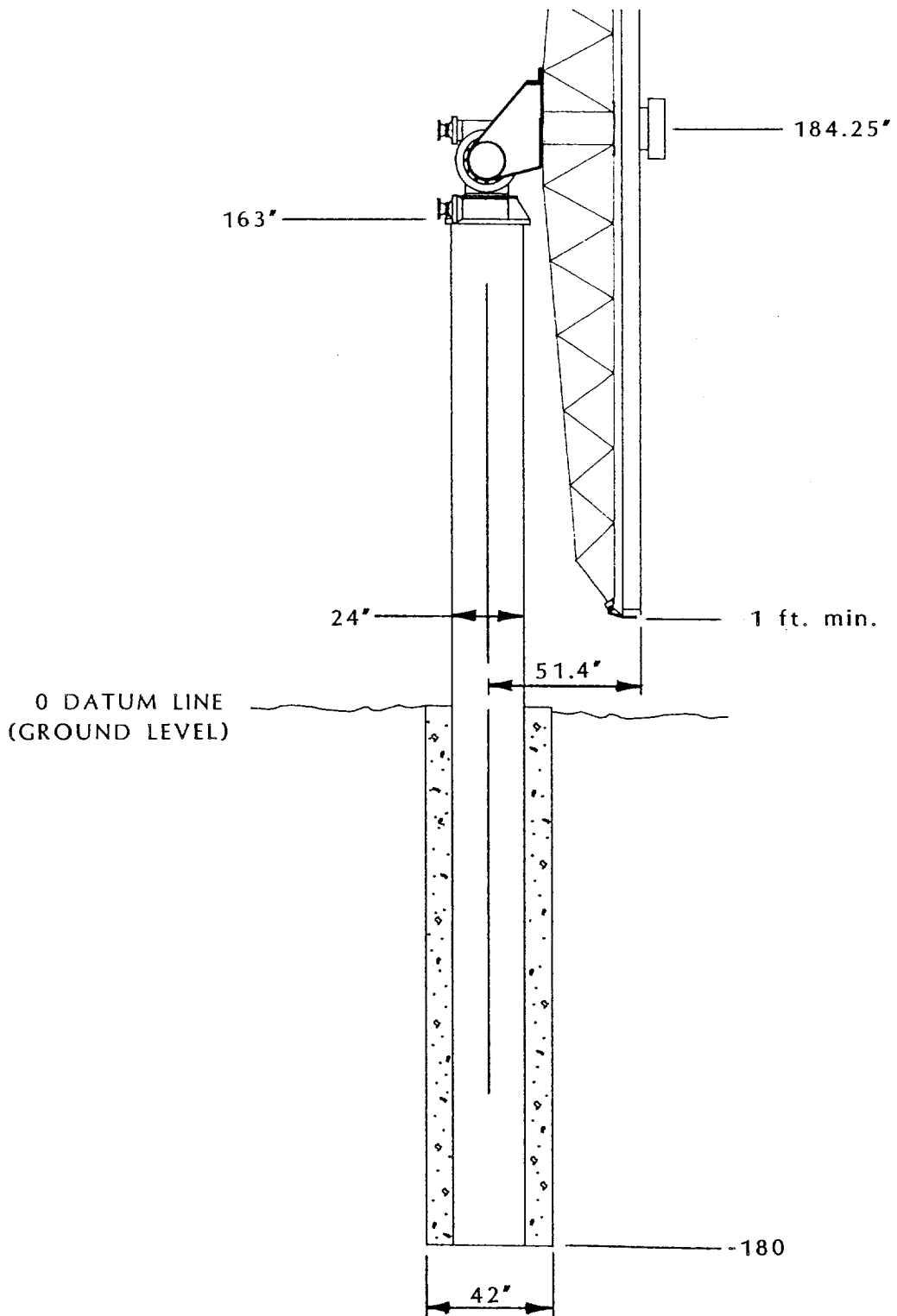
Figure 5.1 Support and Foundation Geometry.
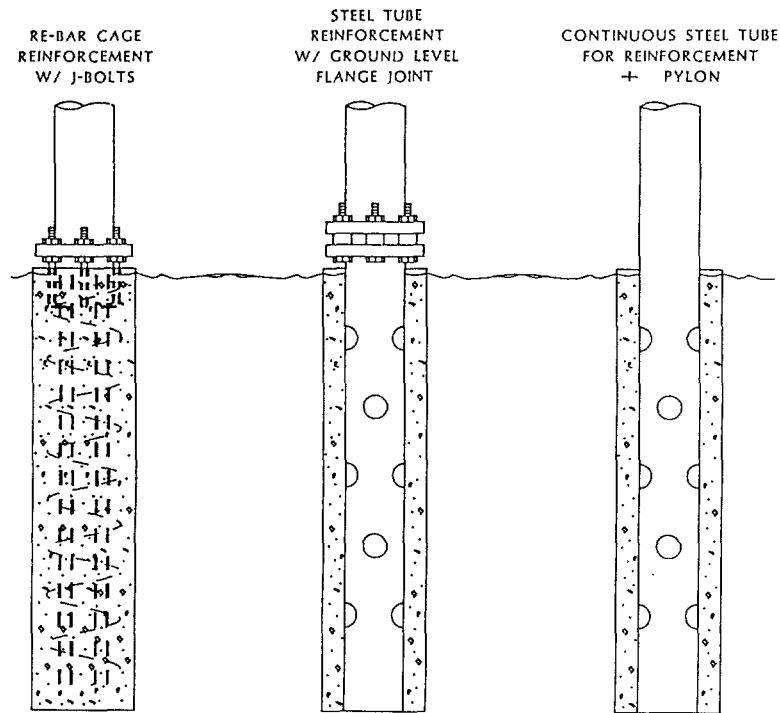
Figure 5.2 Alternative Pier and Pylon Interface Designs.

The pylon is modeled as a cantilever beam with both compressive and transverse loading combined with an axial and transverse moment. Bending moment at the base is derived from two sources. A couple is created by the offset of the mirror-module center of gravity from the vertical axis of the pylon. Added to this is the moment created by the transverse wind drag off the mirror module acting at a distance from the pylon base equal to the height of the center-of-wind effort above the ground. The axial moment results from combined drag and aerodynamic lift forces on the mirror module acting through a center- of-force offset from the pylon axis (See Section 2.0).

The analysis used was based upon work in Roark[8]. Selected results of pylon maximum stress and tilt error for a variety of loading conditions are shown in Table 5.1.

Initial design work resulted in selecting a pylon of 20- inch diameter and a .625-inch wall thickness. Selection of the Peerless-Winsmith low-cost drive, as a potential drive for low-volume production heliostats, dictated a 24-inch pylon. The Peerless-Winsmith unit requires clearance inside the upper portion of the pylon for the azimuth drive motor. Calculations were repeated for the larger diameter pylon using a .375-inch wall, representative of 24-inch schedule-20 pipe material. This material was chosen based upon its availability, as opposed to its optimal sizing. As production quantities increase, availability is less of a problem. Vendors' charges to special order material are amortized over more units and are, therefore, less significant, allowing economical use of more optimally sized elements.

Table 5.1
Pylon Stresses and Tilt Errors Resulting from Various Load Conditions

Pylon	Load Case A		Load Case B		Load Case C	
	50 mph	27 mph	50 mph	27 mph	50 mph	27 mph
20" Sch 40, .593" wall						
Stress, psi					4000	1200
Error, mrad					2	.6
20" Sch 20. .375" wall						
Stress, psi	11000	3000	6000	1800	6000	1900
Error, mrad	3	.8	3.1	.9	3	1
20" Sch 10, .25" wall						
Stress, psi					9000	3000
Error, mrad					4.6	1.6
24" Sch 40, .687" wall						
Stress, psi					2200	700
Error, mrad					1	.3
24" Sch 20, .375" wall						
Stress, psi					3900	1300
Error, mrad					1.7	.6
24" Sch 10, .25" wall						
Stress, psi	11000	3000	6200	1800	8500	1900
Error, mrad	2.5	.5	2.6	.8	2.6	.8

After acceptable stresses and deflections were confirmed, the resonant frequency of the pylon and drive system was considered. Designers of large dish structures in the telecommunications industry typically design for a natural frequency greater than 1 Hz, preferably greater than 2 Hz. This has been determined to help protect against oscillations induced by wind and seismic forces. The pylon and drive system was modeled two ways: as a single mass, single spring and as a dual mass, dual spring system (see Figure 5.3). The single mass model assumes an infinitely stiff drive gear box and serves as a check for reasonableness to the dual mass model. In the dual mass model, a value for stiffness of the drive must be used. This value is not well defined by the drive manufacturers.

Therefore, a range of drive stiffness values was considered to determine the sensitivity of the model to this variable.

The dual mass model handles the mirror module as one inertial load. Its mass includes the mirror module itself and half the drive mass to represent the moveable azimuth

M 1

K 1

M 2

K 2

M eff

K eff
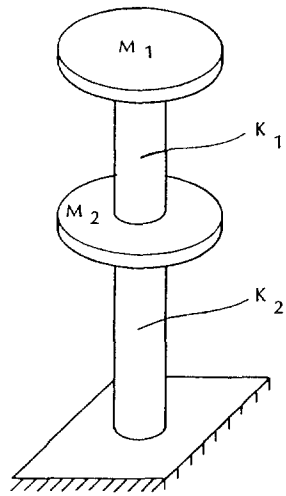
DUAL MASS, DUAL SPRING
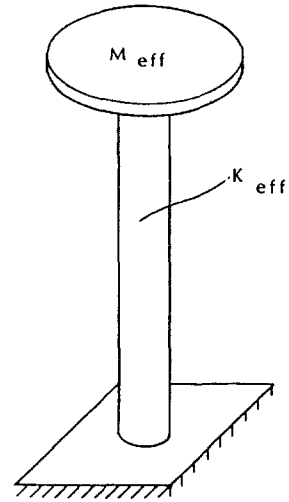
SINGLE MASS, SINGLE SPRING

**Figure 5.3   Mass and Spring Model of Support Pylon and
Drive for Natural Frequency Determination.**

stage. This mass is linked by a torsional spring, representing the drive gear train, to the
other half of the drive and the pylon top flange. A second torsional spring, representing
the pylon body, connects the second mass to ground. This spring represents the pylon.

Some results of this model are shown in Table 5.2. The natural frequency of the final
design is estimated to be 10 Hz based on best information on the drive stiffness. At
some time in the future, a finite element analysis of this system should be considered
to identify combined natural frequencies.

**Table 5.2
Support Structure Natural Frequencies
(Hz.)**

	Drive Stiffness Coefficient (ft-lb/radian)		
	Actual 16×10^6	Low 1.6×10^6	High 160×10^2
Pylon			
20" Sch 20	9.87		
24" Sch 10	10.36	3.37	23.87

41

5.2 Foundation

A cast-in-place concrete pier was selected as the most cost-effective approach to anchoring the support pylon. The pier design was based upon soil conditions at the CRTF in Albuquerque. A generic pier design is not possible because of the widely varying soil conditions likely from one site to another. The cast-in-place pier is likely to be a constant. The length and diameter will vary.

The foundation or pier analysis was conducted based upon soil conditions reported at the CRTF (9, 10). Data were available from previous test borings and soil analysis done in earlier contracts for SNLA.

The design was based upon a single pier for each heliostat. The pier is to be cast in place in a bored hole. The steel reinforcing is to be in the form of a steel pipe. Holes will be flame cut in the pipe in the part to be imbedded in the concrete to let the concrete flow into and fill the interior of the pipe.

The analysis considered both twisting of the foundation and tilting. It was performed in three steps:

1. Determine acceptable range of pier diameters and depths to resist twist moments.

2. Determine acceptable range of pier diameters and depths for soil to support lateral loads and moments. Resulting deflections are evaluated here.

3. Confirm adequate strength of the pier itself for the selected diameter, steel reinforcement configuration, and material properties.

5.2.1 Pier Resistance to Twisting Moment

The pier experiences a twisting moment about its vertical axis from wind effects on the heliostat when it is skewed to the wind vector. This twisting moment is resisted by the friction between the pier outer surface and the soil. The soil friction coefficient is found from on-site soil tests and from handbook values for the applicable soil type. Soil pressure can be found by on-site measurements, or more typically, from a combination of observations of site soil conditions and handbook tables and charts.

The analytical approach assumes that the overburden pressure of the soil increases linearly with depth down to a certain critical depth (11). This depth, usually expressed in diameters, is a function of soil conditions and pier diameter. Typically, this critical depth occurs at 10 to 20 diameters depending upon soil density. This is true for cohesionless soil, as found at the CRTF.

Maximum moment about the vertical axis is 460,000 in.-lbs. A design safety factor of 2 is typical for footings when soil conditions are well defined; the hazard is not great,

and full design loads are not likely. A safety factor of 2 is referenced as typical for bored piles, as opposed to 2 to 3 for driven piles (12). Table 5.3 shows twist resistance of several possible pier geometries. Those shown within the block are acceptable.

Table 5.3
Pier Resistance to Twist
(ft-lbs x 10^2)

Pier Diameter	36 inch	42 inch
Pier Depth		
12 ft	43.3	59.0
15 ft.	67.7	92.1
20 ft.	120.4	163.8

Design load; 38.3 ft-lb x 10^3

5.2.2 Soil and Pier Reaction Analysis

The analysis used determines how a long flexible pier reacts to lateral loading in the given soil conditions. Cohesionless soil is assumed. This part of the analysis is based upon empirical relationships and requires an iterative approach to the solution (12). Table 5.4 shows the final results for several pier geometries and loads. Final results show foundation deflection and ultimate pier load capacity.

Table 5.4
Soil and Pier Reactions
Long Flexible Pier Model

	Ultimate Lateral Load		Lateral Deflection at ground level. at 27 mph.	
	(lbs x 10^3)		(inches)	
Pier Diameter	36 inch	42 inch	36 inch	42 inch
Pier Depth				
12 ft	34.2	39.9	0.05	0.04
15 ft	60.2	70.3	0.07	0.04
20 ft	122.6	143.0	0.05	0.05

To perform this analysis, a series of intermediate results are calculated from the input parameters. These intermediate results are used with an empirically derived graph to establish two deflection coefficients. The deflection coefficients are used in an additional calculation to predict pier ultimate load and deflection. For several load and pier geometry combinations, the calculated intermediate required considerable extrapolation from the empirical graphs. Another analysis technique was used as a check for the long flexible pile model.

43

The second analysis was made assuming a short rigid pier. This analysis was used to predict the ultimate load bearing capacity of the pier. No deflection information could be determined. The results shown in Table 5.5 were compared to those derived from the previous analysis. The match is good for all data combinations, including those with the off-scale intermediate results. The model results did not differ by more than 1.3%, giving confidence in the calculated results.

Table 5.5
Soil and Pier Reactions
Short Rigid Pier Model

Pier Diameter	Ultimate Lateral Load (lbs x 10³)	
	36 inch	42 inch
Pier Depth		
12 ft	34.6	40.4
15 ft	61.0	71.1
20 ft	124.1	144.8

The final step of pier design is to equate the lateral deflections to pier tilt, and therefore, induced optical error. For a stiff pier, the pier tilt is a result of the soil's sub-grade reaction to the force of the pier upon it (see Figure 5.4) The soil's sub-grade reaction coefficient can be obtained from an empirically derived graph relating soil characteristics and density to the sub-grade reaction (12). This leads to determination of the pier's center of rotation and tilt as tabulated in Table 5.6. A 42-inch diameter pier with a depth of 15 feet was selected for the final design based on the deflection occurring at a wind speed of 27 mph.

$$T = \left(\frac{E_{pier}\, I_{pier}}{n} \right)^{1/2}$$

SHORT RIGID PIER IF $L \leq 2T$

DIAM $= 42''$ $2T = 222$

$$Lo/L = \frac{(H + .667L)}{(2H + L)}$$

$$TILT = TAN^{-1} \left(\frac{DEFLECTION}{Lo} \right)$$
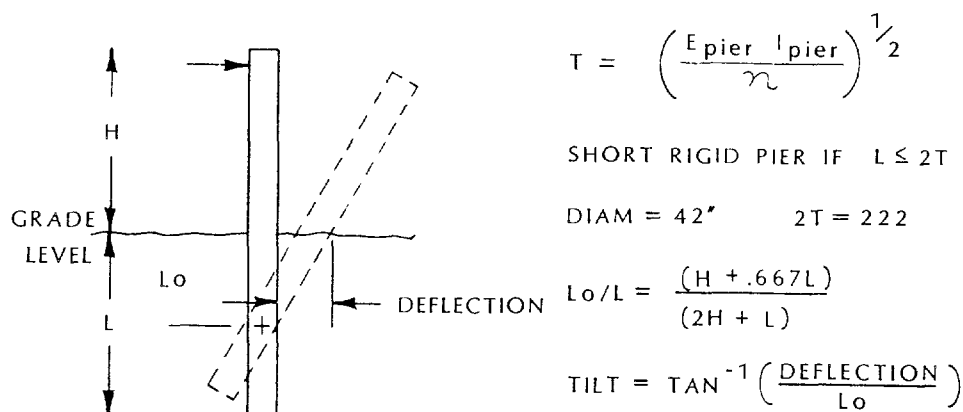
Figure 5.4   Model of Short Rigid Pier in Cohesionless Soil.

44

Table 5.6
Slope Error Resulting From Pier Tilt
(mrad)

Pier Diameter	36 inch	42 inch
Pier Depth		
12 ft	0.63	0.51
15 ft	0.70	0.40
20 ft	0.37	0.37

5.2.3 Stress in Pier

Once pier geometries were determined that would have acceptable performance, the stress in the pier itself was checked. Both the steel and concrete are considered. The model requires an equivalent rectangular pier to be calculated as the first step. Using this equivalent pier and selecting properties of the concrete to be used result in a maximum bending stress the pier can withstand. The analysis assumes a balanced reinforcement, which means compression and tensile failure occur at the same load. This load is compared to the required load capacity to confirm the selected pier geometry. The maximum required bending moment at ground level is 116,600 ft.-lbs. Table 5.7 shows the capacity of several piers. The high ratio of pier capacity to design load indicates the deflection driven nature of this design.

Table 5.7
Bending Stress in Pier

Maximum bending moment in pier at which steel in concrete will yield.

Reinforcing; 24 inch diameter tube, 36 ksi steel.

	($\text{ft-lb} \times 10^6$)	
Pier Diameter	36 inch	42 inch
Steel thickness		
.25 inches	2.2	3.3
.69 inches	2.6	3.8
Design load; $0.1 \text{ ft-lb} \times 10^6$		

45

6.0 TRACKING CONTROLS

6.1 Introduction

The purpose of this analysis was to define a control system suitable for operation of a small (25-100) field of heliostats. The major objective was to reduce communication demands in that control system. The scope of this investigation was limited to development of an azimuth and elevation tracking algorithm for a standard industrial programmable logic controller (PLC). The tracking algorithm, combined with the algorithm for a third control axis (membrane extension) developed for the Mark II stretched-membrane heliostat, was multiplexed to provide simultaneous operation of four heliostats from a single controller to limit costs.

This analysis is presented in four parts:

> 6.2. Solar Azimuth and Elevation,
> 6.3. Ideal Heliostat Azimuth and Elevation,
> 6.4. Actual Heliostat Azimuth and Elevation, and
> 6.5. Local Heliostat Controller.

A schematic program for the tracking algorithm is also provided in an appendix.

The control and communication system used at Solar One used dedicated cabling to periodically transmit the solar azimuth and elevation to all heliostat controllers every few seconds. The status of each heliostat is subsequently transmitted back to the central level. Serially encoded communication is accomplished over dedicated cables. The system has had several problems and is expensive. Alternatives to the dedicated cable communication network for large fields have been explored by other (13).

The small field size associated with this investigation led to a different emphasis. Specifically, the information to be communicated was reviewed to reduce control demands. Rather than transmit solar elevation and azimuth every few seconds, the potential for transmitting the coefficients of a polynomial that approximate solar position was considered. This approach reduced the amount of tracking information to be communicated daily from approximately 28 kilobytes (8 bit words) to about 55 bytes. The reduction by orders of magnitude in information virtually eliminates any problems with communication rate.

This investigation was limited to control strategies that allowed information to be broadcasted. The control algorithm developed in this report does not require thatany heliostat controller be individually addressed. The solar azimuth and elevation can be broadcasted; all controllers require the same information. In a small field, it is unlikely that operation modes for a single heliostat need to be changed automatically. Consequently, the operating mode can be broadcasted as well. The combination of

broadcasted information (no heliostat addresses) and the small amount of information to be transferred reduces communication protocol requirements.

Relatively little control engineering cost can be justified for small production volumes and field sizes. Consequently, only standard, available industrial programmable logic controllers were considered in this analysis. A single controller, specifically the Siemens 100U PLC, was considered for the local heliostat controller in this analysis to focus the investigation on the tracking algorithm rather than on a market review of available controllers. Alarm, mode, and membrane extension algorithms for the Siemens controller were developed for the Mark II stretched-membrane heliostat. This controller had the advantages of low cost, a slightly higher level programming language than competitive controllers, and the ability to communicate through the programming port or via discrete modules.

The first step in the investigation was to consider the accuracy of a polynomial approximation for solar azimuth and elevation over a day. Ultimately, the day was partitioned into five parts, with a separate, third-order polynomial used to represent azimuth or elevation in each partition. This time partition, combined with the daily symmetry about solar noon, yielded an expression with a standard tracking error of less than one milliradian on the summer solstice and smaller errors on shorter days. Polynomial approximations were considered to be a reasonable approach to reduce the communicated information by three orders of magnitude.

The second step in the analysis considered the transfer function between solar and ideal heliostat azimuth and elevation. The ideal heliostat position is peculiar to field location; consequently, the local controller must calculate this information. The Siemens controller does not provide trigonometric relationships. Polynomial approximations were rejected because of the memory requirements imposed on the local controller to store several hundred coefficients. Trigonometric approximations were built with series approximations that required only simple arithmetic operations. Two series approximations were considered. The MacLaurin series was ultimately selected.

The third step in the investigation tested a polynomial transfer function between the ideal and actual heliostat position. This difference is associated with incidental errors such as drive axis tilt (e.g., during installation or from foundation shift), and inherent drive nonlinearities such as those associated with a jack screw elevation drive. A fourth-order polynomial, with two partitions based on position, provided a transfer function with 0.3 mrad of tracking error.

Finally, a schematic program for the Siemens controller was developed. This schematic allowed the processing time and memory requirements to be accurately estimated. The program was configured to allow membrane extension calculations and updates to be done several times during the azimuth and elevation calculations. Special hardware requirements in the local controller were defined consistent with the tracking and membrane algorithms.

The investigation reported on here resulted in an algorithm sufficiently developed to ensure that four heliostat azimuth, elevation, and membrane extension axes could be controlled by a single Siemens 100U PLC. Communication demands were reduced by orders of magnitude. This report provides the basis for a low-risk development of a control system design suitable for small heliostat fields.

6.2 Solar Azimuth and Elevation

The solar azimuth and elevation must be calculated to define the gimbal axis positions for any heliostat. This ephemeris calculation was performed by the field controller at Solar One, and the results were communicated on approximately five-second intervals to each heliostat controller. The viability of two alternate approaches is considered in this report: ephemeris calculation at the local controller to eliminate communication, and a polynomial approximation of the solar azimuth and elevation to reduce communication requirements.

The modified ephemeris calculation proposed by Robert Walraven was used to define solar azimuth and elevation (14). The estimated time to perform this ephemeris calculation on the Siemens PLC heliostat controller was approximately 1.6 seconds. Performance at the heliostat controller eliminated the communication requirement, but the processing time was substantial. Calculation updates should be made on five-second intervals to maintain tracking accuracy; over 30% of the allowable processing time would be used in making this single calculation. The remaining time was insufficient for membrane and drive position calculations.

A polynomial approximation of solar azimuth and elevation executed at the heliostat controller was also considered. The polynomial was of the following form:

$$\text{Azimuth} = \sum_{i=0}^{k} A_i * t^i \quad \text{and} \quad \text{Elevation} = \sum_{i=0}^{k} E_i * t^i$$

$$\begin{aligned}
\text{where} \quad k &= \text{the order of the curve fit,} \\
A,E &= \text{constants, and} \\
t &= \text{time.}
\end{aligned}$$

Communication between the field and local controllers is required for the polynomial, but it is limited to the coefficient of the curve fit. The processing time for a polynomial was potentially less than the modified ephemeris calculation. Consequently, the investigation centered upon the relation between the accuracy, order, and number of time segments required per day.

The scope of the investigation was limited to the following:

1. A single latitude (32° N) and longitude (97° W) were used.
2. Refraction at small elevation angles was considered, but temperature and pressure, which affect the index, were not varied.

3. The accuracy was established for four days only of a single year (summer solstice, winter solstice, and the two equinoxes in 1990).

The day was divided into a number of segment, and a multiple linear regression analysis was performed for each segment. The order of the curve fit was varied to maintain the error or the polynomial approximation below one milliradian. The results of the investigation are summarized in Tables 6.1 through 6.6.

Table 6.1
Sun position, Azimuth, March 21st
Standard Estimate of Error, MRAD

Time	2nd order	3rd order	4th order	5th order
7:15 a.m. - 5:56 p.m.	----	----	----	12.9434
7:15 a.m. - 12:36 p.m.	----	----	1.9595	0.7008
12:36 p.m. - 5:56 p.m.	----	----	1.9032	0.9226
7:15 a.m - 12:02 p.m.	----	0.7862	0.6763	----
12:02 p.m. - 1:08 p.m.	----	0.7915	0.2891	----
1:08 p.m. - 5:56 p.m.	----	0.2888	0.6959	----
7:15 a.m. - 11:45 a.m.	----	0.7950	----	----
11:45 a.m. - 1:25 p.m.	----	0.2917	----	----
1:25 p.m. - 5:56 p.m.	----	0.7884	----	----
7:15 a.m. - 9:28 a.m.	0.8208	----	----	----
9:28 a.m. - 11:20 a.m.	0.9530	----	----	----
11:20 a.m. - 12:36 p.m.	0.7596	----	----	----
12:36 p.m. - 1:50 p.m.	0.6988	----	----	----
1:50 p.m. - 3:41 p.m.	0.9110	----	----	----
3:41 p.m. - 5:56 p.m.	0.8613	----	----	----

Table 6.2
Sun Position, Elevation, March 21st
Standard Estimate of Error, MRAD

Time	2nd order	3rd order	4th order	5th order
7:15 a.m. - 5:56 p.m.	----	----	----	7.2736
7:15 a.m. - 12:36 p.m.	----	1.9364	0.3371	0.3281
12:36 p.m. - 5:56 p.m.	----	1.9185	0.3369	0.3273
7:15 a.m. - 12:02 p.m.	----	1.2425	----	----
12:02 p.m. - 1:08 p.m.	----	0.3077	----	----
1:08 p.m. - 5:56 p.m.	----	1.2596	----	----
7:15 a.m. - 11:45 a.m.	----	0.9370	----	----
11:45 a.m. - 1:25 p.m.	----	0.3171	----	----
1:25 p.m. - 5:56 p.m.	----	0.9468	----	----
7:15 a.m. - 9:28 a.m.	0.4125	----	----	----
9:28 a.m. - 11:20 a.m.	0.6494	----	----	----
11:20 a.m. - 12:36 p.m.	0.3583	----	----	----
12:36 p.m. - 1:50 p.m.	0.3483	----	----	----
1:50 p.m. - 3:41 p.m.	0.6440	----	----	----
3:41 p.m. - 5:56 p.m.	0.4230	----	----	----

Table 6.3
Sun Position, Azimuth, Dec. 21st
Standard Estimate of Error, MRAD

Time	2nd order	3rd order	4th order	5th order
8:16 a.m. - 4:37 p.m.	----	----	4.1862	0.6426
8:16 a.m. - 12:28 p.m.	1.3191	0.9178	0.3039	----
12:28 p.m. - 4:37 p.m.	1.2638	0.9089	0.3050	----
8:16 a.m. - 12:02 p.m.	0.6171	----	----	----
12:02 p.m. - 12:53 p.m.	0.2938	----	----	----
12:53 a.m. - 4:37 p.m.	0.5935	----	----	----
8:16 a.m. - 11:00 a.m.	0.4588	----	----	----
11:00 a.m. - 12:28 p.m.	0.3922	----	----	----
12:28 p.m. - 12:55 p.m.	0.3906	----	----	----
12:55 p.m. - 4:37 p.m.	0.4749	----	----	----

51

Table 6.4
Sun Position, Elevation, Dec 21st
Standard Estimate of Error, MRAD

Time	2nd order	3rd order	4th order	5th order
8:16 a.m. - 4:37 p.m.	----	6.7877	0.7076	0.7078
8:16 a.m. - 12:28 p.m.	3.0854	0.3076	----	----
12:28 p.m. - 4:37 p.m.	3.0258	0.2994	----	----
8:16 a.m. - 12:02 p.m.	2.3556	----	----	----
12:02 p.m. - 12:53 p.m.	0.3201	----	----	----
12:53 a.m. - 4:37 p.m.	2.2555	----	----	----
8:16 a.m. - 11:00 a.m.	0.9123	----	----	----
11:00 a.m. - 12:28 p.m.	0.3038	----	----	----
12:28 p.m. - 12:55 p.m.	0.3073	----	----	----
12:55 p.m. - 4:37 p.m.	0.8578	----	----	----

Table 6.5
Sun Position, Azimuth, June 21st
Standard Estimate of Error, MRAD

Time	2nd order	3rd order	4th order	5th order
6:11 a.m. - 12:30 p.m.	----	----	23.78	7.7000
6:11 a.m. - 11:12 a.m.	----	----	1.538	0.585
11:12 a.m. - 12:30 p.m.	----	----	----	1.050
6:11 a.m. - 10:48 a.m.	----	1.947	0.655	0.331
10:48 a.m. - 12:18 p.m.	----	----	0.549	----
12:18 p.m. - 12:30 p.m.	----	----	0.2904	----
6:11 a.m.-10:17 a.m.	----	0.779	0.344	----
10:17 a.m. - 11:45 a.m.	----	0.961	----	----
11:45 a.m. - 12:30 p.m.	----	1.064	----	----
6:11 a.m. - 8:36 a.m.	0.547	----	----	----
8:36 a.m. - 10:17 a.m.	0.727	----	----	----
10:17 a.m. - 11:12 a.m.	0.758	----	----	----
11:12 a.m. - 11:45 a.m.	0.657	----	----	----
11:45 a.m. - 12:10 p.m.	0.470	----	----	----
12:10 p.m. - 12:30 p.m.	0.647	----	----	----

Table 6.6
Sun Position, Elevation, June 21st
Standard Estimate of Error, MRAD

Time	2nd order	3rd order	4th order	5th order
6:11 a.m. - 12:30 p.m.	----	----	----	----
6:11 a.m. - 11:12 a.m.	----	----	----	0.2922
11:12 a.m. - 12:30 p.m.	----	----	----	0.2711
6:11 a.m. - 10:48 a.m.	----	----	0.2970	----
10:48 a.m. - 12:30 p.m.	----	----	0.3295	----
6:11 a.m. - 10:17 a.m.	----	0.2912	----	----
10:17 a.m. - 11:45 a.m.	----	0.3068	----	----
11:45 a.m. - 12:30 p.m.	----	0.2856	----	----
6:11 a.m. - 8:36 a.m.	0.3387	----	----	----
8:36 a.m. - 10:17 a.m.	0.2970	----	----	----
10:17 a.m. - 11:12 a.m.	0.2971	----	----	----
11:12 a.m. - 11:45 a.m.	0.2980	----	----	----
11:45 a.m. - 12:10 p.m.	0.3009	----	----	----
12:10 p.m. - 12:30 p.m.	0.2875	----	----	----

This investigation clearly demonstrated that relatively few time segments are required per day, even for low-order approximations. For example, three third-order polynomials are required for each axis on the summer solstice. The information transferred would be limited to four 16-bit coefficients and one 8-bit variable (to describe the time for shifting from one expression to the next) per polynomial, along with one 8-bit variable to define sunrise, for a total of (55) 8-bit words to describe solar azimuth and elevation for a full day. This polynomial communication requirement compares to (9096) 8-bit words if the solar position were transmitted at five-second intervals.

A third-order polynomial was selected to approximate solar azimuth and elevation in order to minimize the number of communicated words. A schematic program for the Siemens PLC was developed (see Appendix A); the execution time for the polynomial was 0.08 seconds compared to the 1.6-second requirement for an ephemeris calculation.

The use of a polynomial approximation for solar azimuth and elevation at the local heliostat controller does not eliminate the ephemeris calculation, but shifts the demand to the field level. The ephemeris data must then be regressed upon to define the polynomial coefficients. Finally, an optimization procedure must also be performed to establish the time segments for each day. These calculations would be difficult to implement, even on the more powerful field PLC. The calculations can be performed on a personal computer, however, and the results loaded into a nonvolatile bubble memory module for the field controller. A 32-kilobyte module would provide adequate memory

for more than a year of operation in addition to program backup storage. This approach would relieve both the field and local controllers from ephemeris calculations.

The polynomial approximation was selected for calculation of the solar azimuth and elevation. This process required only 55 words to be communicated to the field on a daily basis. Transmission of a single day or several days of sun position information could be in a few minutes. The processing time for the actual solar azimuth and elevation is short and can be accomplished during each update cycle.

6.3 Ideal Heliostat Azimuth and Elevation

The heliostat azimuth and elevation is distinct from the solar position and must be calculated based on the position of the heliostat with respect to the fixed receiver. Two approaches were considered to calculate the ideal heliostat azimuth and elevation: an approximate polynomial transfer function was defined, and trigonometric functions were built to allow for an exact transfer function.

A polynomial was initially evaluated as an approximate transfer function. The polynomial was of the following form:

$$H_a = C_0 + C_1 a + C_2 e + C_3 a^2 + C_4 ae$$

$$+ C_5 e^2 + C_6 a^3 + C_7 a^2 e + C_8 ae^2 + C_9 e^3$$

$$H_e = K_0 + K_1 a + K_2 e + K_3 a^2 + K_4 ae$$

$$+ K_5 e^2 + K_6 a^3 + K_7 a^2 e + K_8 ae^2 + K_9 e^3$$

where
H_a = heliostat azimuth,
H_e = heliostat elevation,
a = sun azimuth,
e = sun elevation, and
C, K = constants stored in each heliostat controller.

The objective was to describe a unique polynomial for each heliostat based upon field position. This polynomial would be used for several days to modify the solar position to the heliostat azimuth and elevation. Constants would be stored at the local heliostat controller. Communication of the coefficients between the field and heliostat controller was not considered, as this communication would require that heliostats be addressed individually.

The coefficients of the polynomial were defined with regression upon a single "nominal" day (summer solstice and equinox). The same expression was subsequently applied before and after the nominal day to determine the length of time that a single set of coefficients would be accurate. The results are shown in Table 6.7.

54

Table 6.7
Accuracy of the Cubic Position Polynomial
As a Function of Time

Nominal Day	Std. error of approximation, milliradians Days from Nominal Day						
	0	1	2	3	5	10	23
Summer Solstice	0.67	0.65	0.65	0.66	0.84	2.10	1.65
Equinox	0.53	2.06	4.10	8.55	10	20	45

The cubic polynomial approximation used as a transfer function between solar and heliostat azimuth and elevation is, at best, acceptable for four or five days at the solstice, but acceptable for a single day only at the equinox. Approximately 200 polynomials are required for an entire year. More than 30 kilobytes of storage would be required at the heliostat controller for the coefficients for four heliostats. The memory requirements for coefficient storage exceed the capability of the PCL. Consequently, the polynomial approach was abandoned.

An exact transfer function between the solar and ideal heliostat azimuth and elevation requires trigonometric functions. Specifically, two primary functions, sine and cosine, and two reversion functions, arcsine and arccosine, are required. These functions are not available for the heliostat controller, but can be built with arithmetic operations.

Two approximations for sine and cosine were evaluated. A modified series representation of sine and cosine of the form follows:

$$\sin x = x \left(1 - \frac{x^2}{pi^2}\right) \left(1 - \frac{x^2}{2^2 pi^2}\right) \left(1 - \frac{x^2}{3^2 pi^2}\right)....$$

$$\cos x = \left(1 - \frac{4x^2}{pi^2}\right) \left(1 - \frac{4x^2}{3^2 pi^2}\right) \left(1 - \frac{4x^2}{5^2 pi^2}\right)..$$

The advantage of this representation was a single exponentiation (exponentiation is achieved in the Siemens PLC with a set of explicit instructions for multiplication and register shifts), and a single subtraction step that is particularly convenient in binary logic. The execution of arithmetic functions is substantially faster in binary rather than floating point operations.

The ephemeris calculations were performed with this modified series approximation, and the number of series terms was varied to determine the error in the ideal heliostat azimuth and elevation. The results are shown in Table 6.8.

Table 6.8
Accuracy of Sine and Cosine Approximations
using a Modified Series

Ideal Heliostat Axis	Standard error estimate, mrad Number of terms in series				
	25	50	100	200	400
Azimuth	6.334	3.194	1.603	0.803	0.402
Elevation	1.690	0.851	0.427	0.214	0.107

The number of terms required to accurately approximate sine and cosine is substantial; several hundred terms would be required to accurately predict the ideal heliostat azimuth and elevation using this modified series. Table 6.8 indicates a trend; as the number of terms doubles, the error is halved. Using this trend, approximately 6,400 terms would be required to reduce the error in the transfer function to less than 0.02 mrad, a value that can be easily achieved with the second series approximation considered.

The second approximation considered for sine and cosine by a special Taylor's series expansion used the infinite MacLaurin series for all real values of x.

$$\sin x = \sum_{n=0}^{\inf} (-1^n) \frac{x^{(2n+1)}}{(2n+1)!} \qquad \cos x = \sum_{n=0}^{\inf} (-1^n) \frac{x^{(2n)}}{(2n)!}$$

Implementation of the MacLaurin series on a Siemens programmable controller was considered in floating point and binary representations.

The number of terms required for a reasonable approximation of sine and cosine was defined in a similar fashion. The approximations was used to define the ideal heliostat azimuth and elevation based upon the solar position. Positions were calculated on five-second intervals on the summer solstice with the MacLaurin series and compared to a standard double precision compiler approximation. The results are shown in Table 6.9.

Table 6.9
Accuracy of Sine and Cosine Approximations
using the MacLaurin Series

Ideal Heliostat Axis	Standard error estimate, mrad Number of terms in series		
	3	4	5
Azimuth	4.148	0.277	0.012
Elevation	6.946	0.454	0.018

The MacLaurin series converges much faster than the modified series. A five-term MacLaurin series was evaluated in both binary and floating point logic. The com-

parison indicated that sine and cosine could be calculated in optimized 16-bit binary logic in approximately 25 milliseconds versus 33 milliseconds in floating point notation, though the binary logic was considerably more complex. The number of times that a sine or cosine function block must be invoked is relatively small: four calls in the calculation of solar azimuth and elevation, and twenty calls (five per heliostat) for the calculation of heliostat azimuth and elevation. The resultant time savings, 192 milliseconds, did not justify the effort to construct a binary program. A floating point execution of the MacLaurin series, with five terms, was selected. The function block is explicitly defined in Appendix A.

The series expansion for the inverse functions is quite similar to the MacLaurin series in form.

$$\sin^{-1} x = x + \frac{x^3}{2*3} + \frac{1*3}{2*4*5} x^5 + \frac{1*3*5}{2*4*6*7} x^7 + ... \text{ for } -\frac{pi}{2} < \sin^{-1} x < +\frac{pi}{2}$$

$$\cos^{-1} x = \frac{pi}{2} - \sin^{-1} x$$

A similar procedure was used to describe the relationship between the number of terms and accuracy of the approximation. The results of the analysis are shown in Table 6.10. The absence of negative terms resulted in a slower convergence than was achieved in the MacLaurin series for sine and cosine. Nine terms were selected for the approximation. Fortunately, only the arc sine needs to be calculated with the expansion. The arc cosine is obtained with a simple difference.

Table 6.10
Accuracy of Arc Sine and Arc Cosine Approximations

Ideal Heliostat Axis	Standard error estimate, mrad Number of terms in series				
	4	6	8	9	10
Azimuth	0.679	0.168	0.047	0.026	0.014
Elevation	1.072	0.223	0.052	0.026	0.013

Given the primary and inverse trigonometric functions, an exact transfer function between solar and ideal heliostat azimuth and elevation was constructed using a unit cosine approach. The only additional required information was the heliostat position with respect to the tower; a set of three constants. The exact procedure is described schematically for the Siemens PLC heliostat controller in Appendix A.

6.4 Actual Heliostat Azimuth and Elevation

The actual information required to position a heliostat in an elevation and azimuth coordinate frame varies from the ideal position to accommodate the specific drive. These accommodations include incidental variations such as structural sag in the mirror module, tilt in the drive axis, and error in absolute reference position, as well as inherent nonlinearities such as those associated with jack screw drives or cumulative error in gear ratio approximations. A polynomial was selected as a transfer function between the ideal and actual position because this generalized approach was independent of the source of error.

The scope of the investigation was limited to the following:

1. A single receiver position (32° N latitude, 97° W longitude) was used.
2. Refraction at small elevation angles was considered, but temperature and pressure, which affect the index, were not varied.
3. The accuracy was tested on a single day; the summer solstice.
4. Drive tilt was used for incidental error.
   a. An arbitrary tilt error of -10 mrad about an east/west horizontal was assumed in the azimuth drive. The azimuth axis was referenced to ground.
   b. An arbitrary tilt error of +10 mrad about a southern horizontal was assumed in the elevation drive. The elevation axis was referenced to the azimuth drive.
5. A jack screw elevation drive was used to provide inherent drive nonlinearities.

The polynomial was of the following form:

$$\text{Azcorrect} = \text{azh} + \sum_{i=0}^{k} C_i * \text{azh}^i \quad \text{and} \quad \text{Elcorrect} = \text{ezh} + \sum_{i=0}^{k} D_i * \text{ezh}^i$$

where k = order of the curve fit,
       C, D = constants,
       azh = ideal azimuth of theR
       ezh = ideal elevation of the heliostat,
       Azcorrect = actual azimuth, and
       Elcorrect = actual elevation.

Communication between the field and local controllers is not required to execute the polynomial; constants are stored at the local heliostat controller. Drive nonlinearities and axial tilt were assumed to be independent; the standard error estimates were added in RMS fashion.

The difference between the ideal and actual heliostat azimuth and elevation (tracking error) associated with the drive tilts specified above are shown in Figure 6.1. Polynomials of second, third, and fourth order were developed as transfer functions between the ideal and actual positions. The tracking error that resulted in each axis after the polynomial correction is shown in Figures 6.2 and 6.3. A fourth-order fit was selected because the tracking error was less than 0.33 mrad of error in each axis.
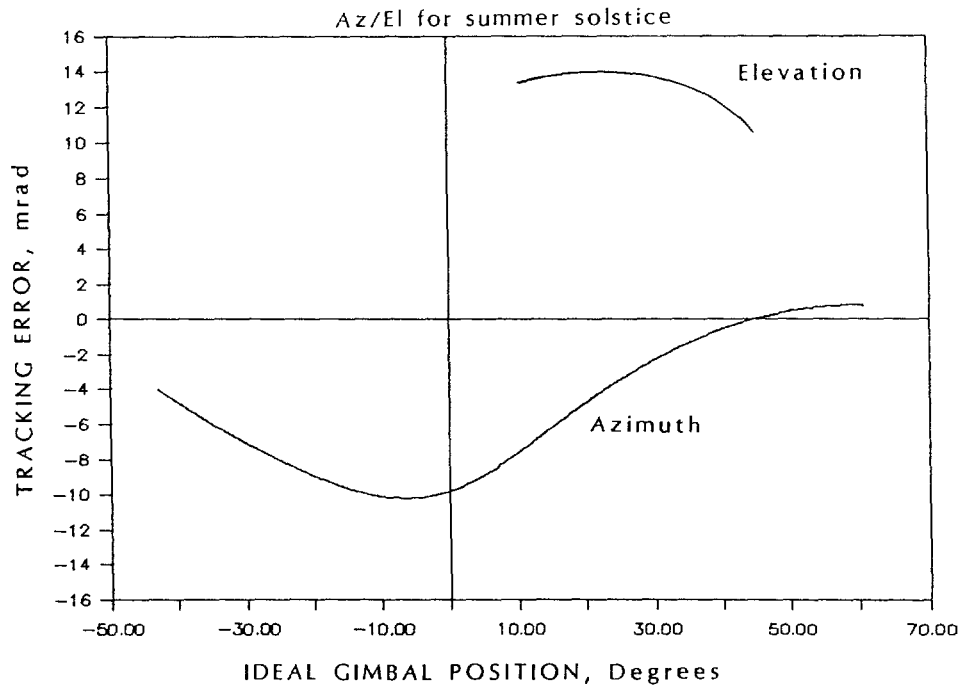
Figure 6.1 Drive Tilt Error, Azimuth, and Elevation.

A sharp increase in elevation error occurred at the extreme range of travel, although the actual magnitude remained acceptable. Investigation of several tower heights and field positions were beyond the scope of this work. A brief analysis was conducted by dividing the elevation range into two segments. The extreme and standard errors for a fourth-order polynomial were substantially reduced; the maximum elevation error for a single segment was 0.4 mrad compared to 0.2 mrad for a two-segment fit; the standard error for a single segment was 0.11 mrad compared to 0.07 mrad for a two-segment fit. This reduction indicated that a minor modification in program implementation for the polynomial correction could be made if an extreme travel is required in the elevation axis at some combination of field position and time of year. No further attempt was made to correct the problem, since the absolute magnitude of the tracking error was small.

Azimuth, summer solstice
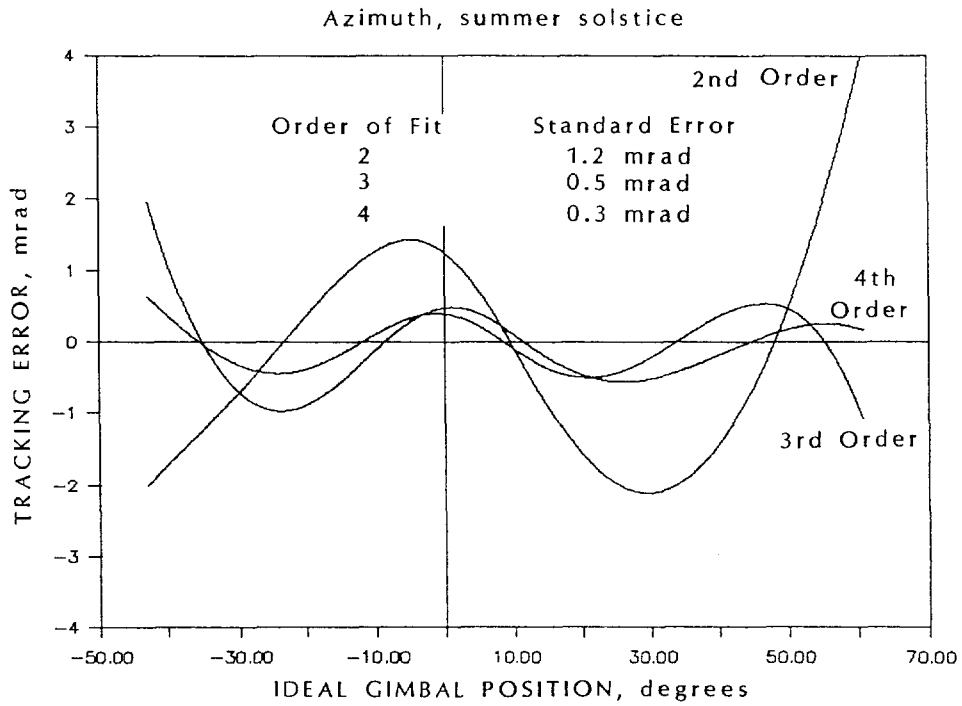
Figure 6.2 Corrected Drive Tilt Error, Azimuth.

Elevation, summer solstice
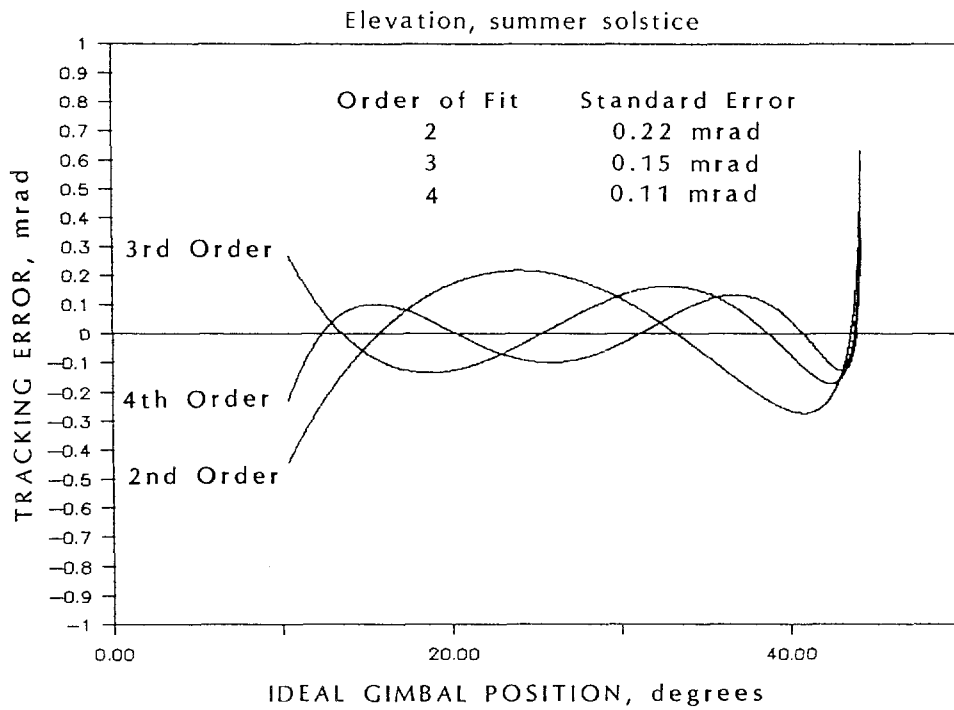
Figure 6.3 Corrected Drive Tilt Error, Elevation.

60

The screw jack drive train is inherently nonlinear. The error associated with a linear relationship between the ideal heliostat elevation and jack extension is shown in Figure 6.4. This nonlinearity can be exactly compensated for with a trigonometric relationship or approximated with a "look up table." An exact transfer function was not considered because of the substantial processing time required; processing time was at a premium with four heliostats per controller. The tabular correction required substantial memory for nonlinear relationships; memory was also at a premium in the heliostat controller. The coefficients' error polynomial were modified to accommodate drive-train nonlinearity, as well as miscellaneous effects such as axial tilt.

k2 = 48, k3 = 72
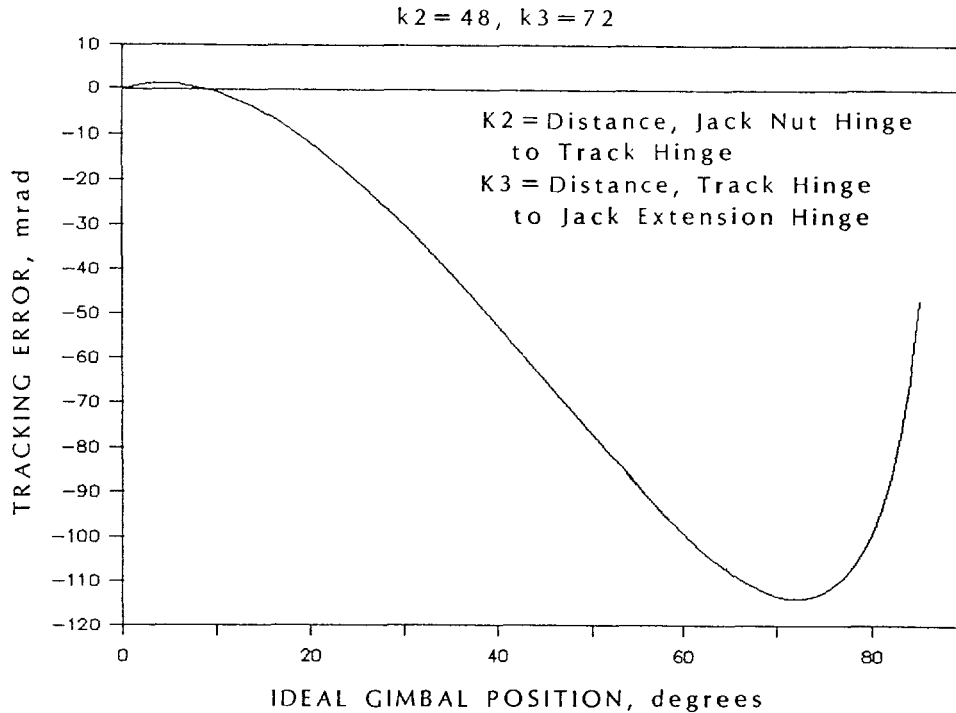
Figure 6.4 Screw Drive Nonlinearity, Uncorrected.

The compensation for screw nonlinearity with a polynomial fit is illustrated in Figure 6.5. The standard error, even for a fourth-order fit, was too high: 3.5 mrad. This error was substantially reduced; however, by dividing the elevation axis into two segments, one polynomial was developed from 0 to 72 degrees from the zenith, and the second addressed the extreme of travel near the horizon. This approach reduced the error, yet added little to the complexity of the algorithm.

The error associated with the jack screw is independent of any drive axis tilt. Consequently, the total standard error is estimated to be:

standard elev error^2	=	$(0.32)^2 + (0.28)^2$,
standard elev error	=	0.42 mrad,
standard azim error	=	0.22 mrad, and
total standard error estimate	=	0.5 mrad

for a fourth-order curve fit in two segments for elevation and a second-order fit of azimuth.

The polynomial approach for correction of incidental and inherent differences between the ideal and actual heliostat azimuth and elevation was similar to the calculation of solar azimuth and elevation. The polynomial was selected based upon position rather than time, but the execution of both conditional and arithmetic operations was virtually identical. The schematic program representation of the actual heliostat position is also included in Appendix A.

$$k2 = 48, \quad k3 = 72$$
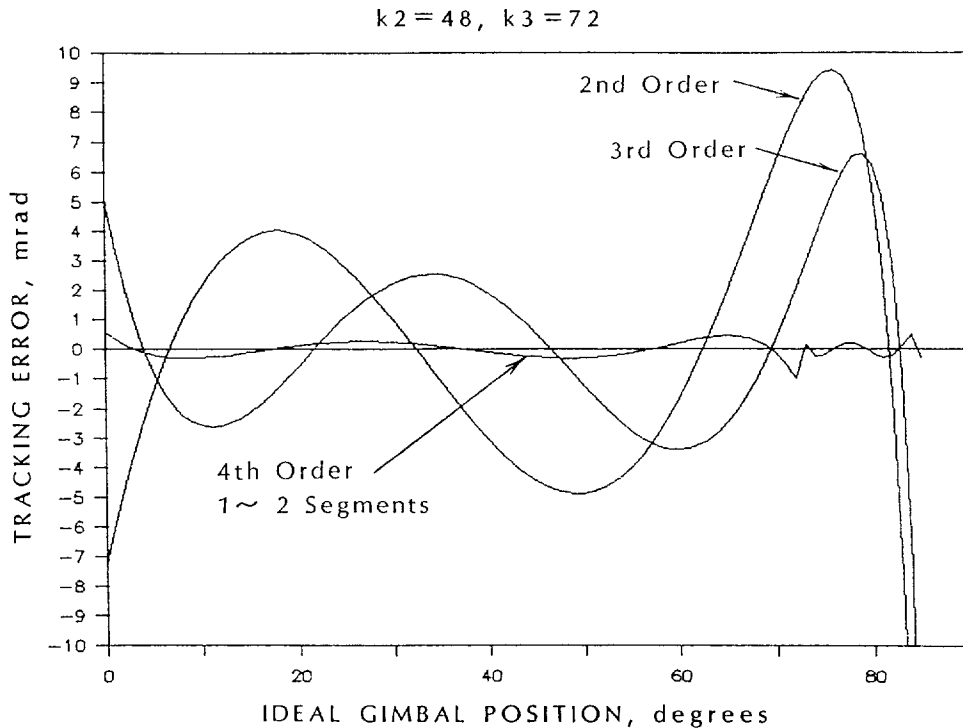
Figure 6.5 Screw Drive Nonlinearity, Corrected.

6.5 Local Heliostat Controller

The development reported in the previous sections, along with the schematic program of Appendix A, defines the procedure for position calculations of two axes per heliostat. This controller must also provide position information for a third axis, membrane extension, based upon a closed-loop PID algorithm. The PID algorithm requires frequent inputs and outputs to remain stable; the calculation of heliostat azimuth and elevation requires a significant processing time by comparison. The cost of the local controllers can also be reduced by supporting several heliostats with a single processor. The support of three axes and several heliostats requires a multiplex program format.

The local controller hardware requirements are developed in this section. These requirements include the processor and modules. Some information in the requirements for the field controller and miscellaneous local and field devices is also provided.

6.5.1 Multiplex Procedure

The primary function of the local PLC is to control three independent position axes: heliostat azimuth, heliostat elevation, and membrane extension. Secondary functions included operation mode and alarm checks. Both the azimuth and elevation axes require that position information be calculated within a five- or six-second interval, with two independent transducers (Hall effect transistors in quadrature on the motor shaft) being monitored at 500 to 750 Hz. The calculation interval for azimuth and elevation is based on a 1-mr deadband. Transducer monitoring is based on a scan rate five times faster than signals from a quarter-turn (90 phase) separation of transistors on a motor shaft turning at 1750 rpm.

The membrane extension axis requires that calculations, transducer (LVDT) monitoring, and analog outputs be modified on a quarter-second interval for loop stability. The calculation, monitoring, and update interval for the membrane extension axis is based on the program developed for the SKI Mark II stretched-membrane heliostat under a previous contract.

Program execution on the PLC selected for the local heliostat controller is slow compared to the monitor rate required for the azimuth and elevation axes. A counting module, with the high-frequency scan rates and buffered output, was selected to monitor the Hall effect transistors. The proportional, integral, and derivative (PID) feedback loop used for membrane extension operates on a 250-ms interval, however. This frequency is well within an acceptable range for program operation, and a separate module is not needed for membrane control.

The scope of this investigation required that a single local controller be used to service four heliostats from the onset. The alarm and PID program blocks for four heliostats can be completed in 120 ms. Consequently, 130 ms per program loop is available for azimuth and elevation axis calculations.

Processing times were established for each step in the calculation of heliostat azimuth and elevation based upon the program schematic presented in Appendix A. These steps were subsequently arranged in blocks that could be executed in less than 130 ms. The blocks are shown in Table 6.11.

The processing time of calculations for three independent axes on each of four heliostats by a single controller is within the limit established by the tracking deadband and membrane stability.

6.5.2 Controller Hardware Requirements

The smallest controller considered for local heliostat control was a Siemen S5-100U Programmable Controller. A CPU 103 processor is required to implement the floating point arithmetic operations used to build the trigonometric functions. This controller must also be supplied with a 110-V AC/24 VDC power supply module. A

Table 6.11
Azimuth/Elevation Calculation Blocks

Block Name	Execution Time Milliseconds	Blocks per Calculation	Total Execution Time, Milliseconds
Equiv Time	3		
Solar Coeff	11		
Time Exp	11		
Solar AZ	29		
Solar EL	29		
Sol AZ Exp 1	24		
	107	1	107
Sol Az Exp 2	24		
Sol El Exp 1	24		
Sol El Exp 2	24		
Sin Sol Az	33		
	105	1	105
Sin Sol El	33		
Cos Sol Al	33		
Cos Sol El	33		
	99	1	99.0
Hel Az/El 1	60		
Elarc Exp	51		
	111	4	444
Elvct Arc 1	37		
Elvct Arc 2	37		
	74	4	296
Hel El Exp 1	24		
Hl El Exp 2	24		
Sin Hel El	33		
Hel Az/El 2	4		
	85	4	340
Azarc Exp	51		
Azvct Arc 1	37		
	88	4	352
Azvct Arc 2	37		
Hel Az Arc 2	16		
El Coeff	6		
Hel Az Crct	28		
Hel El Crct	28		
	115	4	460
Subtotal			2203
PD and ALARM CKS	130	23	2990
			5193/calc

variety of bus units must also be provided to connect the input/output modules to the controller.

Each elevation and azimuth axis requires a Siemens style 385B counter module; eight modules are required per local controller. This module is capable of counting both up and down, based on a quadrature input from the Hall effect transistors. The module can monitor at high frequency and provide a buffered output of position on demand without any program requirements on the central processor itself.

The membrane extension axis requires both analog input and output. The LVDT signal must be resolved into a 0 to 10-V or 4- to 20-ma signal by an external device. Because the standard Siemens analog input module has four channels, a single module is adequate for four heliostats. The analog output can also be voltage or current based. The standard Siemens analog output module provides two channels; two modules are required for each local controller.

The major focus of this study was the development of logic capable of calculating the heliostat azimuth and elevation. The logic corrects for incidental and inherent variations in the drive or mirror module so that tracking accuracy could be maintained. A variety of digital inputs and outputs are required at the local controller to monitor switches or even to provide a simple mode communication approach. The number and size of these modules was not identified within the scope of the current study. The number and cost of these modules should be small by comparison to the counter, analog, and processor modules.

The memory requirements for each program or function block in the azimuth and elevation calculation were also defined based on the schematic development presented in Appendix A. The memory requirements for miscellaneous functions, alarm and mode status, and the PID loop were determined by counting the steps and identifying all flag and data words used in the Mark II program developed by SKI. The miscellaneous, alarm, and PID memory requirements were quadrupled as a conservative estimate of the total memory required for four heliostats. The memory requirements (8-bit words) are shown in Table 6.12.

Table 6.12
Local Controller Memory Requirements

Standard function blocks	960 words program	0 words data
Azim/elev calculation	360 words program	250 words data
Miscellaneous functions	260 words program	20 words data
Alarm and mode monitors	440 words program	60 words data
PID controller	1340 words program	140 words data
	3360 words program	470 words data

These memory requirements are easily within the range of a CPU103. An 8k memory submodule is recommended to provide ample room for program expansion.

The heliostat azimuth and elevation position axes require a fast counter (500 Hz) to monitor mirror position, but a long interval between position updates (5 sec) is allowed with a 1-mr tracking deadband. The membrane extension axis, on the other hand, has moderate monitoring and update demands (250 ms). The calculation of the actual heliostat azimuth and elevation, including effects such as drive nonlinearities or drive axis tilt, requires a significant processing time (3 sec). Consequently, the azimuth and elevation calculations were divided into logical blocks to allow periodic membrane extension updates. The processing time demands on Siemens 100U controller were significant, but four heliostats can be operated by a single controller.

The major input and output modules required for a local controller were identified. The processor was selected to allow floating point arithmetic operations. Local memory requirements were established based on schematic program development for the azimuth and elevation calculations, and programs were developed for control of the Mark II stretched-membrane heliostat. This limited hardware identification also indicated that a single controller could be used to operate four heliostats.

7.0 INTRODUCTION TO DESIGN DRAWINGS

A drawing package has been developed that describes the entire mirror, module, rear support structure, support pylon, focus control system, and tracking control system. The changes to the prototype design discussed in Section 3.0 are reflected therein. The drawings are listed in Table 7.1.

The purpose of the drawings is to minimize any additional engineering or design effort required to initiate fabrication of commercial heliostats. These drawings were used for obtaining most of the quotations and estimates used in the production cost estimates.

The control diagram is drawn as a wiring schematic. Point-to-point and ladder diagrams were not produced. The existing drawing contains all the information required for constructing and troubleshooting the control system.

TABLE 7.1
Drawing Title List

Drwg #	Sheet #	Drawing Title
000	1	Heliostat Assembly Overview
101	1	Mirror Module Assembly
102	1	Heliostat Ring
102	2	Heliostat Ring Details
102	3	Ring/Hinge Connection Details
103	1	Membrane Assembly
103	2	Membrane Reinforcing Ring Details
103	3	Membrane Seal Interface Details
201	1	Rear Support Structure Assembly
202	1	Drive Truss Assembly
202	2	Simple Truss Assembly
202	3	Truss Tip & Secondaries Details
202	4	Tie Rod Details
203	1	Hub Assembly
204	1	Hinge Assembly
204	2	Hinge Details
205	1	Rear Membrane Restraint
206	1	Rear Closure Assembly
206	2	Rear Membrane Sealing Segment Details
301	1	Drive Adapter Assembly
301	2	Drive Adapter Details
301	3	Drive Adapter Details
401	1	Pylon Assembly
401	2	Support Pylon Detail
401	3	Drive Mounting Flange
601	1	Focus Control Assembly
601	2	Fan Mount Weldment
601	3	Fan Mount Details
601	4	Weather Cover Details

8.0 MANUFACTURING COST ESTIMATES

8.1 Introduction to Cost Estimate

The main focus of the manufacturing cost estimates was for low-volume production runs. Near-term requirements for stretched-membrane heliostats are not anticipated to justify the very heavy investment in manufacturing facilities and tooling assumed in the cost estimates for large-volume production reported in several previous studies. This study assumes use of existing central manufacturing facilities. It also assumes use of tooling patterned closely after the prototype tooling used recently by SKI. On-site assembly facilities would still be required for each site. These facilities will be low-cost, temporary structures wherever possible to lower the installed cost.

A detailed cost estimate is presented here for quantities of 25 and of 2000 heliostats per year. This was intended to cover initial stages of development and marketing from engineering prototypes through early market sales. Results are reported in 1990 dollars.

8.2 Approach

The cost estimates are presented in a fairly standard format used for manufacturing estimating. This format separates the direct material and labor costs associated with actual product manufacture from those costs associated with operating the company itself (see Figure 8.1). The indirect costs may differ widely according to the size, type, location, and philosophy of an individual company. This approach should allow users
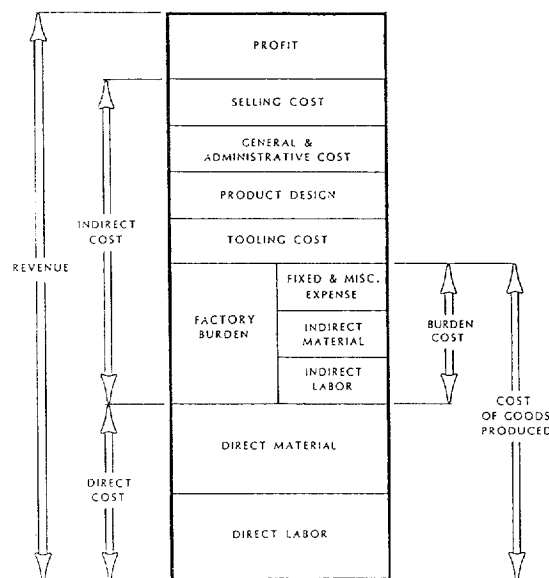
Figure 8.1 Product Cost Structure.

of this report to make valid comparisons of the presented results to the results of other similar reports. It should also permit users to determine the cost of heliostats built under other circumstances than those assumed here. See Appendix 8.A for definition of the terms used in Figure 8.1 and in the following discussion.

The design information used for these estimates is that presented earlier in this report. The cost information in this section is based primarily on actual quotes from manufacturers and suppliers. In some instances, vendors were hesitant to supply firm prices without the confirmation of an actual order. Particularly in the higher quantities, some vendors preferred to give estimates. When a company buys in OEM (original equipment manufacturer) quantities, the price is often a matter of negotiation. Factors such as spot market raw material costs, existing competition, vendor inventory, and likelihood of continuing orders all affect the outcome of such negotiations. For these estimates, a middle of the range value was used when exact pricing was unavailable.

Direct labor estimates are based on moderately detailed process flow sheets developed for the specific component or sub-assembly manufacture. Several are included in the Appendix. Some of the times on the process flow sheets for fabricating were determined from experience assembling the 50-m^2 Mark II prototype. Other times, such as buried cable installation and connection of multi-conductor cable terminations, were determined from published values in commercial estimating guides (15)

Manufacturing overheads and burdens and company overheads were based upon the experience of SKI in its production and prototyping operations for the past 15 years, as well as on common values found in related industries (16).

For 25 heliostats, a more or less prototypical fabrication procedure was assumed. Heavy investment in equipment to carry on simultaneous fabrication operations was not assumed. The cost of obtaining assembly space to carry on all operations simultaneously was not assumed. It was assumed that several large components would be bought from subcontractors where the required capabilities such as machining and welding are widely available. The specialized techniques such as laminating and fabricating 0.010 inches aluminum coil stock would be done by the prime manufacturer.

8.3 Estimates for Direct Costs

Estimates for direct material costs and direct labor hours with cost of benefits included are summarized in Tables 8.1 and 8.2. The details of these estimates are itemized in Appendixes 8.B and 8.C. The material costs, as described earlier, are primarily from vendor quotes and estimates.

TABLE 8.1
Direct costs to manufacture 25 heliostat

INPUT CONSTANTS

Base labor rate	$7.50 / hr
Burden	70%
Material overhead	25%
G & A	15%
Profit/Return on Investment	6%

	labor (hrs)	mat'l ($)	total ($)	total $/m^2	percent (%)
Mirror Module	89	3471	4612	92	20.44
Rear Support Structure	20	3994	4246	85	18.82
Drive and Adapter	8	5427	5529	111	24.51
Pylon	12	1633	1786	36	7.92
Foundation	6	409	486	10	2.15
Focus Control Hardware	1	749	764	15	3.39
Tracking Control Hdwre	40	4025	4536	91	20.11
Field Wiring	19	249	487	10	2.16
Field Installation	9	0	115	2	0.15
Total	203	19957	22560	451	100.00
Material costs			19957	399.13	67.38
Material overhead			4989	99.78	16.85
Labor w/ burden			2603	52.06	8.79
G & A costs on labor			390	7.81	1.32
Profit / Return on investment			1676	33.53	5.66
			29616	592.32	100.00

TABLE 8.2
Direct costs to manufacture 2000 heliostat

INPUT CONSTANTS

Base labor rate	$7.50 / hr
Burden	50%
Material overhead	5%
G & A	15%
Profit/Return on Investment	6%

	labor (hrs)	mat'l ($)	total ($)	total $/m^2	percent (%)
Mirror Module	30	1711	2044	41	17.15
Rear Support Structure	23	1338	1592	32	13.36
Drive and Adapter	2	4239	4263	85	35.77
Pylon	8	918	1006	20	8.44
Foundation	5	399	450	9	3.77
Focus Control Hardware	1	474	487	10	4.09
Tracking Control Hdwre	18	1517	1724	34	14.46
Field Wiring	18	52	252	5	2.12
Field Installation	9	0	101	2	0.85
Total	113	10648	11920	238	100.00

	total ($)	total $/m^2	percent (%)
Material costs	10648	212.96	79.46
Material overhead	532	10.65	3.97
Labor w/ burden	1271	25.43	9.49
G & A costs on labor	191	3.81	1.42
Profit / Return on investment	759	15.17	5.66
	13401	268.02	100.00

It should be noted that the quoted prices for the drives were a major disappointment. In the lowest production volume of 25 units, the drive accounts for 24% of the total cost. For the 2,000 unit production run, this percentage increases to over 35%. Time and resources were not available within this contract for the design of a lower cost drive. SKI feels that development of an in-house drive concept should be possible that would reduce the drive cost 50 to 70%.

It should also be noted that all the costs used for reflective film material is not based on manufacturers's quotations. A completely satisfactory film from a cost and product lifetime perspective may not be currently available. Several manufacturers make standardized silvered reflective films, as well as aluminized films, using both PET and acrylic polymers. Other film manufacturers are capable of making films using them, as well as other potentially higher performance polymers, but offer no standard products. The film cost for the 2,000 heliostat production runs assumes the availability of such a

film. This assumption is based upon the known costs of similar films currently available and on discussions with film manufacturers.

A second exception where costs are not based upon quotation is for the tracking control for the 2,000 unit production run. At the outset of this project, the focus for control design and selection was for 1 to several hundred commercial units. In these quantities, the development of a custom controller could not be cost justified. For the 2,000 unit per year production rate, it is possible that a controller development could be amortized over enough units to offset the cost of the off-the-shelf industrial controller. Such has been assumed for this analysis.

The estimates for direct labor came from several sources. Machining times for in-house work and welding times for in- house work, other than the rear structure trusses, were estimated using specialized commercially available slide rules developed in the fabricating industry for that purpose (17). For the truss assemblies, the fabrication time estimated by a subcontractor in the fabrication business was used. For the wire installation and termination times, a commercial estimating guide was used (15). For the laminating, membrane fabrication, and final assembly, previous experience on production laminating and prototype assembly was used. Other miscellaneous tasks were estimated by observing workers doing similar tasks.

Tables 8.3 and 8.4 summarize the personnel requirements for the manufacturing and assembly operations. These values are used in determining the direct labor costs.

TABLE 8.3
Central Manufacturing Facility
Personnel Requirements

Assy #	Assy Procedure / Personnel Required	Workers Required 1st Shift	2nd Shift
	SUPERVISION		
	Heavy Fabricating Foreman	1	1
	Light Fabricating Foreman	1	
1200,1300	**MEMBRANE FABRICATING**		
	Coil Strip Preparation	2	
	Welding Crew #1	3	
	Welding Crew #2	3	
	Membrane Packing	2	
1200	**MEMBRANE MATERIAL LAMINATING**		
	Lead Man	1	
	Helper	2	
1208-9 1306-9	**MEMBRANE REINFORCING RINGS**		
	Sheetmetal Workers	2	
2100 2200	**TRUSS FABRICATION**		
	Welders	6	6
	Machine Operators	8	8
	Helpers	3	3
2300	**HUB FABRICATION**		
	Welder	1	
	Machine Operator	2	
	Helper	0.5	
2500	**TIE ROD FABRICATION**		
	Machine Operators	3	3
3200	**DRIVE ADAPTER FABRICATION**		
	Welder	1	1
	Machinist	1	
	Machine Operators	2	
	Helper	1	
4100	**PYLON AND FLANGE FABRICATION**		
	Fabricator	1	
	Machine Operator	1	1
	Helper	0.5	

TABLE 8.3
(cont.)
Central Manufacturing Facility
Personnel Requirements

Assy#	Assy Procedure Personnel Required	Workers Required 1st Shift	2nd Shift
2400 6400	BRACKET FABRICATION		
	Fabricator	1	
	Machine operator	1	
	Helper	1	
	MATERIALS HANDLING		
	Jack Truckers	2	
	Forklift Operators	2	
	SHIPPING DEPARTMENT		
	Shipper	1	
	Helper	1	
		57	22
	TOTAL EMPLOYEES		79

TABLE 8.4
On Site Assembly Operation
Personnel Requirements

Assy#	Assy Procedure Personnel Required	Workers Required 1st Shift	2nd Shift
	SUPERVISION		
	Assembly	1	1
	Installation	1	
	ASSEMBLY OPERATIONS		
	Fixture Membrane to Ring	5	5
	Weld Membrane to Ring	3	3
	Finish Out Mirror Module	2	2
	Assemble Main Ring	6	5
		18	16
	INSTALLATION		
	Field Wiring	21	
	Installation	10	
		31	

75

8.4 Indirect Costs

Indirect costs include the factory burden, tooling costs, general and administrative costs, R & D, and selling costs. The first step to determine the factory burden is to estimate the space required for the central manufacturing facility and the on-site assembly operation. The cost of the equipment used in these operations is also needed. Costs of indirect labor such as supervisors and shipping personnel are also a component of these costs.

There are many different assumptions that could be made about how a company would operate in the early stages of marketing heliostats. These assumptions have a very large effect on the predicted direct costs. The authors have not attempted a rigorous consideration of the most likely or most advantageous company policies and practices to be used here. Instead, a single reasonable set of values is used for demonstration purposes. The values are similar to those experienced by Solar Kinetics when manufacturing large volumes (23,000 m^2 per year) of concentrating trough collectors. The analysis is documented so that users of the report may substitute their own values to explore the effects on the overall economics.

The central manufacturing facility is assumed to be rented space. In the early manufacturing stages, a company would probably not invest in real estate until a stable market was proven.

The manufacturing and assembly space required for a central manufacturing facility is about 100,000 ft^2. This was determined from plant layouts made of the specific machinery and processes involved. These layouts are shown in Figures 8.2 to 8.11, and the resulting space requirements are summarized in Table 8.5. Some of these layouts were developed in earlier manufacturing studies by SKI (1). Others were developed specifically for the current work based upon machinery manufacturers data and engineering estimates of the requirements of the operations being performed.
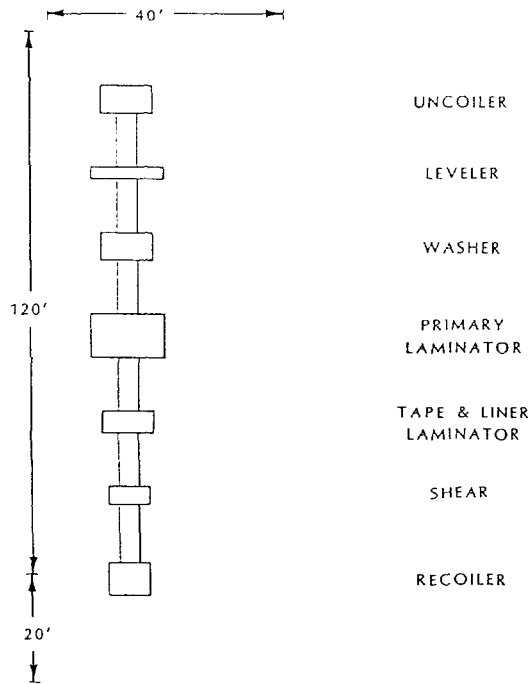
Figure 8.2 Coil Stock Laminating Plant Layout.
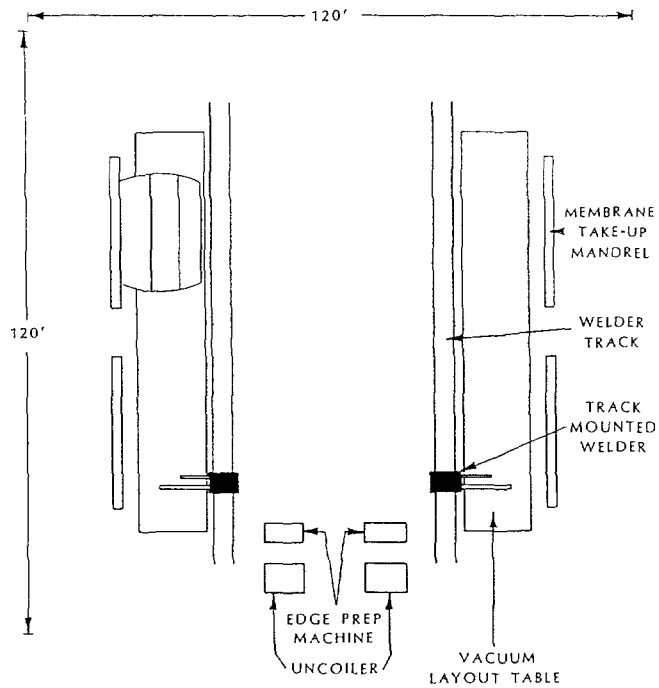
Figure 8.3 Membrane Fabricating Plant Layout.
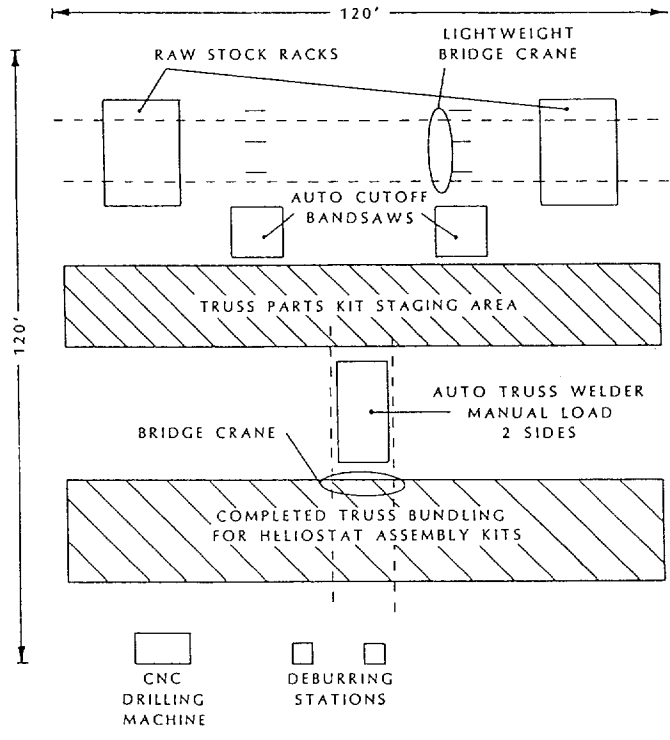
Figure 8.4 Truss Fabrication Plant Layout.
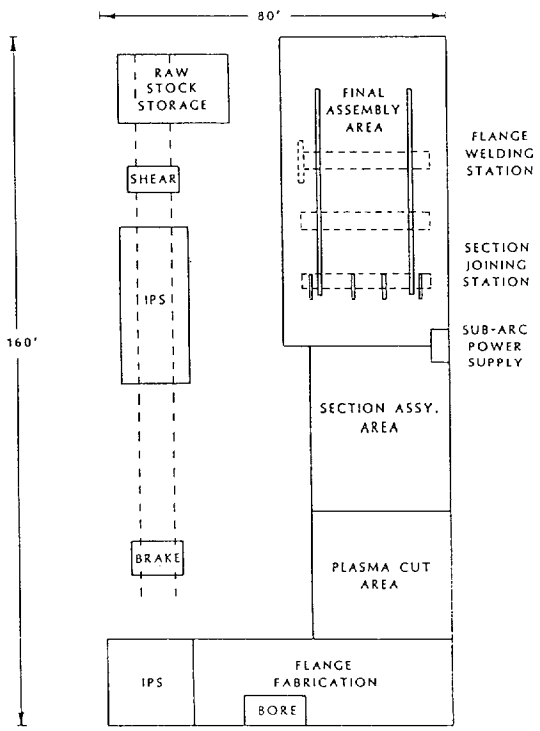
Figure 8.5 Pylon Fabrication Plant Layout.
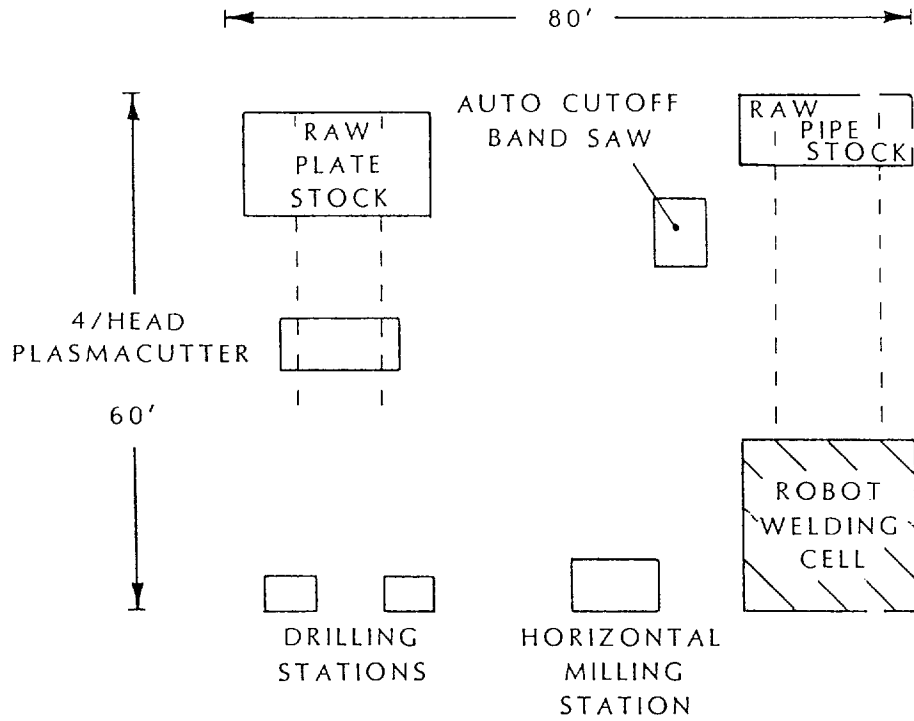
Figure 8.6 Hub Fabricating Plant Layout.
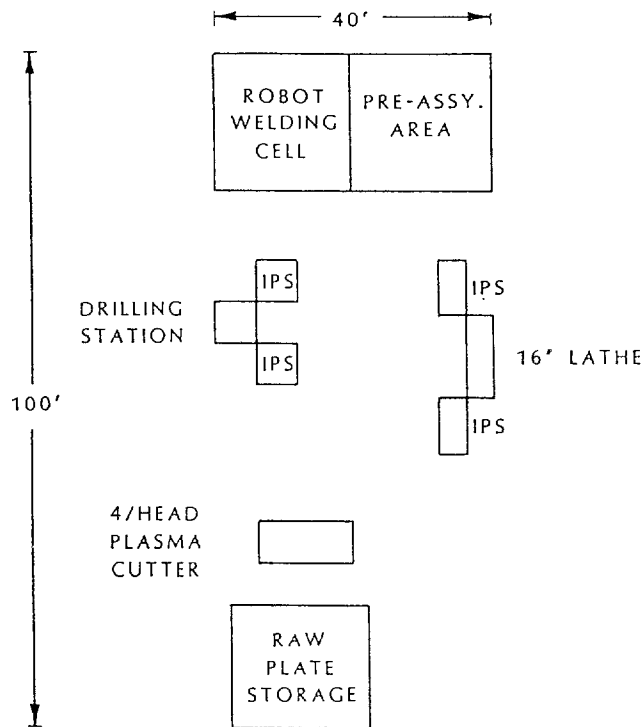
Figure 8.7 Drive Adapter Fabricating Plant Layout.
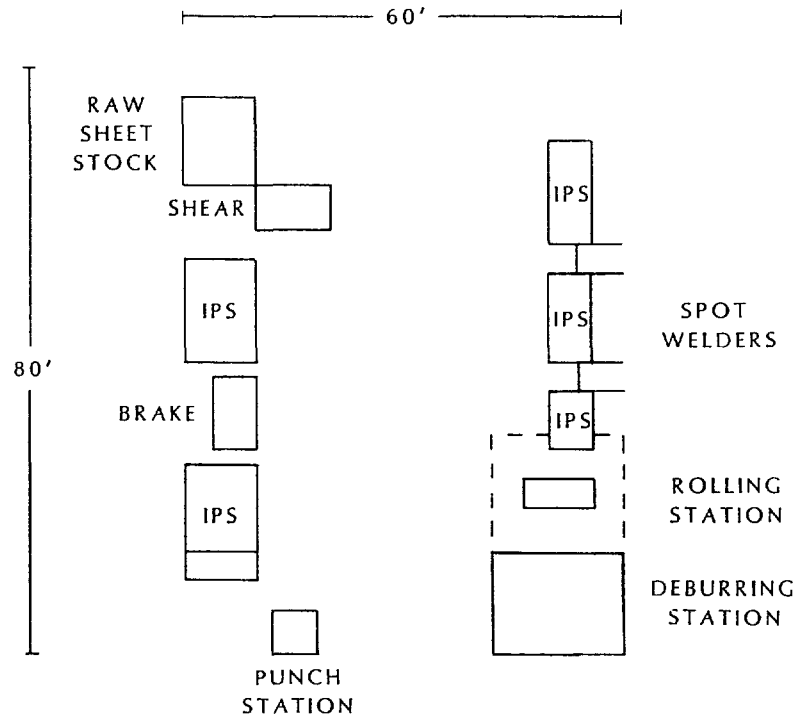
Figure 8.8 Bracket Fabrication Plant Layout.
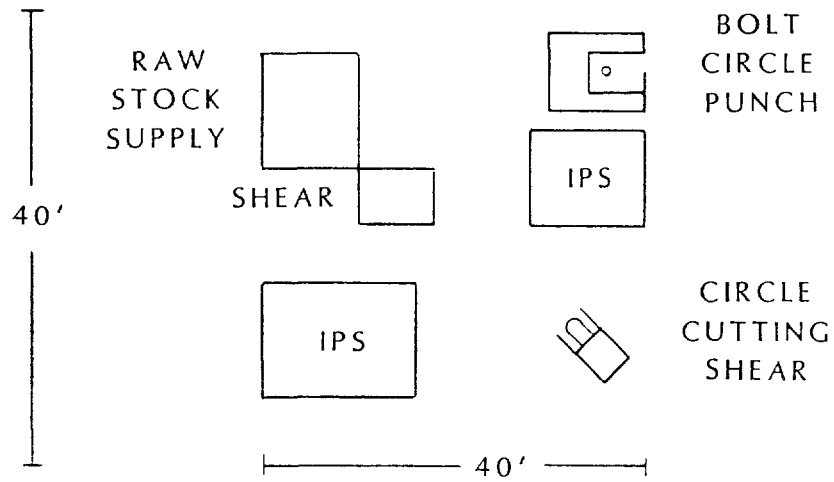
Figure 8.9 Membrane Reinforcing Rings Fabrication Plant Layout.
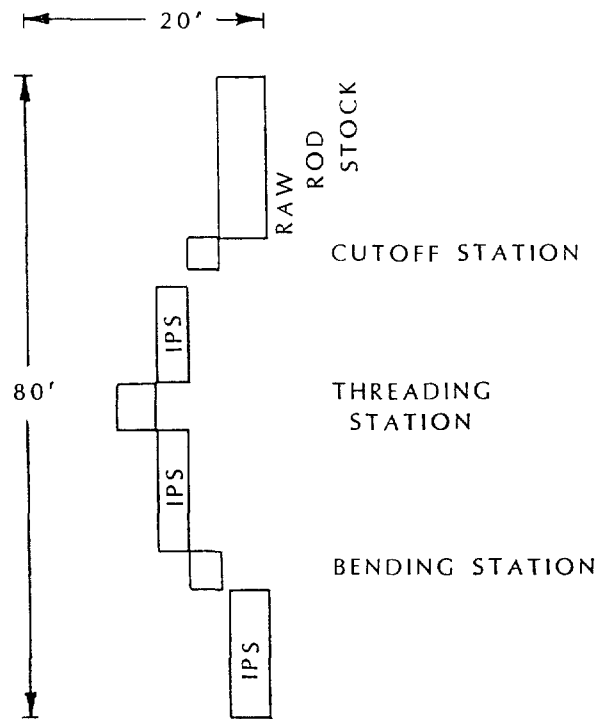
Figure 8.10 Tie Rod Fabricating Plant Layout.
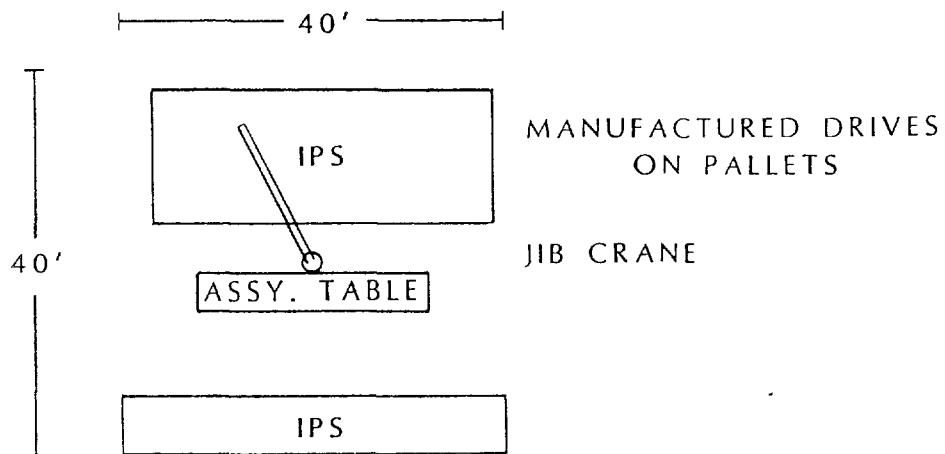
Figure 8.11 Drive Preparation Plant Layout.

TABLE 8.5
Central Manufacturing Facility
Space Requirements

Operation	Length ft	Width ft	Area sq. ft	Sub-Total sq. ft.
MANUFACTURING				
Coil Operation				
Laminating	120	40	4800	
Membrane Fabricating	120	120	14400	
Heavy Fabricating				
Truss Fabrication	120	120	14400	
Pylon Fabrication	160	80	14400	
Hub Fabrication	80	60	4800	
Drive Adapter Fabrication	100	40	4000	
Light Fabricating				
Bracket Fabrication	80	60	4800	
Reinforcing Ring Fabrication	40	40	1600	
Tie Rod Fabrication	80	20	1600	
Assembly Work				
Drive Preparation	40	40	1600	
Control Fabrication	40	40	1600	
Warehousing				
Raw Material Inventory	120	100	12000	
Finished Part Inventory	120	100	12000	
Utilities				
Air comp., heating, power distribution, etc.				
				90400
SUPPORT				
Offices				
Administration			2000	
Engineering			2000	
Service			3000	
				7000
Grand Total				101,400

For the on-site assembly area, an enclosed area of about 29,000 ft^2 is required for the 2,000 unit production rate. The facility layout for this operation is shown in Figure 8.12 and summarized further in Table 8.6. This facility is housed in an air inflated building that provides a combination of minimal site preparation, low building cost, portability and large interior clear spans. No permanent foundations are required for this structure; instead a wide slab is poured where the building sits with an additional paved area surrouding the slab. A small prefabricated steel building serves as an airlock on the primary building entrance to allow removal of the completed heliostat mirror modules. This building is left on site to serve as a mirror module servicing facility during the life of the installation.

TABLE 8.6
On Site Assembly Operation
Space Requirements

Operation	Length ft.	Width ft.	Area sq. ft.	Sub-Total sq. ft.
ASSEMBLY				
Inflatable Structure				
Heliostat Ring Assembly	80	60	4800	
Membrane Fixturing	160	60	9600	
Rear Structure Assembly	100	60	6000	
Final Assembly	80	60	4800	
Receiving/Loading	60	60	3600	
				28800
Rigid Structure				
Entry Truck Size Air-lock	40	40	1600	
				1600
Total, Interior Area				30400
Outdoor Lay Down Area				30000
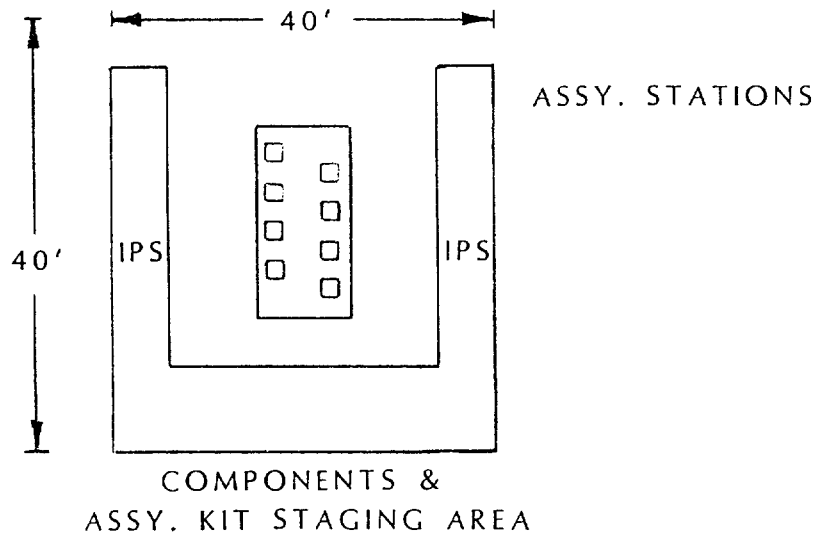
Figure 8.12 Control Cabinet Assembly Plant Layout.

8.5 Start-Up Expenses

Some sort of structure is required in which to perform the on-site assembly work. A sheltered area of approximately 29,000 ft^2 is needed to permit assembly at the required rate of eight heliostats per day. A permanent building of this size is too expensive to build just for assembly purposes and it would probably not be needed on site for any other purpose. Therefore, a temporary, lower cost structure was selected. An air inflated building that can be moved from site to site would be used. As described in Section 8.4 only a concrete pad to which to secure the building and to serve as an assembly area floor requires permanent installation on site. Figure 8.13 shows the on-site assembly operation layout. Because this building can be moved from site to site, its cost is included with the tooling costs as part of the total start-up expense.

The balance of the equipment required for each operation is listed in Table 8.7 and 8.8, which summarizes the costs for tooling and equipment. These costs are used in the next section when evaluating the relationship of price, cost, and return on investment.
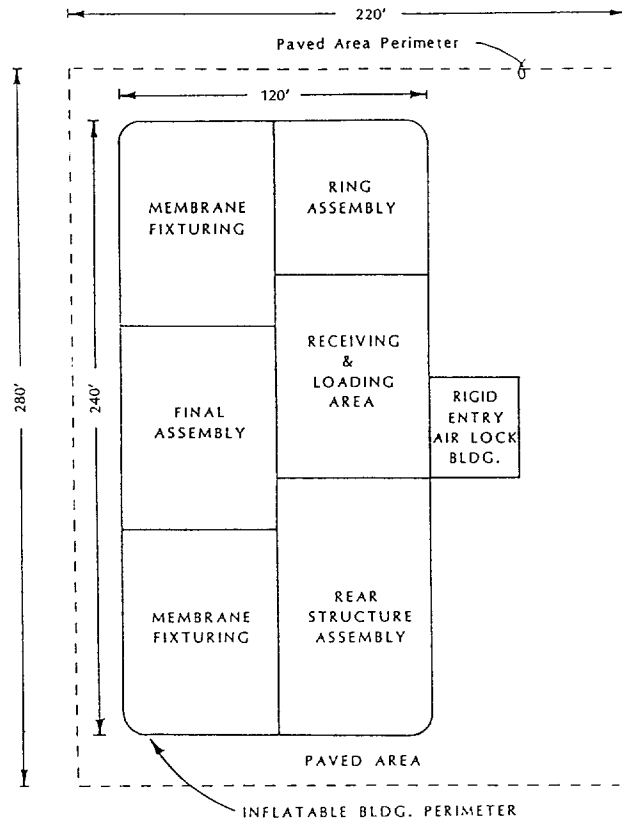
Figure 8.13 On-Site Assembly Facility.

TABLE 8.7
Central Manufacturing Facility
Equipment Requirements

Assy #	Assy Procedure Machinery Required	Qnty	Cost	Subtotal
1200	MEMBRANE FABRICATING			
1300	Dual Head Rolling			
	Resistance Welders	2	$40,000	$80,000
	Dual Membrane Vacuum			
	Layout Tables	2	$10,000	$20,000
	Membrane Mandrel Support &			
	Take Up Rollers	4	$5,000	$20,000
	Membrane Coil Stock Un-			
	coiler w/Edge Prepar-			
	ation Capabilities	1	$24,000	$24,000
1200	MEMBRANE MATERIAL LAMINATING			
	Uncoiler	1	$14,000	$14,000
	Leveler	1	$13,000	$13,000
	Coil Washer	1	$10,000	$10,000
	Dry Laminator	1	$20,000	$20,000
	Tape Applicator	1	$6,000	$6,000
	Release Liner Laminator	1	$6,000	$6,000
	Power Shear	1	$4,100	$4,100
	Recoiler	1	$14,000	$14,000
1208-9	MEMBRANE REINFORCING RINGS			
1306-9				
	52" Power Shear	1	$5,000	$5,000
	50" Radius Power Circle			
	Shear	1	$3,000	$3,000
	Punch Station w/Rotary			
	Table	1	$5,860	$5,860
	Tooling	1	$3,000	$3,000
2100	TRUSS FABRICATION			
2200				
	Automatic Band Saw	2	$32,000	$64,000
	CNC Drilling Machine	1	$38,000	$38,000
	Auto Truss Welder	1	$750,000	$750,000
	Local Material Handling			
	Equip.	1	$40,000	$40,000
	Belt Sanders	2	$700	$700
	Tooling	6	$4,000	$24,000

TABLE 8.7
(Cont.)
Central Manufacturing Facility
Equipment Requirements

Assy #	Assy Procedure Machinery Required	Qnty	Cost	Subtotal
2300	HUB FABRICATION			
	Horizontal Cut Off Band Saw	0.5	$32,000	$16,000
	Plasma Cutting Torch, 4 Head w/Tracer Follower	1	$18,000	$18,000
	Production Drill Press	2	$3,000	$3,000
	Horizontal Milling Machine	1	$10,000	$10,000
	Belt Sander	1	$700	$700
	Manual MIG Welding Station	1	$5,000	$5,000
	Robot MIG Welding Cell	1	$50,000	$50,000
	Tooling	1	$5,000	$5,000
2500	TIE ROD FABRICATION			
	Rod Shear	1	$2,000	$2,000
	Small Turret Lathe	1	$6,899	$6,800
	Power Hand Drill	1	$200	$200
	Tooling	1	$5,000	$5,000
3200	DRIVE ADAPTER FABRICATION			
	Horizontal Cut off Bandsaw	0.5	$32,000	$32,000
	Plasma Cutting Torch, 4 Head w/Tracer Follower	1	$18,000	$18,000
	Production Drill Press	1	$3,000	$3,000
	16" Engine Lathe	1	$13,000	$13,000
	Manual MIG Welding Station	1	$5,000	$5,000
	Robot MIG Welding Cell	1	$50,000	$50,000
	Tooling	1	$10,000	$10,000
4100	PYLON AND FLANGE FABRICATION			
	Hand Held Plasma Torch	1	$3,000	$3,000
	Hand Grinders	5	$200	$1,000
	Production Drill Press	1	$3,000	$3,000
	Powered Weld Rollers	1	$1,000	$1,000
	Semi-automatic MIG Welder	1	$6,000	$6,000
	3/8x10' Shear	1	$35,000	$35,000
	10'x3/8 Press Brake	1	$47,000	$47,000
	Submerged Arc Welder w/ Track	2	$5,000	$10,000

TABLE 8.7
(Cont.)
Central Manufacturing Facility
Equipment Requirements

Assy #	Assy Procedure Machinery Required	Qnty	Cost	Subtotal
2400 6400	BRACKET FABRICATION			
	52"x1/4 Power Shear	1	$12,800	$12,800
	6'x55 Ton Press Brake	1	$17,000	$17,000
	Spot Welders	2	$15,000	$30,000
	Belt Sander	1	$700	$700
	Punch Station	1	$3,860	$3,860
	Power Pyramid Roller	1	$2,000	$2,000
	MATERIAL HANDLING			
	Jack Trucks	10	$700	$7,000
	3000# Forklifts	4	$15,000	$30,000
	6000# Forklifts	2	$29,000	$58,000
	Bar Storage Racks	4	$2,980	$11,920
	Pallet Storage Racks	12	$384	$4,008
	SHIPPING DEPARTMENT			
	Platform Scale	1	$1,000	$1,000
	Radial Arm Saw	1	$1,000	$1,000
	Panel Saw	1	$1,200	$1,200
	Air Compressor	1	$4,000	$4,000
	Air Nailers	6	$100	$600
				$1,723,148

TABLE 8.8
On Site Assembly Operation
Equipment Requirements

Assy #	Assy Procedure Machinery Required	Qnty.	Cost	Subtotal
1100	HELIOSTAT RING			
	Assembly Jig	1	$15,000	$15,000
1200	MEMBRANE FIXTURING			
1300	Vacuum Layout Table	2	$20,000	$40,000
	Tensioning Ring	4	$20,000	$80,000
	Gantry Crane	2	$10,000	$10,000
2000	REAR STRUCTURE			
	Assembly Fixture	1	$20,000	$20,000
	Grooved Bolt Swager	2	$5,000	$10,000
	FINAL ASSEMBLY			
	Support Fixture	1	$15,000	$15,000
	Revolving Seam Welder	2	$20,000	$40,000
	Jib Crane	1	$7,000	$7,000
	Gantry Crane	1	$10,000	$10,000
	MATERIAL HANDLING			
	3000# Forklifts	2	$15,000	$30,000
	6000# Forklifts	2	$29,000	$58,000
	INFLATABLE ENCLOSURE			
	120'x240' Inflatable Building	1	$172,800	$172,800
	40'X40' Rigid Entry Way	1	$25,000	$25,000
	Site Preparation	1	$79,000	$79,000
	INSTALLATION			
	6 Ton All-terrain Hydraulic Crane	1	$75,000	$75,000
	2 Ton, 30' Flatbed Truck	2	$35,000	$70,000
	1 Ton Van with Man Lift	1	$27,750	$27,750
	Platform Man Lift	1	$17,000	$17,000
				$811,550

8.6 Manufacturing Company Analysis

For the annual production rate of 2,000 heliostats, it is likely a dedicated company or company division would be involved. For the fabrication of 25 heliostats, there is probably not enough revenue generated to support major capital investment in specialized tooling. This analysis, therefore, assumed the 25 units would be built on a prototypical basis. The cost breakdowns detailed in Table 8.1 and Appendix 8.B reflect this. Material overheads and G & A rates are higher than an efficient manufacturing

operation would permit. They are, however, typical or even low for a specialty fabricator as would be needed to do this job.

The 2,000 unit production company was analyzed in a situation where it would be in production for 7 years. This would take optimum benefit of allowable depreciation, but not project an indefinite market at this low volume. If volume increased, so would the company viability. As long as sales did not decrease, after 7 years the operation could be liquidated, and all obligations and investors would be satisfied.

It is recognized that after some relatively short product cycle, the current design will be obsolete. Producing larger sizes of heliostats and larger volumes of heliostats has the effect of dramatically reducing the installed cost of the units. Table 8.9 shows how the cost per square meter of stretched-membrane heliostats is reduced with increasing volume and size. However, in order for the industry to get to the stage of producing 7.5×10^6 square meters of heliostats a year, an interim demonstration period is necessary.

Table 8.9
Comparison of Heliostat Manufacturing Costs

Source	SKI II		SKI III		SAIC		SERI	
Qnty.	50000		2000		5000		2500	
Size ...m^2	150		50		100		50	
Dollars	1985		1990		1989		1979	
	$ mtrl.	hrs.	$ mtrl	. hrs.	$ mtrl.	hrs.	$ mtrl.	hrs
Mirror Module	1425.25		1711.00	18.0	5041.49	12.4	1318.29	5.0
Support Structure	768.62		1338.00	23.0	777.22	5.2	382.12	10.0
Drive	1650.00		4239.00	2.0	2910.00	0.0	3930.09	36.6
Pylon	276.00		918.00	8.0	1460.14	0.8	150.60	
Foundation	957.00		399.00	5.0	212.00	0.0	111.13	
Focus Control	250.00		474.00	1.0	1210.67	3.2		
Tracking Control	415.50		1517.00	18.0	100.00	0.0	450.69	8.3
Field Wiring	564.00		52.00	18.0	107.00	4.4	58.41	
Assembly	181.50		0.00	12.0	0.00	3.2		
Installation			0.00	9.0	0.00	4.0	167.01	
Other							100.00	5.0
Instltn contract services							457.07	
	6487.87	0.0	10648.00	114.0	11818.52	33.2	7122.41	64.9
Units per m^2	43.25	0.00	212.96	2.28	118.19	0.33	142.45	1.30
Direct Cost	6487.87		11930.50		12815.52		7901.17	
Direct Cost/m^2	43.25		238.61		128.16		158.02	
Selling Price	8289.00		13401.00		16120.00		9257.00	
Price/m^2	55.26		268.02		161.20		185.14	

TIME ADJUSTED COSTS

	SKI II	SKI III	SAIC	SERI
Adjustment factor	1.16	1.00	1.02	1.54
Direct Cost	7493.49	11930.50	13059.01	12163.91
Direct Cost/m^2	49.96	238.61	130.59	243.28
Selling price	9573.80	13401.00	16426.28	14250.73
Price/m^2	63.83	268.02	164.26	285.01
Annual Production m^2	7500000	100000	500000	125000

After this early stage in manufacturing, stretched-membrane heliostats will have proven their long-term effectiveness to the utility industry. At that time, the major investment in capital equipment necessary to drive down the manufactured cost of heliostats will become attractive to investors and manufacturers serving the utility industry.

Table 8.10 shows the finances of a company producing 2,000 50-m^2 stretched-membrane heliostats. For an investment of $3,200,000, the company can operate profitably even over a relatively short product life.

The scenario shown assumes sufficient demand for 2,000 units a year. When the anticipated opportunities discussed in Section 1 open, a stretched-membrane heliostat company will be able to function autonomously. It would provide investors with a reasonable 15% return. This should be sufficient to bring stretched-membrane heliostat development from its current stage to full-scale market readiness with primarily private sector investment.

Once the technology is proven, full-scale production as outlined in several previous studies can be justified.

Table 8.10
Financial Projections for a Stretched-Membrane
Heliostat Manufacturing Company

INPUT DATA

Manufacturing Equipment	3000000	$	Year 1 Material Cost	10732	$/Unit
Office Equipment	100000	$	Material Overhead	0.05	%/100
Total Capital Expense	3100000		Direct Man Hours	113.00	/Unit
Organizational Expense (nondeductible)	100000	$	Ditirect Labor Rate	7.50	$/MH
Total Startup Costs	3200000	$	Labor Burden	0.50	%/100
Depreciation	7	Years	Shipping Cost	200	$/Unit
Units Sold Per Year	2000		R&D	0.00	% Sales/100
Unit Sale Price	13385	$	G&A	0.15	%/100
Inflation Rate	0.04	%/100	Fed. Tax Rate	0.34	%/100
Discount Rate	0.15	%/100	State Tax Rate	0.04	%/100
Equipment Resale Factor	0.10		Facet Area	50	Sq. M.

Year	1	2	3	4	5	6	7	8
Units Sold	2000	2000	2000	2000	2000	2000	2000	0
Sale Price	13385	13920	14477	15056	15659	16285	16936	0
Gross Sales	26770000	27840800	28954432	30112609	31317114	32569798	33872590	407939
Material Costs	21464000	22322560	23215462	24144081	25109844	26114238	27158807	0
Material O.H.	1073200	1116128	1160773	1207204	1255492	1305712	1357940	0
Direct Labor	1695000	1762800	1833312	1906644	1982910	2062227	2144716	0
Labor Burden	847500	881400	916656	953322	991455	1031113	1072358	0
Shipping Costs	400000	416000	432640	449946	467943	486661	506128	0
R&D Costs	0	0	0	0	0	0	0	0
G&A Expense	441375	459030	477391	496487	516346	537000	558480	0
Gross Margin	848925	882882	918197	954925	993122	1032847	1074161	407939
Depreciation	442857	442857	442857	442857	442857	442857	442857	0
Taxable Income	406068	440025	475340	512068	550265	589990	631304	407939
Fed. Income Tax	138063	149608	161616	174103	187090	200597	214643	138699
State Income Tax	16243	17601	19014	20483	22011	23600	25252	16318
After Tax Profit	251762	272815	294711	317482	341164	365794	391408	252922
Profit as % of Sales	0.009	0.010	0.010	0.011	0.011	0.011	0.012	0.620
Payable Dividend	694619	715673	737568	760339	784021	808651	834266	252922
3200569 = NPV								

93

.

9.0 REFERENCES

1. Development of a Stressed Membrane Heliostat, SAND87-8180, (Solar Kinetics, Inc., Dallas, Texas), Albuquerque, NM: Sandia National Laboratories, April 1987.

2. Design and Demonstration of an Improved Stretched-Membrane Heliostat, SAND89-7028, (Solar Kinetics, Inc., Dallas, Texas), Albuquerque, NM: Sandia National Laboratories, December 1989.

3. K. Beninga, B. Butler, Ph.D., J. Sandubrae, K. Walcott, An Improved Design for Stretched-Membrane Heliostats, SAND89-7027, Albuquerque, NM: Sandia National Laboratories, June 1989.

4. K. Beninga, R. Davenport, J. Sandubrae, Selection and Design of a Stretched-Membrane Heliostat for Today's Markets, SAND89-7040, Albuquerque, NM: Sandia National Laboratories, January 1990.

5. D. J. Alpert, R. M. Houser, A. A. Heckes, W. W. Erdman, An Assessment of Second-Generation Stretched-Membrane Mirror Modules, SAND90-0183, Albuquerque, NM: Sandia National Laboratories, February 1990.

6. J. A. Peterka, A. Tan, B. Bienkiewicz, J. E. Cermak, Mean and Peak Wind Load Reduction on Heliostats, SERI/STR-253-3212, Golden, CO: Solar Energy Research Institute, September 1987.

7. W. H. Heller, J. S. Peters, Development of a Low-Cost Drive Mechanism for Solar Heliostat, SAND90-5753, Albuquerque, NM: Sandia National Laboratories, February 1989.

8. R. J. Roark, Formulas for Stress and Strain, McGraw-Hill.

9. "Geotechnical Investigation Report, Solar Dish Installation," Job No. E83-1179, Sergent, Hauskins and Beckwith Consulting Geotechnical Engineers, Albuquerque, NM: Kirtland Air Force Base.

10. "Soil & Foundation Investigation Report," Job. NO. E76-1018, Sergent, Hauskins and Beckwith Consulting Soil and Foundation Engineers, Albuquerque, New Mexico, April 12, 1976.

11. C. Liu, J. B. Evett, Soils and Foundations, Prentice-Hall, 1981.

12. Hunt, Roy E., Geotechnical Engineering Analysis and Evaluation, McGraw-Hill, 1986.

13. J. Pearson, B. Chen, *An Assessment of Heliostat Control System Methods*, SERI/SP-253-2390, Golden, CO: Solar Energy Research Institute, January 1986.

14. J. C. Zimmerman, *Sun-Pointing Programs and Their Accuracy*, SAND81-0761, Albuquerque, NM: Sandia National Laboratories, May 1981.

15. *Means Facilities Cost Data 1990*, 5th Annual Edition, Kingston, MA: R. S. Means Company, Inc., 1989.

16. K. Drumheller, T. A. Williams, R. A. Dilbeck, G. S. Allison, *The Cost of Heliostats in Low Volume Production*, SERI/TR-8043-2, Golden, Co: Solar Energy Research Institute, January 1980.

17. CO_2 Welding Time Calculator, Bridgewater, NJ: Hunter Assoc.

18. W. H. Heller, Peerless Winsmith, Telephone conversation, April 25, 1990.

APPENDIX ITEM 3.A
List of Assembly Procedures

MEMBRANES

1. Laminate front membrane material.
2. Membrane fabrication
   a. weld membranes
   b. 1 front
   c. 1 rear, and
   d. package membranes.

REAR STRUCTURE

1. Fabricate trusses
   a. install hinge weldments.
2. Fabricate hub.
3. Fabricate drive adapter.

PYLON PREPARATION

1. Fabricate pylon.
2. Machine drive mounting flange.
3. Weld flange to pylon.

CONTROLS

1. Assemble control cabinet.
2. Assemble drive motors to drive.
3. Assemble focus control fan assembly.

ON SITE ASSEMBLY

1. Rear Structure
   a. mount hub in fixture
   b. bolt on trusses
   c. install all tie rods
   d. remove supports at truss tips
   e. tension tie rods as required to level and position trusses, and
   f. move to IPS.

2. Heliostat Ring
   a. roll segments
   b. prep ends of segments
   c. mount segments in fixture
   d. bolt segment joints
   e. install temporary truing spokes, and
   f. move to IPS.
3. Final assembly
   a. mount membranes on tensioning rings
   b. mount first membranes with tensioning ring in assembly fixture
   c. mount heliostat ring in assembly fixture
   d. mount second membranes with tensioning ring in assembly fixture
   f. weld membranes to ring
   g. cut center holes and install reinforcing rings
   h. attach rear support structure to heliostat ring
   j. install focus fan assembly
   k. install membrane seals, and
   l. move to IPS.

FIELD OPERATIONS

1. Install pylons
   a. bore pier hole
   b. set pylon in hole and true, and
   c. pour concrete.
2. Install field wiring
   a. dig trench
   b. lay wire, and
   c. back fill and tamp trench.
3. Install drive on pylon
   a. install adapter on drive, and
   b. mount drive to pylon.
4. Install control box on pylon
   a. mount to pylon, and
   b. connect wires.
5. Mount mirror module to drive adapter
   a. connect wiring.
6. Check out.

APPENDIX 6A

A schematic program for the local heliostat controller was developed during the course of this investigation. The schematic is specific to the Siemens PLC defined as the baseline design. This program was developed to demonstrate the viability of all calculations and estimate processing time and memory requirements. The format was dictated by the Siemens programming language. A verbal description of each programming step was provided rather than lines of actual code. The divisions in this presentation represent major program blocks or function blocks.

The development was limited to a representation of the program required to calculate the actual heliostat azimuth and elevation. Portions of the code that were written under previous contracts, such as the PID (proportional, integral, and derivative) feedback loop used to control membrane position, were not changed. These codes were incorporated in the time estimates required for multiplex strategies, however. Several standard function blocks available from Siemens (e.g. floating point arithmetic operations) were also incorporated into the schematic.

Communication was not addressed in this program, although values that are communicated from the field level controller are identified. The controllers can be addressed through the programming port with a standard language developed by Siemens. The amount of information that must be communicated is small (tracking information requires less than 60 words daily; operation mode requires a single word) and not specific to heliostat field position. Consequently, a simplex communication procedure could be developed over a set of twisted pair cables with minimal protocol instructions. Communication speed is simply not an issue in the proposed tracking regimen.

The field controller program was not developed in this analysis. A table of all tracking coefficients was assumed to be available, and the table requirements were easily within the memory capabilities of a Siemens 115 PLC. Consequently, the program requirements for field tracking commands are limited to selection of coefficients based on the day of the year.

A1. Miscellaneous Function Blocks Available from Siemens.

Several standard function blocks were required for tracking calculations. These blocks are summarized in Table A1.

Table A1
Arithmetic Function Blocks Available from Siemens

Block Number/Name	Block Lgth. in Words	Mean Processing Time in Milliseconds
FB 15 Fixed to Float CONV	93	2.40
FB 16 Float to Fixed CONV	93	3.66
FB 17 Floating point ADD	264	3.74
FB 19 Floating point MULT	174	4.75
FB 20 Floating point DIV	221	3.67
FB 21 Floating point COMPARE	110	1.88
FB RAD:16 Binary square root	126	4.80
Any typ binary operation		0.0016
Any typ one work operation		0.125

A2. Equivalent Time (EQUIV TIME).

An equivalent rather than actual time was used for position calculations to take advantage of the symmetry in solar azimuth and elevation about solar noon. The procedure can also be adjusted to provide an offset between local and solar time to accommodate different longitudes within a time zone.

The following information is required as an input to this procedure:

   a. BNT0, the integer, non-signed local time, in seconds from midnight.
   b. BNT5, the local time at solar noon, in integer seconds after midnight (communicated from field controller).

Program Block.

   1. Move local time, BNT0 to accum1.
   2. Move noon time, BNT5, to accum2.
   3. Compare.
   4. If BNT0 > BNT5 (i.e. afternoon) set aftflag = true else set aft flag = false.
   5. Non-signed subtraction.
Note: BNT0 is still in accum1 and BNT5 is in accum2.
   6. Negate result.
   7. Move negated result to accum1.
   8. Add.
Note: Noon time, BNT5, is still in accum2.
   9. Move result to FB15.
   10. Convert fixed to float.
   11. Move result to R1, the real equivalent morning time.

The results of this procedure are as follows:

    a. R1, the real equivalent morning time.
    b. aftflag, a true flag if it is afternoon.

The estimated execution time and memory requirements are 3 ms and (15) 8-bit words [(12) operational words, (1) binary word, and (1) real word]. This block is executed once per az/el loop.

A3. Solar Azimuth and Elevation Coefficients (SOLAR COEFF)

An array of coefficients are transmitted once daily by the field controller. This procedure selects the particular coefficients to be used during the active time segment. The selection of coefficients is a binary comparative operation. The process is identical for morning and afternoon without regard to sign.

The following information is required as an input to this procedure:

    a. The azimuth coefficients stored after each days transmittal, CA 0 through CA 15. The order is assumed to be A_0,A_1,A_2,A_3 for the first time segment, A_0,A_1,A_2,A_3 for the second time segment, etc. (Communicated from field level controller.)
    b. The elevation coefficients stored after each days transmittal, CE 0 through CE 15. (Communicated from field level controller.)
    c. The time, in seconds before solar noon, that begins each time segment, BNT1 through BNT4. (Communicated from field level controller.)
    d. Solar noon in seconds after midnight, BNT5. (Communicated from field level controller.)
    e. The current time in seconds after midnight, BNT0.
Note: Times are expressed as binary, non-signed numbers and can be expressed as a 16-bit word.

Program Block 1.

    1. Set noon time, BNT5 to accum1.
    2. Set current time, BNT0 to accum1.
    3. Non-signed subtraction.
Note: Subtraction of a current time of 43500 (12:05) from a solar noon of 45000 (12:30) yields 1500 (25 minutes). Subtraction of a current time of 46500 (12:55) from a solar noon of 45000 also yields 1500. There is no sign. That is acceptable since it is the distance from solar noon, in seconds, that defines the time segment, and the solar path is symmetrical about solar noon.
    4. Set result to BNT6.
    5. a. Set first time segment begin time, BNT1 to accum1.
         b. Set result, BNT6, to accum2.
         c. Compare.

d. If BNT1 < time before noon (i.e. accum1 < accum2), conditionally call Block 2.

e. Increment (BNI0) begin time register by one.

6. Repeat steps 5a through 5b 3 more times, 4 times total.

Program Block 2.

1. Set increment from Block1 (BNI0) to accum1.

Note: The increment from block 1 is 0 if the first time segment should be used, 1 for the second, 2 for the third, and 3 for the fourth time segment.

2. Set accum2 equal to 4.

3. Binary multiply.

4. Set the result to accum1.

5. Set a Block 2 increment, BNI1, to 0.

6. a. Set BNI1 to accum2.

b. Add.

c. Set the result to a block 2 temporary number, BNT0.

d. Set the current azimuth coefficient register, AA(BNI1), equal to the transmitted azimuth register, CA(BNT0).

e. Set the current elevation coefficient register, EE(BNI1), equal to the transmitted azimuth register, CE(BNT0).

f. Increment BNI1 by 1.

7. Repeat steps 6a through 6f three times, i.e. execute 4 times total.

Note: At step 4, accum1 contains the product of the block1 increment and the constant, 4. If, for example, this was the third time segment, accum1 would contain a value of 8. CA8 is the azimuth constant in the third segment time polynomial. CA9, CA10, and CA11 are the first, second, and third order coefficients, respectively. They are assigned in the repetition of steps 6a through 6f.

Note: At the end of the Block 2 call, operation returns to Block 1. The Block 2 call will typically occur more than once, but the final call will always contain the proper coefficients.

The results of this procedure are as follows:

a. Azimuth
0th order coefficient (constant) in AA0.
1st order coefficient in AA1,
2nd order coefficient in AA2, and
3rd order coefficient in AA3.

b. Elevation
0th order coefficient (constant) in EE0,
1st order coefficient in EE1,
2nd order coefficient in EE2, and
3rd order coefficient in EE3

The estimated time and memory requirements are 11 ms and (45) 16-bit words [(29) operation words, (0) permanent binary words, and (8) real words]. This block is executed once per az/el loop.

A4. Time Exponentiation (TIME EXP)

This block provides time raised to the first, second, and third power as required for the third order approximation of solar azimuth and elevation in each time segment.

The following information is required as an input to this program block:

    a. The real equivalent morning time, R1.

Program Block

    1. Move floating point time, R1, to multiplier in FB 19.
    2. Move R1 to multiplicand in FB 19.
    3. Define the initial variable storage word as R2.
    4. a. Multiply.
        b. Store product in variable register.
        c. Move product to multiplicand in FB 19.
        d. Increment register number for variable storage.
    5. Repeat steps 4a-4d once, execute 2 times total.

The results of this procedure are as follows:

    Note: Equivalent morning time, R1 is calculated in Section 2.1.4.
            a. t^2 in R2.
            b. t^3 in R3.

The estimated time and memory requirements are 11 ms, and (14) 8-bit words [(10) operational words, (0) binary words, and (2) real words]. This block is executed once per az/el loop.

A5. Calculation of the Solar Azimuth and Elevation.

The solar azimuth and elevation are calculated in essentially identical procedures. The processing time is significant (57 ms), however. To increase flexibility, a single block may be defined and executed twice. This division would provide two sections, SOLAR AZ and SOLAR EL.

The following information is required as an input to this program block:

    a. Azimuth coefficients, AA0, AA1, AA2, AA3.
    b. Elevation coefficients, EE0, EE1, EE2, EE3.
    c. Time and exponentials of time, R1, R2, R3.
    d. The afternoon flag, aftflag, calculated in the following section.

The procedure for the calculation is as follows:

1. Set index1 to 1.
2. Set AA0 to add1 of FB17.
3. a. Move AA(index1) to multiplicand of FB19.
   b. Move R(index1) to multiplier of FB19.
   c. Multiply.
   d. Move result to add2 of FB17.
   e. Add.
   f. Move result to add1 of FB17.
   g. Increment index1 by 1.
4. Repeat steps 3a-3g twice, execute three times total.
5. Move result to SA1.
6. Reset index1 to 1.
7. Set AA0 to add1 of FB17.
8. a. Move EA (index1) to multiplicand of FB19.
   b. Move R(index1) to multiplier of FB19.
   c. Multiply.
   d. Move result to add2 of FB17.
   e. Add.
   f. Move result to add1 of FB17.
   g. Increment index by 1.
9. Repeat steps 8a-8g twice, execute three times total.
10. Move result to SE1.
11. If aftflag = true then negate SA1.

The results of this procedure are as follows:

a. The underacted solar azimuth, SA1.
b. The underacted solar elevation, SE1.

The estimated time and memory requirements are 57 ms and (36) 8-bit words [(32) operational words, (0) permanent binary words, and (2) real words]. Each block is executed one per az/el loop.

A6. Exponentiation of Solar Azimuth (SOL AZ EXP).

Exponentials of an angle are required for calculation of sine and cosine. The block is divided into two parts (SOLL AZ EXP 1 and SOL AZ EXP 2) to increase flexibility in the multiplex arrangement.

The following information is required as an input to this procedure:

   a. The underacted solar azimuth, SA1.

Program Block.

   1. Set SA1 to the floating point angle.
   2. Call Sin Exponentiation Function Block.

Sin Exponentiation Function Block.

   1. Move floating point angle to multiplier in FB 19.
   2. Move floating point angle to multiplicand in FB 19.
   3. Define the initial variable storage word as R1.
   4. a. Multiply.
      b. Store product in variable register.
      c. Move product to multiplicand in FB 19.
      d. Increment register number for variable storage.
   5. a. Repeat steps 4a-4d four times.
   5. b. Repeat steps 4a-4d four times again.

The results of this procedure are as follows:

   a. x in R1, x^2 in R2, x^3 in R3, ... x^9 in R9, where x is the angle and Rn is the variable word used for product storage.

The estimated time and memory requirements are 48 ms and (28) 8-bit words [(10) operational words, (0) permanent binary words, and (9) real words]. Each block is executed once per az/el loop.

A7. Exponentiation of Solar Elevation (SOL EL EXP).

Exponentials of the solar elevation are required for calculation of sine and cosine. The block is divided into two parts (SOL EL EXP 1 and SOL EL EXP 2) to increase flexibility in the multiplex arrangement. The process is identical to step A6, and uses A6 Blocks 1 and 2 as function blocks.

The following information is required as an input to this procedure:

   a. The underacted solar elevation, SE1.

Program Block.

   1. Set SE1 to the floating point angle.
   2. Call Sin Exponentiation Function Block.

The results of this procedure are as follows:

    a. X in R1, x^2 in R2, x^3 in R3, ... x^9 in R9, where x is the angle and Rn is the variable word used for product storage.

The estimated time and memory requirements are 48 ms and (20) 8-bit words [(2) operational words, (0) permanent binary words, and (9) real words]. Each block is executed once per az/el loop.

A8. Sine of Solar Azimuth (SIN SOL AZ).

The sine function block requires previous exponentiation before implementation. This program block uses the sine function block.

The following information is required as an input to this program block:

    a. x in R1, x^2 in R2, x^3 in R3, ... x^9 in R9, where x is the solar azimuth angle and Rn is the variable word used for product storage.
    b. The constants -6, 120, -5040, and 362880 are stored as floating point numbers in C3, C5, C7, and C9. (This line is a permanent storage, not an active programming step.).

Program Block.

1. Move exponential output to proper registers.
2. Call sine block.
3. Move R0 to sin sol az storage register.

Sine Function Block.

1. Move R1 to add1 of FB 17.
2. Define R3 and C3 as the initial constants and variables.
3.   a. Move Rn to dividend of FB 20.
     b. Move Cn to divisor of FB 20.
     c. Divide.
     d. Move quotient to add2 of Fb 17.
     e. Add.
     f. Move sum to Add1 of FB 17.
     g. Increment variable and constant registers by 2.
4. Repeat steps 3a-3g three times.
5. Move the sum to variable storage register R0.

The results of this procedure are as follows:

    a. sin (x) in R0, where x is the angle in radians.

The estimated time and memory requirements are 33 ms and (22) 8-bit words [(12) operational words, (0) permanent binary words, and (5) real words]. Each block is executed once per az/el loop.

A9. Sine of Solar Elevation (SIN SOL EL).

The sine of elevation program block is virtually identical to A8 requires previous exponentiation before implementation. This program block uses the sine function block.

The following information is required as an input to this program block:

a. x in R1, x^2 in R2, x^3 in R3, ... x^9 in R9, where x is the solar elevation angle and Rn is the variable word used for product storage.

b. The constants -6, 120, -5040, and 362880 are stored as floating point numbers in C3, C5, C7, and C9. (This line is a permanent storage, not an active programming step.)

Program Block.

1. Move exponential output to proper registers.
2. Call sine block.
3. Move R0 to sin sol el storage register.

The results of this procedure are as follows:

a. sin (x) in R0, where x is the angle in radians.

The estimated time and memory requirements are 33 ms and (13) 8-bit words [(3) operational words, (0) permanent binary words, and (5) real words]. Each block is executed once per az/el loop.

A10. Cosine of Solar Azimuth (COS SOL AZ).

The cosine function block requires previous exponentiation before implementation. This program block uses the cosine function block.

The following information is required as an input to this program block:

a. x in R1, x^2 in R2, x^3 in R3, ... x^9 in R9, where x is the solar azimuth angle and Rn is the variable word used for product storage.

b. The constants -2, 24, -720, and 40320 are stored as floating point numbers in C2, C4, C6, and C8. (This line is a permanent storage, not an active programming step.)

Program Block.

1. Move exponential output to proper registers.
2. Call cosine block.
3. Move R10 to sin sol el storage register.

Cosine Function Block.

1. Move 1 to add1 of FB 17.
2. Define R2 and C2 as the initial constants and variables.
3. a. Move Rn to dividend of FB 20.
   b. Move Cn to divisor of FB 20.
   c. Divide.
   d. Move quotient to add2 of FB 17.
   e. Add.
   f. Move sum to Add1 of FB 17.
   g. Increment variable and constant registers by 2.
4. Repeat step 3a-3g three times.
5. Move the sum to variable storage register R10.

The results of this procedure are as follows:

a. cos (x) in R10, where x is the angle in radians.

The estimated time and memory requirements are 33 ms and (22) 8-bit words [(12) operational words, (0) permanent binary words, and (5) real words]. Each block is executed once per az/el loop.

A11. Cosine of Solar Elevation (COS SOL EL).

The cosine of elevation program block is virtually identical to A8 requires previous exponentiation before implementation. This program block uses the sine function block.

The following information is required as an input to this program block:

a. x in R1, x^2 in R2, x^3 in R3, ... x^9 in R9, where x is the solar elevation angle and Rn is the variable word used for product storage.
b. The constants -2, 24, -720, and 40320 are stored as floating point numbers in C2, C4, C6, and C8. (This line is a permanent storage, not an active programming step.)

Program Block.

1. Move exponential output to proper registers.
2. Call cosine block.
3. Move R10 to cos sol el storage register.

108

The results of this procedure are as follows:

     a. $\cos(x)$ in R10, where x is the angle in radians.

The estimated time and memory requirements are 33 ms and (13) 8-bit words [(3) operational words, (0) permanent binary words, and (5) real words]. Each block is executed once per az/el loop.

A12. Heliostat Azimuth and Elevation, Part 1 (HEL AZ/EL 1).

The translation from solar to heliostat azimuth and elevation is a function of the heliostat's position in the field. The translation was divided into parts to reduce the time associated with any one block. The result of part 1 is the Cartesian vector representation of the underacted mirror normal.

The following information is required as an input to this program block:

     a. Sine of solar azimuth.
     b. Sine of solar elevation.
     c. Cosine of solar azimuth.
     d. Cosine of solar elevation.
     e. The constant distances south, east, up, and total to the tower are stored as floating point numbers. (This line is a permanent storage, not an active programming step.)

<u>Program Block</u>.

   1. Load sine of the sun elevation into temp register T0,T1.
   2. Load 1.0 into temp register T2.
   3. Load cosine of the sun azimuth into temp register T3.
   4. Load sine of the sun azimuth into temp register T4.
   5. Load cosine of the sun elevation into temp register T5.
   6. Load distance south to tower into temp register T6.
   7. Load distance east to tower into temp register T7.
   8. Load distance up to tower into temp register T8.
   9. Load total distance to tower into divisor of FB 20.
  10. a. Load T0 into multiplicand of FB 19.
       b. Load T3 into multiple of FB 19.
       c. Multiply.
       d. Load product into add1 of FB 17.
       e. Load T6 into add2 of FB 17.
       f. Add.
       g. Load sum into dividend of FB 20.
       h. Divide.
       i. Move quotient into temp register T9.
  11. Repeat steps 10a-i 3 times, incrementing all temp registers by one.

12. Move 0 into add1 of FB 17.
13. a. Move T9 into multiplicand and multiplier of FB 17.
    b. Multiply.
    c. Move product into add2 of FB 17.
    d. Add.
    e. Move sum into add1 of FB 17.
14. Repeat steps 13 a-c 3 times, incrementing all temp registers by one.
15. Move sum into convert to binary register of FB 16.
16. Convert.
17. Convert 32 bit binary to 16 bit binary.
Note: At this point T0 contains the square of the unit cosine of the mirror normal in floating point real number format. If the distances south, east, and up to the tower are expressed in relative terms such that the maximum value is one, the temporary register T0 will contain a number that can be expressed as a 16-bit binary without loss of very many significant figures.
18. Load result into radicand of FB RAD:16.
19. Find square root.
20. Convert 8-bit root and 16-bit remainder to floating point with FB 15.
21. Store floating point number in temporary storage register T0.

The results of this procedure are as follows:

a. The Cartesian unit vectors for i, j, and k in registers T9, T10, and T11 with the unit cosine in T0.

The estimated time and memory requirements are 60 ms and (45) 8-bit words [(35) operational words, (0) permanent binary words,and (5) real words]. Each block is executed one per az/el loop.

A13. Exponentiation of Elevation Vector (ELARC EXP)

The arcsine and arccosine functions require an exponentiation for odd powers only. The procedure for exponentiation is similar to that described in Section A6. The difference is that only the odd powers are retained.

The following information is required as an input to this program block:

a. The floating point elevation.

Program Block.

1. Move floating point angle to variable register R11.
2. Call arc exponentiation function block.

<u>Arc Exponentiation Function Block</u>.

1. Move floating point angle to multiplier in FB 19.
2. Move floating point angle to multiplicand in FB 19.
3. Multiply.
4. Move product to multiplier of FB19.
5. a. Multiply.
   b. Store product in variable register.
   c. Move product to multiplicand in FB 19.
   d. Increment register number for variable storage.
6. Repeat step 5a-5d eight times.

The results of this procedure are as follows:

x in R11, x^3 in R12, X^5 in R13, ... x^{17} in R19, where x is the angle and Rn is the variable word used for product storage.

The estimated time and memory requirements are 51 ms and (30) 8-bit words [(12) operational words, (0) permanent binary words, and (9) real words]. Each block is executed once per az/el loop.

A14. Arc Function of Elevation Vector

The arcsine and arccosine functions are dependent and cannot be separated. Consequently, both functions are executed when either are required. This step returns both the arc sine and arc cosine of the elevation vector, but only the arc cosine is required.

The procedure for calculation of arcsine is similar to sine, described in A8. The major differences are the constants, the number of executions, and the increment. This block is broken into two parts (ELVCT ARC 1 and ELVCT ARC 2) to provide time flexibility in the multiplex arrangement.

The following information is required as an input to this program block:

a. The exponentiated values from A13 is R11, R12, ... R19.
b. The constants 6, 13.33333, 22.4, ... 633.9048 are stored as floating point numbers in C12, C13, C14, ... C19. (This line is a permanent storage, not an active programming step.

<u>Program Block</u>.

1. Move floating point angle to variable register R11.
2. Call arcsine function block.
3. Call arccosine function block.

Arcsine Function Block.

1. Move R11 to add1 of FB 17.
2. Define R12 and C12 as the initial constants and variables.
3. a. Move Rn to divisor of FB 20.
   b. Move Cn to divisor of FB 20.
   c. Divide.
   d. Move quotient to add2 of FB 17.
   e. Add.
   f. Move sum to Add1 of FB 17.
   g. Increment variable and constant registers by 1.
4. Repeat steps 3a-3g seven times.
5. Move the sum to variable storage register.

Arccosine Function Block.

1. Move the constant -1 to the multiplier of FB 19.
2. Move the arcsine of the angle to the multiplicand of FB 19.
3. Multiply.
4. Move the product to add2 in FB 17.
5. Move the constant pi/2 to add1 in FB 17.
6. Add.
7. Move the sum to a variable storage register.

The results of this procedure are as follows:

   a. The arc cosine of the elevation vector, i.e. the ideal heliostat elevation angle, in radians.

The estimated time and memory requirements are approximately 37 ms for each part and (27) 8-bit words [(25) operational words, (0) permanent binary words, and (1) real words]. Each block is executed once per az/el loop.

A15. Exponentiation of the Ideal Heliostat Elevation.

The sine of the elevation vector is used as an intermediate variable in the calculation of the ideal azimuth. The execution of this procedure is similar to A6 or A7. This block was broke into two parts (HEL EL EXP 1 and HEL EL EXP 2) for time flexibility in the multiplex procedure.

The following information is required as an input to this procedure:

   a. The ideal heliostat elevation.

<u>Program Block.</u>

    1.   Set the ideal heliostat elevation to the floating point angle.
    2.   Call Sin Exponentiation Function Block.

The results of this procedure are as follows:

    a.   x in R1, x^2 in R2, x^3 in R3, ... x^9 in R9, where x is the angle and Rn is the variable word used for product storage.

The estimated time and memory requirements are 48 ms and (20) 8-bit words [(2) operational words, (0) permanent binary words, and (9) real words]. Each block is executed once per heliostat.

A16. Sine of Ideal Elevation Angle (SIN HEL EL).

This block is, in execution, similar to A8 or A9. The sine function requires exponentiation before implementation.

The following information is required as an input to this program block:

    a.   x in R1, x^2 in R2, x^3 in R3, ... x^9 in R9, where x is the ideal elevation angle and Rn is the variable word used for product storage.
    b.   The constants -6, 120, -5040, and 362880 are stored as floating point numbers in C3, C5, C7, and C9. (This line is a permanent storage, not an active programming step.)

<u>Program Block.</u>

    1.   Move exponential output to proper registers.
    2.   Call sine block.
    3.   Move R0 to sin ideal el storage register.

The results of this procedure are as follows:

    a.   sin (x) in R0, where x is the angle in radians.

The estimated time and memory requirements are 33 ms and (13) 8-bit words [(3) operational words, (0) permanent binary words, and (5) real words]. Each block is executed once per heliostat.

A17. Heliostat Azimuth and Elevation, Part 2 (HEL AZ/EL 2)

Part 2 in the heliostat azimuth development requires a single multiplication to establish the azimuth product vector.

The following information is required as an input to this program block:

      a. Azimuth vector from A12.
      b. Sine of elevation vector from A16.

Program Block.

    1. Load the azimuth vector into the multiplicand position of FB19.
    2. Load the sine of the elevation vector into the multiplier position of FB19.
    3. Multiply.
    4. Store the result in the azimuth product vector register.

The results of this procedure are as follows:

      a. The azimuth product vector.

The estimated time and memory requirements are 4 ms and (6) 8-bit words [(4) operational words, (0) permanent binary words, and (1) real word]. This block is executed once per heliostat.

A18. Exponentiation of Azimuth Vector (AZARC EXP)

The arcsine and arccosine functions require an exponentiation for odd powers only. The procedure for exponentiation is similar to that described in section A13.

The following information is required as an input to this program block:

      a. The floating point azimuth.

Program Block.

    1. Move floating point angle to variable register R11.
    2. Call arc exponentiation function block.

The results of this procedure are as follows:

x in R11, x^3 in R12, x^5 in R13, ... x^{17} in R19, where x is the angle and Rn is the variable word used for product storage.

The estimated time and memory requirements are 51 ms and (20) 8-bit words [(2) operational words, (0) permanent binary words, and (9) real words]. Each block is executed once per az/el loop.

A19. Arcsine of Azimuth Product Vector

This step returns the arcsine of the azimuth product vector. The arc sine of the azimuth product vector is the ideal heliostat azimuth angle, in radians. This block requires a substantial amount of processing time. Consequently, it is broken into two parts (AZVCT ARC 1 and AZVCT ARC 2).

The following information is required as an input to this program block:

    a. The exponentiated values from A18 in R11, R12,... R19.
    b. The constants 6, 13.33333, 22.4,... 633.9048 are stored as floating point numbers in C12, C13, C14,... C19. (This line is a permanent storage, not an active programming step.

Program Block.

    1. Move floating point angle to variable register R11.
    2. Call arcsine function block.
    3. Move result to arcsine of az prod vector register.

The results of this procedure are:

    a. The ideal heliostat azimuth.

The estimated time and memory requirements are approximately 37 ms for each part and (5) 8-bit words [(3) operational words, (0) permanent binary words, and (1) real words]. Each block must be executed once per heliostat per az/el loop.

A20. Exponentiation of the Ideal Azimuth (HEL AZ EXP)

The correction of the azimuth angle to accommodate drive tilt or other miscellaneous errors requires exponentiation before the correction polynomial can be solved. Exponentiation of the ideal elevation was completed as a part of another step (A15). These values can be used to correct the elevation for drive type, tilt, and other miscellaneous errors.

The following information is required as an input to this program block:

    a. The ideal heliostat azimuth.

Program Block.

    1. Move floating point ideal azimuth to multiplier in FB 19.
    2. Move floating point ideal azimuth to multiplicand in FB 19.
    3. Define the initial variable storage word.

4. a. Multiply.
    b. Store product in variable register.
    c. Move product to multiplicand in FB 19.
    d. Increment register number for variable storage.
5. Repeat steps 4a-4d twice, execute 3 time total.

The results of this procedure are as follows:

a. Ideal azimuth^2.
b. Ideal azimuth^3.
c. Ideal azimuth^4.

The estimated time and memory requirements are 16 ms, and (16) 8-bit words [(10) operational words, (0) binary words, and (3) real words]. This block must be executed once per heliostat per az/el loop.

A21. Selection of the Elevation Correction Coefficients (EL COEFF).

Two polynomials were allowed for in the correction of the elevation axis. A single set of azimuth correction coefficients are required. Consequently, no selection block is required for azimuth.

The following information is required as an input to this program block:

a. The ideal heliostat elevation.
b. The correction coefficients for each relationship, formatted as CE0, CE1, CE2, and CE3 for the first relationship, followed by the coefficients for the second correction polynomial in the same order.

The procedure for selection is as follows:

1. Transfer the ideal elevation to compare 1 of FB21.
2. Transfer the elevation at which the 2nd relationship will be used.
3. Compare.
4. Set index1 to 0.
5. Set index2 to 0.
6. If ideal elev > elev for 2nd polynomial, set index2 to 4.
7. a. Set dataword(index2) to elevation correction coefficient EC(index1).
    b. Increment index1 by 1.
    c. Increment index2 by 1.
8. Repeat steps 7a-c three times, execute four times total.

The results of this procedure are as follows:

a. The appropriate elevation correction coefficient stored in EC0, EC1, EC2, and EC3.

The estimated time and memory requirements are 6 ms and (20) 8-bit words [(12) operational words, (0) binary words, (4) real words].

The selection must be executed once per heliostat per az/el loop.

A22. Correction of the Azimuth Position (HEL AZ CRCT)

This program block implements the corrective polynomial. In execution, it is similar to block A5.

    a. Azimuth correction coefficients, AC0, AC1, AC2, AC3.
    b. Ideal azimuth, UA0, and exponentials, UA1, UA2, UA3.

The procedure for the calculation is as follows:

1. Set index1 to 1.
2. Set AC0 to add1 of FB17.
3.   a. Move AC(index1) to multiplicand of FB19.
     b. Move UA(index1) to multiplier of FB19.
     c. Multiply.
     d. Move result to add2 of FB17.
     e. Add.
     f. Move result to add1 of FB17.
     g. Increment index1 by 1.
4. Repeat steps 3a-3g twice, execute three times total.
5. Move result to HA1.

The results of this procedure are as follows:

    a. The actual heliostat azimuth, HA1.

The estimated time and memory requirements for this procedure are 28 ms and (17) 8-bit words [(15) operational words, (0) permanent binary words, and (1) real words]. The actual correction for drive errors must be executed once per heliostat per az/el loop.

A23. Correction of the Elevation Position (HEL EL CRCT)

This program block implements the corrective polynomial. In execution, it is similar to block A22.

    a. Elevation correction coefficients, EC0, EC1, EC2, EC3.
    b. Ideal elevation, UE0, and exponentials, UE1, UE2, UE3.

The procedure for the calculation is as follows:

1. Set index1 to 1.
2. Set EC0 to add1 of FB17
3. a. Move EC(index1) to multiplicand of FB19.
   b. Move UE(index1) to multiplier of FB19.
   c. Multiply.
   d. Move result to add2 of FB17.
   e. Add.
   f. Move result to add1 of FB17.
   g. Increment index1 by 1.
4. Repeat steps 3a-3g twice, execute three times total.
5. Move result to HE1.

The results of this procedure are:

   a. The actual heliostat elevation, HE1.

The estimated time and memory requirements for this procedure are 28 ms and (17) 8-bit words [(15) operational words, (0) permanent binary words, and (1) real words]. The actual correction for drive errors must be executed once per heliostat per az/el loop.

Twenty-three major program blocks were developed to calculate the actual heliostat azimuth and elevation. Some of these blocks were, subsequently, divided into two parts to reduce the contiguous processing time, and therefore, increase the flexibility in the multiplex procedure required to operate four heliostats from a single controlle. Summaries of the memory requirements and processing times are provided in Section 5.0 of this report.

APPENDIX ITEM 8.A
Definition of Terms Used in Financial Analysis.

DIRECT COSTS are the costs traceable to a specific product. This often includes only the material and labor. These costs are roughly proportional to the quantity of product produced.

DIRECT LABOR costs are the wages of the people that do tasks in the manufacturing process for a specific product. In this study, the labor costs usually includes labor taxes, unemployment insurance, and fringe benefits.

DIRECT MATERIALS is the cost of the materials that end up as part of the specific product. This is the cost paid to the original supplier.

INDIRECT COSTS are costs that are "considered" as not being traceable to a specific product. These costs are not directly proportional to the quantity of product produced. The costs included here vary greatly from one company's accounting practices to another's. Typical costs are building rent, utilities, selling expenses, R & D expenses, and general and administrative costs.

INDIRECT LABOR refers to wages of people that do not do tasks directly related to the manufacturing processes of a specific product. This could include janitors, maintenance workers, inspectors, and machine set-up persons.

INDIRECT MATERIAL refers to purchase of materials that do not end up as part of the specific product. This could include cutting fluids, cleaning solutions, and abrasives.

FIXED EXPENSES are defined as those not directly related to the manufacturing process. This could include telephone bills, energy bills, taxes, equipment depreciation, etc. Fixed expenses can also include salaries of persons not considered directly related to the manufacturing process. They may include industrial engineers, production supervisors, buyers, etc.

TOOLING is the cost to design and build durable tools, or revise existing ones to manufacture a specific product or its components.

GENERAL AND ADMINISTRATIVE costs are the costs required to keep a company in business, but not directly related to production operations. These may include executive salaries, R & D, public relations expenses, etc.

SELLING COSTS are the costs directly related to selling the specific product. This could include salespersons' salaries, marketing studies, etc.

INPUT CONSTANTS
    Base labor rate $7.50
    Burden   0.70
    Material overhead   0.25
    G & A   0.15
    Profit   0.06

PART #	PART DESCRIPTION	QNTY	+-----LABOR---------+			+-------MATERIAL--------------------++			++-------SUB-ASSEMLY TOTALS---------------				
	Assy #		mfg	set up	w/burden	Units	Unit cost		Raw $	labor	mtrl	total	$/m^2	% total
		#/hlst	(hrs)	(hrs)	($)		($/unit)	Unit/Prt	($)	($)	($)	($)	($)	(%)
	MIRROR MODULE													
		1	16.0		204					$204	$0	$204	$4.07	0.9%
	1100 Ring	1								$122	$987	$1,108	$22.17	4.9%
1101	Main ring segments	3	9.6	0.0	122	lbs	1.49	101.3	453.03					
1102	Joint/Hinge doubler	6			0	@	73.66	1.0	441.96					
1191	Doubler swage bolt	48			0	@	1.14	1.0	54.72					
1192	Doubler swage nuts	48			0	@	0.77	1.0	36.96					
1193	Tooling attachment nuts	24			0	@			0.00					
	1200 Front Membrane	1								$509	$2,188	$2,698	$53.95	12.0%
1201	Panel #1	2	23.9	3.9	306	lbs	1.79	2.7	9.49					
1202	Panel #2	2			0	lbs	1.79	9.5	34.01					
1203	Panel #3	2			0	lbs	1.79	11.4	40.81					
1204	Panel #4	3			0	lbs	1.79	12.2	65.51					
1206	Reflective laminate	1	5.4	14.0	76	ft^2	2.35	808.0	1900.42					
1207.1	Laminate edgesealng tape,.50	1			0	ft	0.07	620.0	45.26					
1207.2	Laminate edgesealing tape,.75	1			0	ft	0.11	268.0	29.48					
1207.3	Laminate edgesealing tape,1	1			0	ft	0.15	268.0	39.13					
1208	Outer hole reinforcement	1			0	lbs	1.38	3.1	4.28					
1209	Inner hole reinforcement	1			0	lbs	1.38	1.6	2.21					
1291	Selfclinching rivts,3/16xshrt	52	10.0		128	100	3.07	0.0	1.60					
1292	Rivet washers	104			0	100			2.00					

120

1293	Adhesive				0	-			14.00				
	1300 Rear Membrane	1								$306	$296	$602	$12.04	2.7%
1301	Panel #1	2	23.9	3.9	306	lbs	1.79	2.7	9.49				
1302	Panel #2	2			0	lbs	1.79	9.5	34.01				
1303	Panel #3	2			0	lbs	1.79	11.4	40.81				
1304	Panel #4	3			0	lbs	1.79	12.2	65.51				
1306	Outer hole reinforcemnt 1	2			0	lbs	1.38	18.3	50.51				
1307	Outer hole reinforcemnt 2	1			0	lbs	1.38	17.9	24.70				
1308	Inner hole reinforcemnt 1	1			0	lbs	1.38	18.6	25.67				
1309	Inner hole reinforcemnt 2	1			0	lbs	1.38	16.4	22.63				
1391	Selfclinching rivts,3/16xmed.	192			0	100	2.91	0.0	5.59				
1392	Rivet washers	384			0	100			3.00				
1393	Adhesive				0	-			14.00				
	REAR SUPPORT STRUCTURE												
	Assembly	1	12		149					149	0	$149	$2.98	0.7%
	2100 Truss-drive	3				@	397.00	1.0	1191.00	$1	$1,416	$1,416	$28.32	6.3%
2101	Front primary	3			0	-			0.00				
2102	Rear primary	3			0	-			0.00				
2103	Tip hinge plate	3			0	-			0.00				
2104	Tip hinge tube	3			0	-			0.00				
2105	Hinge tube bushing	6	0.1		1	@			0.00				
2106	Secondary #1	3			0	-			0.00				
2107	Secondary #2	3			0	-			0.00				
2108	Secondary #3	3			0	-			0.00				
2109	Secondary #4	3			0	-			0.00				
2110	Secondary #5	3			0	-			0.00				
2111	Secondary #6	3			0	-			0.00				
2112	Secondary #7	3			0	-			0.00				
2113	Secondary #8	3			0	-			0.00				
2114	Secondary #9	3			0	-			0.00				
2115	Secondary #10	3			0	-			0.00				
2116	Secondary #12	3			0	-			0.00				
2117	Rear tierod doubler-inner	3			0	-			0.00				
2118	Rear tierod doubler-outer	3			0	-			0.00				
2119	Rear middle primary dbler	3			0	-			0.00				
2120	Primary root doublers				0	-			0.00				
2121	Secondary root doublers				0	-			0.00				
2122	Drive interface bracket	3			0	-			0.00				
2191	Truss to hub swage bolt, L	21			0	@	2.30	1.0	48.30				

2192	Truss to hub swage bolt, S	24		0	@	1.85	1.0	44.40				
2193	Truss to hub swage nuts	45		0	@	0.83	1.0	37.35				
	Galvanizing	3		0	100 lb.	15.37	2.1	94.53				
	2200 Truss-simple	3			@	397.00	1.0	1191.00	$1	$1,416	$1,416	$28.32	6.3%
2201	Front primary	3		0	-			0.00				
2202	Rear primary	3		0	-			0.00				
2203	Tip hinge plate	3		0	-			0.00				
2204	Tip hinge tube	3		0	·			0.00				
2205	Hinge tube bushing	6	0.1	1	@			0.00				
2206	Secondary #1	3		0	-			0.00				
2207	Secondary #2	3		0	-			0.00				
2208	Secondary #3	3		0	-			0.00				
2209	Secondary #4	3		0	-			0.00				
2210	Secondary #5	3		0	-			0.00				
2211	Secondary #6	3		0	-			0.00				
2212	Secondary #7	3		0	-			0.00				
2213	Secondary #8	3		0	-			0.00				
2214	Secondary #9	3		0	-			0.00				
2215	Secondary #10	3		0	-			0.00				
2216	Secondary #12	3		0	-			0.00				
2217	Rear tierod doubler-inner	3		0	-			0.00				
2218	Rear tierod doubler-outer	3		0	-			0.00				
2219	Rear middle primary dbler	3		0	-			0.00				
2220	Primary root doublers			0	-			0.00				
2221	Root kink doubler	3		0	-			0.00				
2291	Truss to hub swage bolt, L	21		0	@	2.30	1.0	48.30				
2292	Truss to hub swage bolt, S	24		0	@	1.85	1.0	44.40				
2293	Truss to hub swage nuts	45		0	@	0.83	1.0	37.35				
	Galvanizing	3		0	100 lb.	15.37	2.1	94.53				
	2300 Hub	1			@	428.00	1.0	428.00	$0	$447	$447	$8.94	2.0%
2301	Hub body	1		0	-			0.00				
2302	Front flange	1		0	-			0.00				
2030	Rear flange	1		0	-			0.00				
2034	Drive fins	6		0	-			0.00				
2305	Simple fins	6		0	-			0.00				
2306	Hub bottom cover	1		0	-			0.00				
	Galvanizing	1		0	100 lb.	15.37	1.2	18.80				
	2400 Hinge	6							$0	$506	$506	$10.13	2.2%

2401.1	Hinge main plate	6		0	@	37.00	1.0	222.00					
2401.2	Hinge mounting ears	12		0	-			0.00					
2402	Rear hinge pin	6		0	@	10.00	1.0	60.00					
2403	*Hinge urethane bushing*	6		0	@	11.67	1.0	70.00					
2404	Hinge inner bushing washer	6		0	@	6.34	1.0	38.04					
2405	Hinge bushing liner	6		0	@	6.15	1.0	36.90					
2406	Hinge outer bushing spacer	6		0	@	7.85	1.0	47.10					
2491	Rear hinge pin nut	12		0	@	2.00	1.0	24.00					
2492	Rear hinge thrust bushing	12		0	@			0.00					
2493	Rear hinge thrust spring	12		0	@			0.00					
2494	Rear hinge thrust washer	12		0	@			0.00					
2495	Rear hinge locking washer	6		0	@			0.00					
2496	Rear hinge locking pin	12		0	@			0.00					
2497	Hinge SHCS, 1"-8	6		0	@			0.00					
2498	*Hinge SHCS nut*	6		0	@			0.00					
2499	Hinge SHCS belleville washers	6		0	@			0.00					
	Galvanizing	6		0	100 lb.	15.37	0.1	8.41					
2500	Tie rods								$102	$209	$311	$6.23	1.4%
2501	Rod-A	1	8.0	102	lbs.	0.59	151.0	89.09					
2502	Rod-B			0	@			0.00					
2503	Rod-C			0	@			0.00					
2504	Rod-D			0	@			0.00					
2505	Common rod-E			0	@			0.00					
2506	Common rod-F			0	@			0.00					
2507	Turnbuckle body	36		0	@	2.70	1.0	97.20					
2591	Acorn nut, 3/8 NC, S.S.			0	@			0.00					
2592	Washer, flat, 3/8, Galv.			0	@			0.00					
	Galvanizing	1		0	100 lb.	15.37	1.5	23.21					
	DRIVE AND ADAPTER												
3100	Az/El drive								$0	$5,000	$5,000	$100.00	22.2%
3101	Az-El torque tube drive.	1		0	@	5000.00	1.0	5000.00					
3191	Drive-flange bolt			0	@			0.00					
3192	Drive-flange safety washer			0	@			0.00					
3200	Drive adapter								$102	$427	$529	$10.58	2.3%
3201 R&L	Drive adapter weldment, R&L	2	8.0	102	@	0.35	500.0	350.00					
3201.1	adapter mounting flange	1		0	@			0.00					
3201.2	adapter stub tube	1		0	@			0.00					
3201.3	*adapter main web*	1		0	@			0.00					

3201.4	adapter upper flange	1		⸳	0	@			0.00				
3201.5	adapter lower flange	1			0	@			0.00				
3201.6	adapter upper face plate	1			0	@			0.00				
3201.7	adapter lower face plate	1			0	@			0.00				
3201.8	adapter cross bar plate	1			0	@			0.00				
3202	Adapter top cross bar	1			0	@			0.00				
3291	Adapter to drive bolt	12			0	@			0.00				
3292	Adapter to drive safety washer	12			0	@			0.00				
3293	Galvanizing	1			0	100 lb.	15.37	5.0	76.85				
	PYLON												
4100	Pylon									$153	$1,633	$1,786	$35.72	7.9%
4101	Pylon body	1	8.3	106	ft	41.58	28.5	1185.03				
4102	Pylon top flange	1	3.7	47	@	158.30	1.0	158.30				
	Galvanizing	1		0	100 lb.	15.37	18.9	289.76				
	FOUNDATION												
5100	Hole, 42" diam, 15 ft dp	1		0	ft	10.00	15.0	150.00	$0	$150	$150	$3.00	0.7%
5200	Steel reinforcement	1		0	@			0.00	$0	$0	$0	$0.00	
5300	Concrete	1	6.0	77	yd^3	48.90	5.3	259.17	$77	$259	$336	$6.71	1.5%
	FOCUS CONTROL HARDWARE												
6100	Fan assembly	1	0.5	6	@			0.00	$6	$210	$217	$4.34	1.0%
6101	Fan motor	1		0	@	103.75	1.0	103.75				
6102	Fan blade	1		0	@	10.40	1.0	10.40				
6103.1	Fan shroud assembly	1		0	@		1.0	0.00				
6103.2	Fan shroud ring	1		0	@	18.18	1.0	18.18				
6103.3	Fan shroud brackets	3		0	@	7.50	1.0	22.50				
6103.4	Weather cover brackets	3		0	@	7.50	1.0	22.50				
6103.5	Weather ring brackets	3		0	@	3.10	1.0	9.30				
6103.6	Fan motor mounting bracket	1		0	@	6.50	1.0	6.50				
6104	Motor strap	2		0	@	7.10	1.0	14.20				
6191	Shroud assy mounting screw	2		0	@			0.00				
6192	Motor strap bolt	2		0	@			0.00				
	Galvanizing	1		0	100 lb.	15.37	0.2	3.07				
6200	Sensor assembly & accessr's								$0	$397	$397	$7.95	1.8%
6201	LVDT	1		0	@	134.00	1.0	134.00				
6202	LVDT mounting clips	2		0	@			0.00				
6203	LVDT core	1		0	@			0.00				
6204	Core mounting rod	1		0	@			0.00				

6205	Sensor mounting bracket	1			0	@			0.00				
6206	Rod jam nut	1			0	@			0.00				
6207	Rivnut	1			0	@			0.00				
6208	LVDT excitation module	1			0	@	200.00	1.0	200.00				
6209	Module socket	1			0	@	15.00	1.0	15.00				
6210	Proximity limit switch	1			0	@	48.38	1.0	48.38				
	6300 Weather covers									$9	$141	$150	$3.00	0.7%
6301	Fan weather plate	1			0	@			0.00				
6302	Fan weather ring	1			0	@	9.60	1.0	9.60				
6303	Sealing bellows (front)	1			0	0	83.30	1.0	83.30				
6304	Seal strap	1			0	@			0.00				
6305	Sealing bellows clamp flange	2			0	@			0.00				
6306	Rear sealing pan segments	6			0	@			0.00				
6307	Rear seal segment retainer	6			0	@			0.00				
6308	Rear membrane flange ring	1	0.7	1.5	9	@	6.30	1.0	6.30				
6309	Rear seal strip	1			0	@	41.65	1.0	41.65				
6310	Rear seal strip clamp strap	2			0	@			0.00				
6311	Weather cover bolts	3			0	@			0.00				
6312	Weather cover nuts	3			0	@			0.00				
6313	Weather cover seal washers	3			0	@			0.00				
6314	Weather ring bolts	3			0	@			0.00				
6315	Weather ring nuts	3			0	@			0.00				
6316	Rear seal segment screws	12			0	@			0.00				
6317	Rear seal segment washers	12			0	@			0.00				
6318	PVC foam tape,adhesive back	1			0	@			0.00				
	TRACKING CONTROL HARDWARE												
	7100 Motors & accessories									$0	$863	$863	$17.27	3.8%
7101	90vdc,56c,TENV 1/4hp PMC motor	2			0	@	177.63	1.0	355.26				
7102	Intermediate adapter flange	2			0	@			0.00				
7103	Proximity shaft positn sensr	4			0	@	48.38	1.0	193.54				
7104	Axis reference position switch	2			0	@	60.48	1.0	120.96				
7105	Axis end travel limit switch	4			0	@	48.38	1.0	193.54				
						@							
	7200 Logic controller					@				$0	$2,216	$2,216	$44.31	9.8%
7201	CPU 103	0.50			0	@	701.25	1.0	350.63				
7202	Power supply	0.50			0	@	123.75	1.0	61.88				
7203	Digital I/O module	0.50			0	@	397.50	1.0	198.75				
7204	Analog input module	0.50			0	@	315.00	1.0	157.50				
7205	Analog output module	0.50			0	@	375.00	1.0	187.50				

7206	Counter module	2.00			0	@	225.00	1.0	450.00					
7207	Digital DC input, 8 chnl	2.50			0	@	138.75	1.0	346.88					
7208	Digital DC output, 8 chnl	2.50			0	@	86.25	1.0	215.63					
7209	BUSS units	2.00			0	@	48.75	1.0	97.50					
7210	Battery	0.50			0	@	12.00	1.0	6.00					
7211	8K EEPROM	0.50			0	@	275.63	1.0	137.81					
7212	Connector	0.50			0	@	11.25	1.0	5.63					
					0	@			0.00					
7300	Control components									$0	$633	$633	$12.65	2.8%
7301	Fan reversing relay	1.00			0	@	21.28	1.0	21.28					
7302	Fan motor controller	1.00			0	@			0.00					
7302.1	main control chassis	1.00			0	@	130.90	1.0	142.80					
7302.2	harness w/ fuse block	1.00			0	@	16.44	1.0	12.75					
7302.3	plug in power resistor	1.00			0	@	1.25	1.0	1.25					
7303	Defocus scram relay	1.00			0	@	17.02	1.0	17.02					
7304	Drive motor starter				0									
7304.1	Drive motor contactor	0.00			0	@	25.70	1.0	0.00					
7304.2	Drive motor overload relay	0.00			0	@	30.24	1.0	0.00					
7305	Drive motor reversing relay	2.00			0	@	15.20	1.0	30.40					
7306	Drive motor SCR controller	2.00			0	@	47.06	1.0	94.12					
					0	@			0.00					
7400	Electrical hardware				0	@			0.00	$511`	$313	$824	$16.48	3.7%
7401	Enclosure	0.50	40.0	2.0	511	@		1.0	0.00					
7402	Back panel	0.50			0	@		1.0	0.00					
7403	Front sub-panel	0.50			0	@		1.0	0.00					
7404	35mm DIN rail	3.00			0 6.5 ft		6.12	1.0	18.36					
7405	Feed tru terminal block	50.00			0	@	0.68	1.0	34.00					
7406	Ground terminal block	5.00			0	@	2.27	1.0	11.35					
					0	@			0.00					
					0	@			0.00					
	FIELD WIRING				0	@			0.00	$237	$249	$487	$9.73	2.2%
	Main Trunk	0.0005	10.6		135	@	587.13	1.0	0.29					
	Heliostat to Heliostat	0.50	8.0		102	@	498.23	1.0	249.12					
					0	@			0.00					
	FIELD INSTALLATION				0	@			0.00	$115	$0	$115	$2.30	0.5%
	Transport/rig module to drive	1.00	7.0		89	@			0.00					
	Install box on pylon & wire	1.00	2.0		26	@			0.00					
	TOTALS		203		25 $2,603.21					$19,394	$2,603	$19,957	$22,560	$451.20	100.0%

INPUT CONSTANTS

Base labor rate	$7.50
Burden	0.50
Material overhead	0.05
G & A	0.15
Profit	0.06

PART # Assy #	PART DESCRIPTION	QNTY #/hlst	+------LABOR--------+			+------MATERIAL------------------+			+-------SUB-ASSELY TOTAL--------------				
			mfg (hrs)	set up (hrs)	w/burden ($)	Units	Unit cost ($/unit)	Unit/Prt	Raw $ ($)	labor ($)	mtrl ($)	total ($)	$/m^2 ($)	% total (%)
	MIRROR MODULE	1	12.0		135					$135	$0	$135	$2.70	1.1%
1100	Ring	1								$81	$675	$755	$15.11	6.3%
1101	Main ring segments	3	7.2	0.0	81	lbs	1.48	101.3	449.99					
1102	Joint/Hinge doubler	6			0	@	27.08	1.0	162.47					
1191	Doubler swage bolt	48			0	@	0.80	1.0	38.40					
1192	Doubler swage nuts	48			0	@	0.50	1.0	24.00					
1193	Tooling attachment nuts	24			0	@			0.00					
1200	Front Membrane	1			0					$66	$817	$883	$17.66	7.4%
1201	Panel #1	2	3.3		37	lbs	1.18	2.7	6.25					
1202	Panel #2	2			0	lbs	1.18	9.5	22.42					
1203	Panel #3	2			0	lbs	1.18	11.4	26.90					
1204	Panel #4	3			0	lbs	1.18	12.2	43.19					
1206	Reflective laminate	1	2.2	0.7	25	ft^2	0.75	808.0	606.00					
1207.1	Laminate edgesealng tape,.50	1			0	ft	0.06	620.0	35.34					
1207.2	Laminate edgesealing tape,.75	1			0	ft	0.09	268.0	22.78					
1207.3	Laminate edgesealing tape,1	1			0	ft	0.11	268.0	30.28					
1208	Outer hole reinforcement	1	0.2		2	lbs	1.38	3.1	4.28					
1209	Inner hole reinforcement	1	0.2		2	lbs	1.38	1.6	2.21					
1291	Selfclinching rivts,3/16xshrt	52			0	100	2.49	0.0	1.29					
1292	Rivet washers				0	100			2.00					
1293	Adhesive				0	–			14.00					

127

Code	Description	Qty			Unit								
1300	Rear Membrane	1		0					$52	$219	$271	$5.41	2.3%
1301	Panel #1	2	3.3	37	lbs	1.18	2.7	6.25					
1302	Panel #2	2		0	lbs	1.18	9.5	22.42					
1303	Panel #3	2		0	lbs	1.18	11.4	26.90					
1304	Panel #4	3		0	lbs	1.18	12.2	43.19					
1306	Outer hole reinforcemnt 1	1	0.3	4	lbs	1.38	18.3	25.25					
1307	Outer hole reinforcemnt 2	1	0.3	4	lbs	1.38	17.9	24.70					
1308	Inner hole reinforcemnt 1	1	0.3	4	lbs	1.38	18.6	25.67					
1309	Inner hole reinforcemnt 2	1	0.3	4	lbs	1.38	16.4	22.63					
1391	Selfclinching rivts,3/16xmed.	192		0	100	2.63	0.0	5.05					
1392	Rivet washers			0	100			3.00					
1393	Adhesive			0	-			14.00					
				0									
	REAR SUPPORT STRUCTURE			0									
	Assembly	1	9	99					99	0	$99	$1.97	0.8%
2100	Truss-drive	3	2.2	25	lbs	0.30	205.0	184.50	$26	$369	$395	$7.90	3.3%
2101	Front primary	3		0	-			0.00					
2102	Rear primary	3		0	-			0.00					
2103	Tip hinge plate	3		0	-			0.00					
2104	Tip hinge tube	3		0	-			0.00					
2105	Hinge tube bushing	6	0.1	1	@			0.00					
2106	Secondary #1	3		0	-			0.00					
2107	Secondary #2	3		0	-			0.00					
2108	Secondary #3	3		0	-			0.00					
2109	Secondary #4	3		0	-			0.00					
2110	Secondary #5	3		0	-			0.00					
2111	Secondary #6	3		0	-			0.00					
2112	Secondary #7	3		0	-			0.00					
2113	Secondary #8	3		0	-			0.00					
2114	Secondary #9	3		0	-			0.00					
2115	Secondary #10	3		0	-			0.00					
2116	Secondary #12	3		0	-			0.00					
2117	Rear tierod doubler-inner	3		0	-			0.00					
2118	Rear tierod doubler-outer	3		0	-			0.00					
2119	Rear middle primary dbler	3		0	-			0.00					
2120	Primary root doublers			0	-			0.00					
2121	Secondary root doublers			0	-			0.00					
2122	Drive interface bracket	3		0	-			0.00					
2191	Truss to hub swage bolt, L	21		0	@	1.40	1.0	29.40					
2192	Truss to hub swage bolt, S	24		0	@	1.35	1.0	32.40					
2193	Truss to hub swage nuts	45		0	@	0.63	1.0	28.35					
	Galvanizing	3		0	100 lb.	15.37	2.1	94.53					

	2200 Truss-simple	3	2.2	25	lbs	0.30	205.0	184.50	$26	$369	$395	$7.90	3.3%
2201	Front primary	3		0	-			0.00					
2202	Rear primary	3		0	-			0.00					
2203	Tip hinge plate	3		0	-			0.00					
2204	Tip hinge tube	3		0	-			0.00					
2205	Hinge tube bushing	6	0.1	1	@			0.00					
2206	Secondary #1	3		0	-			0.00					
2207	Secondary #2	3		0	-			0.00					
2208	Secondary #3	3		0	-			0.00					
2209	Secondary #4	3		0	-			0.00					
2210	Secondary #5	3		0	-			0.00					
2211	Secondary #6	3		0	-			0.00					
2212	Secondary #7	3		0	-			0.00					
2213	Secondary #8	3		0	-			0.00					
2214	Secondary #9	3		0	-			0.00					
2215	Secondary #10	3		0	-			0.00					
2216	Secondary #12	3		0	-			0.00					
2217	Rear tierod doubler-inner	3		0	-			0.00					
2218	Rear tierod doubler-outer	3		0	-			0.00					
2219	Rear middle primary dbler	3		0	-			0.00					
2220	Primary root doublers			0	-			0.00					
2221	Root kink doubler	3		0	-			0.00					
2291	Truss to hub swage bolt, L	21		0	@	1.40	1.0	29.40					
2292	Truss to hub swage bolt, S	24		0	@	1.35	1.0	32.40					
2293	Truss to hub swage nuts	45		0	@	0.63	1.0	28.35					
	Galvanizing	3		0	100 lb.	15.37	2.1	94.53					
				0									
	2300 Hub	1	3.0	34	lbs	0.30	122.3	36.69	$34	$55	$89	$1.78	0.7%
2301	Hub body	1		0	-			0.00					
2302	Front flange	1		0	-			0.00					
2303	Rear flange	1		0	-			0.00					
2304	Drive fins	6		0	-			0.00					
2305	Simple fins	6		0	-			0.00					
2306	Hub bottom cover	1		0	-			0.00					
	Galvanizing	1		0	100 lb.	15.37	1.2	18.80					
	2400 Hinge			0					$11	$343	$354	$7.09	3.0%
2401.1	Hinge main plate	6	1.0	11	lbs	1.50	8.6	77.40					
2401.2	Hinge mounting ears	12		0	-			0.00					
2402	Rear hinge pin	6		0	lbs	3.00	1.5	27.00					

129

Code	Description	Qty		Val	Unit	Rate	Factor	Cost					
2403	Hinge urethane bushing	6		0	@	8.14	1.0	48.85					
2404	Hinge inner bushing washer	6		0	@	4.87	1.0	29.22					
2405	Hinge bushing liner	6		0	@	4.39	1.0	26.34					
2406	Hinge outer bushing spacer	6		0	@	5.73	1.0	34.38					
2491	Rear hinge pin nut	12		0	@	7.67	1.0	92.00					
2492	Rear hinge thrust bushing	12		0	@		1.0	0.00					
2493	Rear hinge thrust spring	12		0	@		1.0	0.00					
2494	Rear hinge thrust washer	12		0	@		1.0	0.00					
2495	Rear hinge locking washer	6		0	@		1.0	0.00					
2496	Rear hinge locking pin	12		0	@		1.0	0.00					
2497	Hinge SHCS, 1"-8	6		0	@		1.0	0.00					
2498	Hinge SHCS nut	6		0	@		1.0	0.00					
2499	Hinge SHCS belleville washers	6		0	@		1.0	0.00					
	Galvanizing	6		0	100 lb.	15.37	0.1	7.93					
2500	Tie rods			0	@				$59	$201	$260	$5.19	2.2%
2501	Rod-A	1	5.2	59	lbs	0.59	151.0	89.09					
2502	Rod-B			0	@		1.0	0.00					
2503	Rod-C			0	@		1.0	0.00					
2504	Rod-D			0	@		1.0	0.00					
2505	Common rod-E			0	@		1.0	0.00					
2506	Common rod-F			0	@		1.0	0.00					
2507	Turnbuckle body	36		0	@	2.43	1.0	87.48					
2591	Acorn nut, 3/8 NC, S.S.			0	@		1.0	0.00					
2592	Washer, flat, 3/8, Galv.			0	@		1.0	0.00					
	Galvanizing	1		0	100 lb.	15.37	1.6	24.59					
				0									
	DRIVE AND ADAPTER			0									
3100	Az/El drive			0					$0	$3,900	$3,900	$78.00	32.7%
3101	Az-El torque tube drive.	1		0	@	3900.00	1.0	3900.00					
3191	Drive-flange bolt			0	@			0.00					
3192	Drive-flange safety washer			0	@			0.00					
3200	Drive adapter			0					$24	$339	$363	$7.26	3.0%
3201 R&L	Drive adapter weldment, R&L	2	2.1	24	@	0.26	500.0	262.50					
3201.1	adapter mounting flange	1		0	@			0.00					
3201.2	adapter stub tube	1		0	@			0.00					
3201.3	adapter main web	1		0	@			0.00					
3201.4	adapter upper flange	1		0	@			0.00					
3201.5	adapter lower flange	1		0	@			0.00					
3201.6	adapter upper face plate	1		0	@			0.00					
3201.7	adapter lower face plate	1		0	@			0.00					
3201.8	adapter cross bar plate	1		0	@			0.00					

Code	Description	Qty		Count	Unit	Cost	Factor	Total	$	$	$	$	%
3291	Adapter to drive bolt	12		0	@			0.00					
3292	Adapter to drive safety washer	12		0	@			0.00					
3293	Galvanizing	1		0	100 lb.	15.37	5.0	76.85					
				0									
	PYLON			0									
4100	Pylon			0					$89	$918	$1,006	$20.13	8.4%
4101	Pylon body	1	7.9	89	lbs.	0.26	1807.0	475.24					
4102	Pylon top flange	1		0	@	147.92	1.0	147.92					
	Galvanizing	1		0	100 lb.	15.37	19.2	294.43					
				0									
	FOUNDATION			0									
5100	Hole, 42" diam, 15 ft dp	1		0	ft	9.33	15.0	139.95	$0	$140	$140	$2.80	1.2%
5200	Steel reinforcement	1		0	@			0.00	$0	$0	$0	$0.00	
5300	Concrete	1	4.5	51	yd^3	48.90	5.3	259.17	$51	$259	$310	$6.20	2.6%
				0									
	FOCUS CONTROL HARDWARE			0									
6100	Fan assembly	1	0.5	6	@		1.0	0.00	$6	$112	$117	$2.35	1.0%
6101	Fan motor	1		0	@	39.26	1.0	39.26					
6102	Fan blade	1		0	@	10.40	1.0	4.24					
6103.1	Fan shroud assembly	1		0	@		1.0	0.00					
6103.2	Fan shroud ring	1		0	@	17.25	1.0	17.25					
6103.3	Fan shroud brackets	3		0	@	4.70	1.0	14.10					
6103.4	Weather cover brackets	3		0	@	4.70	1.0	14.10					
6103.5	Weather ring brackets	3		0	@	2.04	1.0	6.12					
6103.6	Fan motor mounting bracket	1		0	@	4.38	1.0	4.38					
6104	Motor strap	2		0	@	4.60	1.0	9.20					
6191	Shroud assy mounting screw	2		0	@		1.0	0.00					
6192	Motor strap bolt	2		0	@		1.0	0.00					
	Galvanizing	1		0	100 lb.	15.37	0.2	3.07					
6200	Sensor assembly & accessr's			0					$0	$238	$238	$4.77	2.0%
6201	LVDT	1		0	@	80.00	1.0	80.00					
6202	LVDT mounting clips	2		0	@			0.00					
6203	LVDT core	1		0	@			0.00					
6204	Core mounting rod	1		0	@			0.00					
6205	Sensor mounting bracket	1		0	@			0.00					
6206	Rod jam nut	1		0	@			0.00					
6207	Rivnut	1		0	@			0.00					
6208	LVDT excitation module	1		0	@	112.50	1.0	112.50					
6209	Module socket	1		0	@	7.50	1.0	7.50					
6210	Proximity limit switch	1		0	@	38.40	1.0	38.40					

6300	Weather covers				0					$8	$124	$132	$2.63	1.1%
6301	Fan weather plate	1			0	@			0.00					
6302	Fan weather ring	1			0	@	8.20	1.0	8.20					
6303	Sealing bellows (front)	1			0	@	72.20	1.0	72.20					
6304	Seal strap	1			0	@			0.00					
6305	Sealing bellows clamp flange	2			0	@			0.00					
6306	Rear sealing pan segments	6			0	@			0.00					
6307	Rear seal segment retainer	6			0	@			0.00					
6308	Rear membrane flange ring	1	0.7	1.5	8	@	6.30	1.0	6.30					
6309	Rear seal strip	1			0	@	37.35	1.0	37.35					
6310	Rear seal strip clamp strap	2			0	@			0.00					
6311	Weather cover bolts	3			0	@			0.00					
6312	Weather cover nuts	3			0	@			0.00					
6313	Weather cover seal washers	3			0	@			0.00					
6314	Weather ring bolts	3			0	@			0.00					
6315	Weather ring nuts	3			0	@			0.00					
6316	Rear seal segment screws	12			0	@			0.00					
6317	Rear seal segment washers	12			0	@			0.00					
6318	PVC foam tape,adhesive back	1			0	@			0.00					
					0									
					0									
	TRACKING CONTROL HARDWARE				0									
7100	Motors & accessories				0					$0	$558	$558	$11.16	4.7%
7101	90vdc,56c,TENV 1/4hp PMC motor	2			0	@	77.32	1.0	154.64					
7102	Intermediate adapter flange	2			0	@		1.0	0.00					
7103	Proximity shaft positn sensr	4			0	@	38.40	1.0	153.60					
7104	Axis reference position switch	2			0	@	48.00	1.0	96.00					
7105	Axis end travel limit switch	4			0	@	38.40	1.0	153.60					
					0	@								
7200	Logic controller				0	@				$0	$500	$500	$10.00	4.2%
7201	CPU 103	1.00			0	@	500.00	1.0	500.00					
7202	Power supply	0.00			0	@	82.50	1.0	0.00					
7203	Digital I/O module	0.00			0	@	265.00	1.0	0.00					
7204	Analog input module	0.00			0	@	210.00	1.0	0.00					
7205	Analog output module	0.00			0	@	250.00	1.0	0.00					
7206	Counter module	0.00			0	@	150.00	1.0	0.00					
7207	Digital DC input, 8 chnl	0.00			0	@	92.50	1.0	0.00					
7208	Digital DC output, 8 chnl	0.00			0	@	57.50	1.0	0.00					
7209	BUSS units	0.00			0	@	32.50	1.0	0.00					
7210	Battery	0.00			0	@	8.00	1.0	0.00					
7211	8K EEPROM	0.00			0	@	183.75	1.0	0.00					
7212	Connector	0.00			0	@	7.50	1.0	0.00					

						0	@			0.00					
						0	@			0.00					
						0	@			0.00					
						0	@			0.00					
						0	@			0.00					
						0	@			0.00					
						0	@								
7300	Control components					0					$0	$395	$395	$7.90	3.3%
7301	Fan reversing relay	1.00				0	@	11.23	1.0	11.23					
7302	Fan motor controller	1.00				0	@			0.00					
7302.1	main control chassis	1.00				0	@	119.00	1.0	142.80					
7302.2	harness w/ fuse block	1.00				0	@	14.93	1.0	12.75					
7302.3	plug in power resistor	1.00				0	@	0.63	1.0	0.63					
7303	Defocus scram relay	1.00				0	@	8.99	1.0	8.99					
7304	Drive motor starter					0									
7304.1	Drive motor contactor	0.00				0	@	20.40	1.0	0.00					
7304.2	Drive motor overload relay	0.00				0	@	24.00	1.0	0.00					
7305	Drive motor reversing relay	2.00				0	@	8.55	1.0	17.10					
7306	Drive motor SCR controller	2.00				0	@	42.79	1.0	85.58					
						0	@			0.00					
						0	@			0.00					
7400	Electrical hardware					0	@			0.00	$207	$64	$271	$5.41	2.3%
7401	Enclosure	0.50	18.4	2.0		207	@		1.0	0.00					
7402	Back panel	0.50				0	@		1.0	0.00					
7403	Front sub-panel	0.50				0	@		1.0	0.00					
7404	35mm DIN rail	3.00				0 6.5 ft		6.12	1.0	18.36					
7405	Feed tru terminal block	50.00				0	@	0.68	1.0	34.00					
7406	Ground terminal block	5.00				0	@	2.27	1.0	11.35					
						0	@			0.00					
						0	@			0.00					
	FIELD WIRING					0	@			0.00	$200	$52	$252	$5.04	2.1%
	Main trunk	0.0005	10.6			119	@	134.72	1.0	0.07					
	Heliostat to Heliostat	0.50	7.2			81	@	104.53	1.0	52.27					
						0	@			0.00					
						0	@			0.00					
	FIELD INSTALLATION					0	@			0.00	$101	$0	$101	$2.03	0.8%
	Transport/rig module to drive	1	7.0			79	@			0.00					
	Install box on pylon & wire	1	2.0			23	@			0.00					
						0	@			0.00					
TOTALS			113	4 $1,271.30							$10,532	$1,271	$10,648	$11,920	$238.39	100.0%

U.S. Department of Energy (3)
Forrestal Bldg.
Code CE-132
1000 Independence Avenue, SW
Washington, DC 20585
Attn: S. Gronich
        M. Scheve
        R. Shivers

U.S. Department of Energy
Forrestal Bldg.
Code CE-13
1000 Independence Avenue, SW
Washington, DC 20585
Attn: R. Annan

U. S. Department of Energy
Deputy Assistant Secretary
for Renewable Energy
CE-10, Forrestal Bldg, Room 6C-026
1000 Independence Avenue, SW
Washington, DC 20585
Attn: R. L. San Martin

U.S. Department of Energy (2)
Albuquerque Operations Office
P.O. Box 5400
Albuquerque, NM 87115
Attn: D. Graves
        G. Tennyson

U.S. Department of Energy
San Francisco Operations Office
1333 Broadway
Oakland, CA 94612
Attn: R. Hughey

Advanced Thermal Systems
7600 East Arapahoe
Suite 215
Englewood, CO 80112
Attn: D. Gorman

Agua Y Energia Electrica
Sociedad del Estado
Attn: eng. Eduardo A. Sampayo
Gabato 3713
1826 Remedios de Escalada
Buenos Aires, ARGENTINA

Allegheny Ludlum Steel (2)
Market and Product Development
Alabama and Pacific Avenues
Brackenridge, PA 15014
Attn: Joseph M. Hunt
        John P. Ziemianski

Allegheny Ludlum Steel
80 Valley St.
Wallingford, CT 06492
Attn: John J. Halpin

Analysis Review & Critique
6503 81st Street
Cabin John, MD 20818
Attn: C. LaPorta

Arizona Public Service Company
P.O. Box 53999
M/S 9110
Phoenix, AZ 85072-3999
Attn: W. J. McGuirk

Arizona Solar Energy Office
Dept. of Commerce
1700 W. Washington, 5th Floor
Phoenix, AZ 85007
Attn: Dr. Frank Mancini

Asinel
Ctra. Villaviciosa
de Odón a Móstoles
Km 1,700
28935 Móstoles
Madrid SPAIN
Attn: Jesús M. Mateos

Atlantis Energy Ltd.
Thunstrasse 43a
3005 Bern, SWITZERLAND
Attn: Mario Posnansky

Babcock and Wilcox
91 Stirling Avenue
Barberton, OH 44203
Attn: D. Young

Battelle Pacific Northwest
 Laboratory
P.O. Box 999
Richland, WA 99352
Attn: T. A. Williams

Bechtel National, Inc. (4)
50 Beale Street
50/15 D8
P. O. Box 3965
San Francisco, CA 94106
Attn: P. DeLaquil
         B. Kelly
         J. Egan
         R. Leslie

Black & Veatch Consulting
 Engineers (4)
P.O. Box 8405
Kansas City, MO 64114
Attn: J. C. Grosskreutz
         J. E. Harder
         L. Stoddard
         J. Arroyo

Bomin Solar
Industriestr. 8
D-7850 Lorrach
FEDERAL REPUBLIC OF GERMANY
Attn: Dr. Hans Jurgen Kleinwachter

Tom Brumleve
1512 Northgate Road
Walnut Creek, CA 94598

California Energy Commission
1516 Ninth Street, M-S 43
Sacramento, CA 95814
Attn: A. Jenkins

California Polytechnic University
Dept. of Mechanical Engineering
3801 West Temple Ave.
Pomona, CA 91768-4062
Attn: W. Stine

California Public Utilities Com.
Resource Branch, Room 5198
455 Golden Gate Avenue
San Francisco, CA 94102
Attn: T. Thompson

Center for Energy and
Environmental Research
GPO Box 3682
San Juan, PR 00936
Attn: Director

Centro de Investigacions   (4)
   Energeticas Medioambientales
   y Technologicas (CIEMAT)
Instituto de Energias Renovables
Avda. Complutense, 22
28040 Madrid
SPAIN
Attn: M. Macias
         M. Romero
         E. Conejero
         J. M. Figarola

Danka Products
3905 S. Mariposa St.
Englewood, CO 80110
Attn: Dan Sallis

DLR EN-TT (2)
Institute for Technical
 Thermodynamics
Pfaffenwaldring 38-40
7000 Stuttgart 80
FEDERAL REPUBLIC OF GERMANY
Attn: Dr. R. Koehne
         Dipl. Ing R. Buck

DLR (2)
Linder Hohe
5000 Koln 90
FEDERAL REPUBLIC OF GERMANY
Attn:　　Dr. Manfred Becker
　　　　Dr.-Ing. Manfred Bohmer

El Paso Electric Company
303 N. Oregon
10th Floor
P.O. Box 982
El Paso, TX 79960
Attn:　　David Gutierrez

Electric Power Research
 Institute (2)
P.O. Box 10412
Palo Alto, CA 94303
Attn:　　J. Bigger
　　　　E. DeMeo

Engineering Perspectives
20 19th Avenue
San Francisco, CA 94121
Attn:　　John Doyle

Flachglas Solartechnik GmbH
Muhlengasse 7
D-5000 Koln 1
FEDERAL REPUBLIC OF GERMANY
Attn:　　Joachim Benemann

Flachglas Solartechnik GmbH (2)
Sonnesstr. 25
D-8000 Munchen 1
FEDERAL REPUBLIC OF GERMANY
Attn:　　Dr. Michael Geyer
　　　　Ingo Susemihl

Foster Wheeler Solar Development
 Corporation (2)
12 Peach Tree Hill Road
Livingston, NJ 07039
Attn:　　S. F. Wu
　　　　R. Zoschak

Georgia Institute of Technology
GTRI/EMSL Solar Site
Atlanta, GA 30332
Attn:　　T. Brown

Georgia Power
7 Solar Circle
Shenandoah, GA 30265
Attn:　　Ed. Ney

Leo Gutierrez
434 School Street
Livermore, CA 94550

HGH Enterprises, Inc.
23011 Moulton Parkway
Suite C-13
Laguna Hills, CA 92653
Attn:　　Dick Holl

Industrial Solar Technology (2)
5775 West 52nd Ave.
Denver, CO 80212
Attn:　　R. Gee
　　　　K. May

Interatom GmbH (2)
P. O. Box
D-5060 Bergisch-Gladbach
FEDERAL REPUBLIC OF GERMANY
Attn:　　M. Kiera
　　　　W. Meinecke

Lawrence Berkeley Laboratory
MS 90-2024
One Cyclotron Road
Berkeley, CA 94720
Attn:　　Arlon Hunt

Los Angeles Department of Water
 and Power
Alternate Energy Systems
Room 661A
111 North Hope Street
Los Angeles, CA 90012
Attn:　　Bill Engels

Luz International (2)
924 Westwood Blvd.
Los Angeles, CA 90024
Attn: D. Kearney
       M. Lotker

Clayton Mavis
626 Tina Way
Livermore, CA 94550

Meridian Corporation
4300 King St.
Suite 400
Alexandria, VA 22302-1508
Attn: D. Kumar

MITI
Electrotechnical Laboratory
Solar Energy Applications Section
1-1-4 Umezono, Tsukuba
Ibaraki 305, JAPAN
Attn: Koichi Sakuta

Nevada Power Co.
P. O. Box 230
Las Vegas, NV 89151
Attn: Mark Shank

ORMAT Energy Systems, Inc.
610 East Glendale Ave.
Sparks, NV 89431-5811
Attn: Dr. Lucien Bronicki

Pacific Gas and Electric Company (3)
3400 Crow Canyon Road
San Ramon, CA 94526
Attn: G. Braun
       T. Hillesland
       R. Dracker

Peerless Winsmith, Inc.
172 Eaton St.
P. O. Box 530
Springville, NY 14141
Attn: W. Hellar

Platforma Solar de Almeria
Aptdo. 7
Tabernas (Almeria)
E-04200 SPAIN
Attn: M. Sanchez

Polydyne, Inc.
1900 S. Norfolk Street, Suite 209
San Mateo, CA 94403
Attn: P. Bos

PSI (2)
CH-5303 Wurenlingen
SWITZERLAND
Attn: W. Durish
       P. Kesselring

Public Service Company of New Mexico
M/S 0160
Alvarado Square
Albuquerque, NM 87158
Attn: T. Ussery
       A. Martinez

Public Service Company of Colorado
System Planning
5909 E 38th Avenue
Denver, CO 80207
Attn: D. Smith

San Diego Gas and Electric Company
P.O. Box 1831
San Diego, CA 92112
Attn: R. Figueroa

SCE (2)
P.O. Box 800
Rosemead, CA 91770
Attn: W. von KleinSmid
       C. Lopez

Schlaich, Bergermann & Partner
Hohenzollernstr. 1
D-7000 Stuttgart 1
Federal Republic of Germany
Attn: Wolfgang Schiel

Sci-Tech International
Advanced Alternative Energy
 Solutions
5673 W. Las Positas Boulevard
Suite 205
P.O. Box 5246
Pleasanton, CA 84566
Attn: Ugur Ortabasi

Science Applications
 International Corporation
10260 Campus Point Drive
San Diego, CA 92121
Attn: B. Butler

Science Applications
 International Corporation (2)
10343 Roselle Street
San Diego, CA 92121
Attn: J. Sandubrae
         K. Beninga

Solar Energy Research Institute (6)
1617 Cole Boulevard
Golden, CO 80401
Attn: B. Gupta
         L. M. Murphy
         P. Schissel
         T. Wendelin
         A. Lewandowski
         M. Carasso

Solar Kinetics, Inc. (12)
P.O. Box 540636
Dallas, TX 75354-0636
Attn: J. A. Hutchison
         A. Konnerth (10)
         P. Schertz

Solar Power Engineering Company
P.O. Box 91
Morrison, CO 80465
Attn: H. C. Wroton

Solar Steam
P.O. Box 32
Fox Island, WA 98333
Attn: D. Wood

South Coast AQMD
9150 Flair Dr.
El Monte, CA 91731
Attn: L. Watkins

Stearns Catalytic Corporation
P.O. Box 5888
Denver, CO 80217
Attn: T. E. Olson

Stone and Webster Engineering
 Corporation
P.O. Box 1214
Boston, MA 02107
Attn: R. W. Kuhr

Sulzer Bros, Ltd.
New Technologies
CH-8401 Winterthur
SWITZERLAND
Attn: Hans Fricker, Manager

Tom Tracey
6922 South Adams Way
Littleton, CO 80122

United Solar Tech, Inc.
3434 Martin Way
Olympia, WA 98506
Attn: R. J. Kelley

University of Arizona
Engineering Experimental Station
Harvil Bldg., Room 151-D
Tucson, AZ 85721
Attn: Don Osborne

University of Houston (3)
Solar Energy Laboratory
4800 Calhoun
Houston, TX 77704
Attn: A. F. Hildebrandt
         L. Vant-Hull
         C. Pitman

Eric Weber
302 Caribbean Lane
Phoenix, AZ 85022

WG Associates
6607 Stonebrook Circle
Dallas, TX 75240
Attn: V. Goldberg

David White
3915 Frontier Lane
Dallas, TX 95214

3M Corp.
3M Center
Building 207-1W-08
St. Paul, MN 55144
Attn: B. A. Benson

3141	S. A. Landenberger (5)
3145	Document Processing (8)
	for DOE/OSTI
3151	G. C. Claycomb (3)
6200	B. W. Marshall, Actg.
6220	A. Van Arsdall
6210	J. T. Holmes, Actg.
6215	P. Best
6215	C. P. Cameron, Actg.
6215	W. Erdman
6215	A. A. Heckes
6215	R. M. Houser
6215	Library (15)
6216	D. J. Alpert (5)
6216	J. W. Grossman
6216	T. R. Mancini
6216	J. E. Pacheco
6216	M. R. Prairie
6216	C. E. Tyner
6216	L. Yellowhorse
6217	J. M. Chavez
6217	P. C. Klimas
6217	G. J. Kolb
8133	A. C. Skinrood
8523	R. C. Christman

Dist-6